Comparative LC-MS Analysis of Proteomics Profile in Cells Incubated with S- or R-Ibuprofen and Its Inhibitory Effect on Angiogenesis Induced by HBV Replication

By: Mr Zhang Jianhua

School of Chemical and Biomedical Engineering

Nanyang Technological University

2011

ACKNOWLEDGEMENTS

I would like to express my most heartfelt and sincere gratitude to the following people, without whom the completion of this project would not have been possible.

It is hard to overstate my gratitude to my Ph.D supervisor, Professor Chen Wei Ning, William. It is due to his valuable guidance, ever-friendly nature and cheerful enthusiasm that I am able to finish my Ph.D research in a respectable manner. I am also thankful to him for allowing me some extra time to manage my unforeseen family matters. Without his unselfish help, I could never finish my doctoral work in Nanyang Technological University. For me, he is not only a scientific mentor but also a lifetime advisor.

I warmly thank my co-supervisor Professor Ching Chi Bin for his most valuable support throughout the course of the whole project.

I am grateful for Singapore Millennium Foundation for supporting my Ph.D training with their research scholarship.

I would like to express my thanks to Dr Tan Tuan Lin, Dr Lu Yiwei, Dr Sui Jianjun, Dr Feng Huixing, Dr Niu Dandan, for their valuable discussions and cooperation with my experiments. I thank Ms Tan Li Ling Jane and Mr. Tan Kee Yang for thesis grammar correcting, I also thank Ms Laleh, Ms Bahar, Ms Zhou Yusi, for accompanying in NTU. Thanks for all other lab colleagues.

I specially thank Ms Zhang Tianyu for giving me continuous encouragement and support.

Finally I wish to express my gratitude to my family for their moral support.

Table and contents

List of Figures

List of Tables

Summary:

Ibuprofen is a member of the proprionic acid group of nonsteroidal anti-inflammatory drugs (NSAIDs), with the *S*-enantiomer being more active compared with the *R*-enantiomer. It has been shown to have protective effect against neuroinflammation which is linked to the pathogenesis of several neurodegenerative disorders, including Alzheimer disease. While its prophylactic effect on Alzheimer disease has been suggested, a comprehensive understanding of its mechanism of action remains unclear. Using iTRAQ-coupled two-dimensional liquid chromatography-mass spectrometry (2D LC-MS/MS) analysis, we report here the first study of protein profile of neuroblastoma cells incubated separately with the two enantiomers of ibuprofen. Three types of cellular proteins including metabolic enzymes, signaling molecules and cytoskeletal proteins displayed changes. The changes in the level of a number of enzymes, involved in fatty acid synthesis and antioxidant activity in cells incubated with the *S*-enantiomer, was further supported by the real-time PCR analysis.

Chronic Hepatitis B Virus (HBV) carriers may develop hepatocellular carcinoma (HCC) by a wide range of mechanisms including angiogenesis. HCC progresses from a small nodule with no blood vessels to a large hypervascular tumor by going through an angiogenic switch. HBV infection and in particular hepatitis B virus x protein (HBx) have been shown to modulate angiogenesis. However, a comprehensive and coordinated mechanism in the HBV-induced angiogenesis still remains to be established. In this study, transient transfection of replicative HBV genome was

carried out in rat primary hepatocytes (RPHs) as well as HepG2 cells. A cell-based HBV replication was established in both RPHs and HepG2 cells. 2D LC-MS/MS analysis was used to detect differentially expressed proteins in cells supporting HBV replication compared with those transfected with the empty vector. HBV replication induced angiogenesis was indicated by tube formation of endothelial cells cultured in condition medium from RPHs or HepG2 cells supporting HBV replication. Enzymes associated with angiogenesis, namely fumarate hydratase and tryptophanyl-tRNA synthetase, were identified by 2D LC-MS/MS analysis in HBV replicating RPHs and HepG2 cells.

On the other hand, the expression levels of 38 known angiogenic genes were screened on mRNAs of HBV replicating HepG2 cells by Real Time RT-PCR. We showed that the known angiogenic proteins such as interleukin 6 (IL6), cyclooxygenase-2 (Cox-2) were regulated by HBV infection. Interestingly, ibuprofen (a Cox2 inhibitor) was found to attenuate the level of IL6 and Cox 2 which was induced by HBV replication.

The mechanism of attenuation of angiogenic proteins by ibuprofen was further investigated. Our results showed that HBx was involved in the increase of the expression of Cox2 through NFκB pathway. However, the expression of Cox2 was decreased when the HBx-expressing cells were incubated with ibuprofen. The contrasting effect of HBx on Cox2 was found to be determined by differential dimer formation among the members of the NFκB family of proteins, including NFκB, RelA and C-Rel. Specifically, HBx alone resulted in the dimer formation between NFκB and

RelA while the combined presence of HBx and ibuprofen led to the formation between NFκB and C-Rel. Additional information on interaction network involving HBx, ibuprofen and NFκB pathways was revealed by 2D LC-MS/MS proteomics analysis.

Taking together, in spite of anti-inflammatory effects, chiral ibuprofen affects other physiological process such as reducing Reactive Oxygen Species (ROS) for Alzheimer disease (AD) development and inhibiting angiogenesis induced by HBV replication. Chiral ibuprofen as existing S and R form ibuprofen showed obvious drug chirality in disease therapy, S ibuprofen is more efficient on protection of neurodegeneration, while R ibuprofen is more efficient on inhibit Cox2 expression with HBx expression. The study of ibuprofen chirality on molecular mechanism may supply meaningful reference for chiral drug further development. The angiogenesis-associated proteins identified in our study may eventually lead to novel anti-angiogenic HCC cancer therapy based on tumor vascular targeting or be the markers for HCC diagnosis.

Chapter 1 Introduction

1.1 History of chiral drug

The molecules are termed chiral, when they have the same structural formulas but differ from each other only in the way the atoms or groups are oriented in space [1], as for example shown in Figure 1.1. However, most enantiomers (one of two stereoisomers) of racemic drugs possess vastly different biological functions in terms of their pharmacology, pharmacokinetics, toxicology and metabolism. Most new chiral drugs for specific disease therapy are developed in single-enantiomer form.

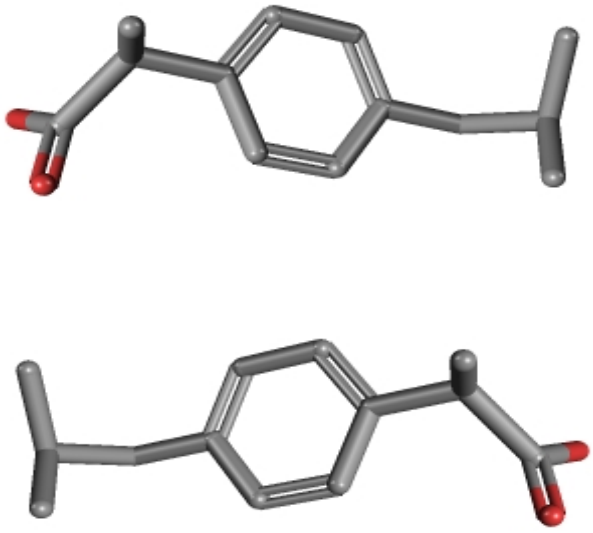

Figure 1.1 Ibuprofen drug Chirality. Ibuprofen demonstrates the definition of the term ‘chirality’, in which both top and bottom chemicals have the same composition of atoms but do not superimpose on each other spatially.

During the 20th century, thousands of new chiral compounds were synthesized,

many of them were examined for therapeutic effects and potential [2], many of them were found to have enantioselectivity for disease therapies. The chirality in drug function and metabolism was firstly studied in 1933, when Easson set up a basic model [3], by which cardiac dysrhythmias therapy effects of (R)-(-) form epinephrine was the more potent enantiomer showed a 300 time greater than the other [4]. The enantiomers of cardiac drugs were reported lately to have significant pharmacokinetics biological variations. For example, the β-adrenergic-antagonist activity of propranolol, was verified to be potent in the S enantiomer, and several other related adrenergic antagonists were found in similar selectivity [5]. Table 1.1 listed some chiral drugs which racemic drugs are obviously different in biological activities. In the 1970s, a lot of information had been obtained on the role of chirality in drug action and metabolism, and some reviews have been published on the subject [6-10].

During the 1980s, new powerful methods for synthesizing unichiral drugs were developed, techniques for the separation of drug enantiomers were improved, and enantioselective analytical methods were set up to selectively detect and measure the individual enantiomers without separation [11]. With the help of these tools, a broad and serious examination was begun on the role of chirality in new-drug action. But some of the chiral drugs are more complex than two enantiomers, and some new drugs were marketed as a mixture more racemic mixtures, such as cyclothiazide (4 race-mates) [12]. In such cases it was often claimed that all or most of the stereoisomers provide the useful activities. But in some cases the reason for the use of

drug mixture could be the high cost of separating enantiomers or the stereochemical instability of chiral center, such as carbenicillin.

Main pharmacological effects of drugs	Isomer potency
β-Adrenoreceptor blocking drugs (β -blockers): propranolol, acebutolol, atenolol, carvedilol	Ex: S(-)-propranolol > R(+)-propranolol
Calcium channel antagonists : verapamil, nicardipine, nimodipine,	Ex: S(-)-verapamil > R(+)-verapamil
β 2-Adrenoceptor agonists : Bronchodilators: Albuterol, salmeterol and terbutaline	Ex: R(-)-albuterol > S(+)- albuterol
Hypnotics, Sedatives : hexobarbital, secobarbital, mephobarbital,	Ex: S(-)-secobarbital> R-(+)secobarbital
Anesthetics : Ketamine, isoflurane	Ex: S(+)-ketamine > R(-)-ketamine
Central-acting analgesic (μ-opiod receptors): Methadone	Ex: R(-)-methadone > S(+)-methadone
Analgesics, Anti-inflammatory drug (NSAID): Ibuprofen, ketoprofen,	Ex: S(+)-Ibuprofen > R(-)-Ibuprofen
Tranquilizers : 3-hydroxy-benzodiazepines : oxazepam, lorazepam, temazepam	Ex: S(+)-oxazepam > R(-)- oxazepam

Table 1.1 Comparison of isomer potency of racemic drugs. Main pharmacological drugs are listed on the table with isomer potency of representative drugs set as examples.

1.2 Cluster of chiral drug

In pharmacology, racemic drugs can be divided into three main groups according to their activities. The first and most common category is that of racemic

pharmaceuticals which have one major bioactive enantiomer, while the other is less active, inactive or toxic. The next class consists of enantiomers with equal activity and identical pharmacodynamics. Finally, the last category is made up of racemic drugs with one major bioactive enantiomer, but when in body the less active enantiomer could be metabolized into its bioactive enantiomer by chiral inversion [13] [14].

Group 1. Racemic drugs having one major bioactive enantiomer.

A number of cardiovascular drugs, agents which used for the therapy of hypertension, arrhythmias, heart failure belong to this group. These drugs include the β-adrenergic blocking agents, angiotensin converting enzyme inhibitors and calcium channel antagonists.

Group 2. Racemic drugs having equally bioactive enantiomers.

Only a small number of racemic drugs belong to this group such as antineoplastic (cyclophosphamide), antiarrhythmic (flecainide), antidepressant (fluoxetine).

Group 3. Racemic drugs having chiral inversion.

A number of nonsteroidal anti-inflammatory drugs (NSAIDs) like Ibuprofen, benoxaprophen, ketoprofen, fenprofen etc, belong to this group. Ibuprofen in this group is active and has an analgesic and anti-inflammatory effect. S-Ibuprofen is 100-fold more potent than the R-Ibuprofen as a cyclo-oxygenase I inhibitor. *In vivo*, the R-Ibuprofen can undergo chiral inversion to S-enantiomer by the action of hepatic enzymes [15, 16]. *In vivo* studies have demonstrated high plasma concentrations of

S-Ibuprofen after administration of the R-enantiomer. This inversion of Ibuprofen has been estimated to reach 57-71% of the dose [17].

1.3 Mechanism of representative chiral drug

Ibuprofen or 2-(4-isobutylphenyl) propanoic acid belongs to the third group of chiral drug that possesses analgesic and antipyretic properties [18]. Like acetylsaliscylic acid (aspirin), Ibuprofen works by inhibiting cyclooxygenases (COX) activity. These enzymes catalyze the synthesis of prostaglandins which have both positive and negative effects. For example, prostaglandins are effective blocking the development of stomach ulcers, but they can cause inflammation and pain response.

Human COX enzymes have three isoforms. Knowing each COX isoform respective functions is important for studying the therapeutic effects of Ibuprofen. Cox1 is present at near constant expression levels *in vivo* under all conditions, while the levels of Cox2 increase under inflammatory conditions. The newly identified Cox3, a splice variant of Cox1 mRNA, seems to be also involved in the effects of NSAID. Researchers suspect that the side effects of aspirin and Ibuprofen may arise from Cox1 enzyme inhibition, whereas the therapeutic benefits may be caused by the inducible Cox2 enzyme inhibition [19].

Ibuprofen and aspirin inhibit Cox1 and Cox2 via different mechanisms. Ibuprofen binds to COX enzymes non-covalently and competes with the enzyme's natural substrate. On the other hand, aspirin bind to a serine residue by a covalent bond in the COX enzyme. Acetaminophen cannot interact with either Cox1 or Cox2, but may interact with newly identified Cox3. It is an exciting area of pharmacology

for selective targeting of the COX enzymes, and challenges still exist for the development of drugs that can interact with specific COX enzymes [20]. Other studies have indicated that Ibuprofen may be useful in the prophylaxis of Alzheimer disease. However, the mechanism of this action remains unclear [21].

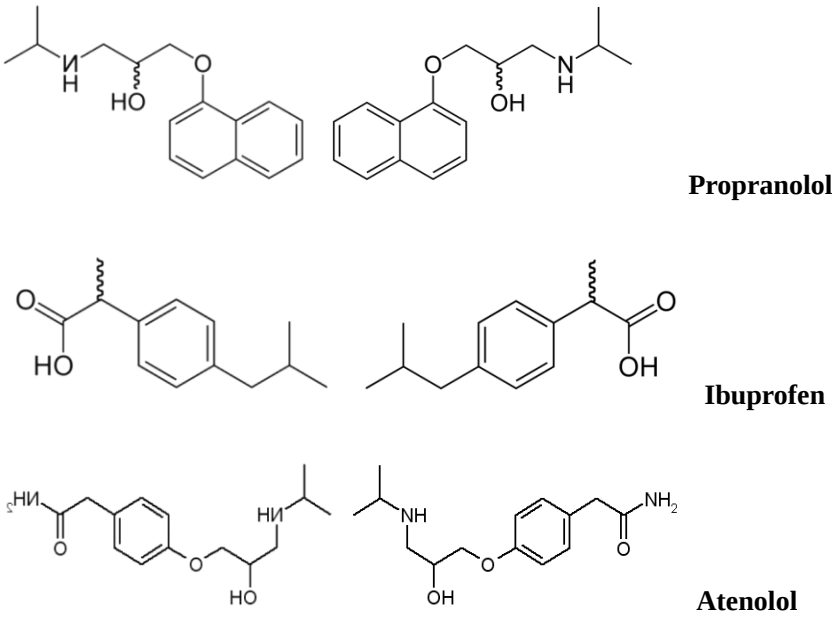

Figure 1.2 Chemical formulas of chiral Propranolol, Ibuprofen and Atenolol.

β-blockers (*β*-adrenoceptor antagonists) are compounds that bind to *β*-adrenoceptor, but compete with *β*-adrenergic agonists, and thus inhibit their physiological effects. The mechanism of action of *β*-blockers has been studied at gene expression level [22]. Propranolol and Atenolol (shown in Figure 1.2) are *β*-blockers belonging to Group 1 chiral drug. Propranolol is the first beta adrenergic receptor antagonist in clinical applying for the medical management of angina pectoris, and is

regarded as one of the most important contributions to the 20th century pharmacology [23]. Atenolol, a β_1 receptor specific antagonist, introduced in 1976, was developed as a replacement for propranolol in the treatment of hypertension [24]. Unlike Propranolol, Atenolol avoid various central nervous systems (CNS) side effects as it is unable to pass through the blood-brain barrier [25].

1.4 Toxicology

Enantiomers may result in stereoselective toxicity, since there are pharmacodynamic and pharmacokinetic differences between enantiomers. The different toxic effects of chiral drugs can be from either one enantiomer or both [26, 27].

Toxicity resides exclusively in distomer of some chiral drug such as ketamine, penicillamine, ethambutol [27, 28]. The levodopa (L-3,4-dihydroxyphenylalanine racemic mixture was used to treat for Parkinson's disease but it was quickly found that its D-enantiomer causes unacceptable toxicity in patients. Subsequently, the unichiral levodopa was developed in L-form [29]. Some racemic drugs were stopped to clinical use due to chiral toxicity, such as tocainide (the antiarrhythmic agent) and benoxaprofen (the analgesic and anti-inflammatory drug) [30]. However, it does not mean that unichiral drugs are always preferred over racemic drugs, since in some cases the unichiral form could be less safe than its corresponding racemic mixture, such as labetalol [31] and sotalol [9]. The reasons of this phenomenon may be that stereoisomers have direct pharmacodynamic or pharmacokinetic competition/interaction, and this competition/interaction results in one stereoisomer

toxicity reduced by the other, such as labetalol, or one stereoisomer specific protective effect in the racemic mixture [32].

1.5 Pharmacokinetics and metabolism

The biological effect of the drug is affected by the processes of digestion, distribution, metabolism and elimination. The potential for enantiomers discrimination at every stage is therefore important, and stereo-pharmacokinetic studies and stereospecific drug assays are needed in every step of procedure [33].

Numerous studies have demonstrated that stereoisomers of some chiral drug quantitatively and qualitatively display differences in their pharmacokinetic and metabolic profiles [34]. For example, many antiarrhythmic drugs such as disopyramide, flecainide, encainide, mexiletine, propafenone, etc are marketed as racemates. Their distribution, metabolism and excretion profiles, however, usually favor one enantiomer.

Most chiral drugs belonging to β-blockers have different pharmacokinetic profiles. The pharmacokinetic profile of propranolol and its sulfate and glucuronide metabolites showed that the S/R ratio was about 1.4 fold in serum and urine, 2 fold for the sulfate conjugate and 3 fold for the major glucuronide metabolite in human serum and urine. In most cases a modest degree of stereoselectivity is shown in the β-blockers enantiomers. However, in certain cases for some drugs the enantiomers concentration relative dose in plasma varied. Furthermore, other factors such as dosing rate, enantiomer-enantiomer interaction of drugs, patients heart function, race and metabolic phenotype also affect the β-blockers stereospecific pharmacokinetics

and pharmacodynamics [35-37].

Research on the development of chiral drugs enables the discovery of the merits and pitfalls of unichiral agents versus racemic mixtures as new drugs [38]. A great deal of evidence accumulated prefers unichiral drugs instead of a mixture of stereoisomers. This is because the unichiral drug as a single agent is easy to study with respect to the therapeutic and toxic effects, pharmacokinetic properties as well as its efficacy dependency on its plasma concentration. Other advantages of using a unichiral drug over a racemate may include reduced drug dosage, prevention of racemic drug interactions and reduced drug toxicity. However, this is a complex issue and each drug must be reviewed by its own merits.

1.6 Neuroprotective effects of chiral Ibuprofen

Alzheimer disease (AD) is a neurodegenerative disease characterized by progressive cognitive deterioration and declining activities of daily living. Abundant evidences now show that neuroinflammation contributes to the pathogenesis of several neurodegenerative disorders, including AD [39, 40]. In addition to the analysis in transgenic mouse with AD, clinical trial data have shown that NSAIDs may have protective effects against the onset of AD [41-43].

Ibuprofen is a member of the proprionic acid group of NSAIDs. Some studies have indicated that S-Ibuprofen can be useful in the prophylaxis of AD. However, the mechanism of action remains unclear [21]. In order to investigate the mechanism of S-enantiomer Ibuprofen effects on AD, S-enantiomer and R-enantiomer of Ibuprofen were used and their protein profiles were compared in our study. The particular

proteins expression affected by S-enantiomer may play important roles in AD therapy.

1.7 Anti-angiogenesis effects of chiral Ibuprofen

Angiogenesis, new blood vessel formation, occurs in the liver of patients infected with hepatitis B or C virus. Most chronic liver diseases leads to an angiogenic switch, causes the upregulation of vascular endothelial growth factor (VEGF) among other proangiogenic factors, and finally results in the formation of new blood vessels [44]. In patients with chronic viral hepatitis, a significant change in the vascular architecture takes place with neovascularization, suggesting that angiogenesis could contribute to the increased risk of HCC in patients with HBV or HCV chronic infection [45].

Recent studies have indicated that NSAIDs as Cox2 inhibitors might be an effective approach to colorectal cancer prevention [46]. Rothwell et al. reported that high-dose aspirin (≥500 mg daily) reduces long-term incidence of colorectal cancer [47]. Yao group showed fewer occurrences of liver cancer metastasis in individuals taking NSAIDs, which presumably reduce the risk of liver cancer at least in part by inhibiting Cox. Ibuprofen has activity on tumor metastasis inhibition, at least in part, by modulating tumor angiogenesis in the colorectal cancer mouse model [48].

The enantiomers of chiral Ibuprofen may differ in the way they biologically participate in cancer prevention. In our study, 2D LC/MS proteomics was used to find target proteins of chiral Ibuprofen in HepG2 cells, and the efficacy of R and S Ibuprofen for HCC angiogenesis inhibition was investigated.

At present, there is considerable progress in the research of chiral drug, although it is still at the very initial stages of development. Chiral drug study is improving at an accelerated speed with advanced biotechnology development, especially with the

wide use of LC/MS application in the drug industry. Proteomics based on LC/MS is a fast developing research field which can be applied in exploring the effects of chiral drug on diseases therapy.

1.8 LC/MS technology development

HPLC and mass spectrometry have advanced greatly in recent years. At present, HPLC is commonly used on molecules separation, and mass spectrometry is a fairly routine tool which has been applied for molecular weight determination and for complex structure identification. LC/MS has become a useful tool and a highly productive analysis platform for drug development. The reasons are: (1) technological advances in the LC/MS interface, (2) improved HPLC and mass spectrometer performance, and (3) an increased need for rapid, high-throughput analysis of trace mixtures. The basic structure of the LC/MS equipment is shown in Figure 1.3. In the following sections, HPLC and mass spectrometry improvements are introduced one by one.

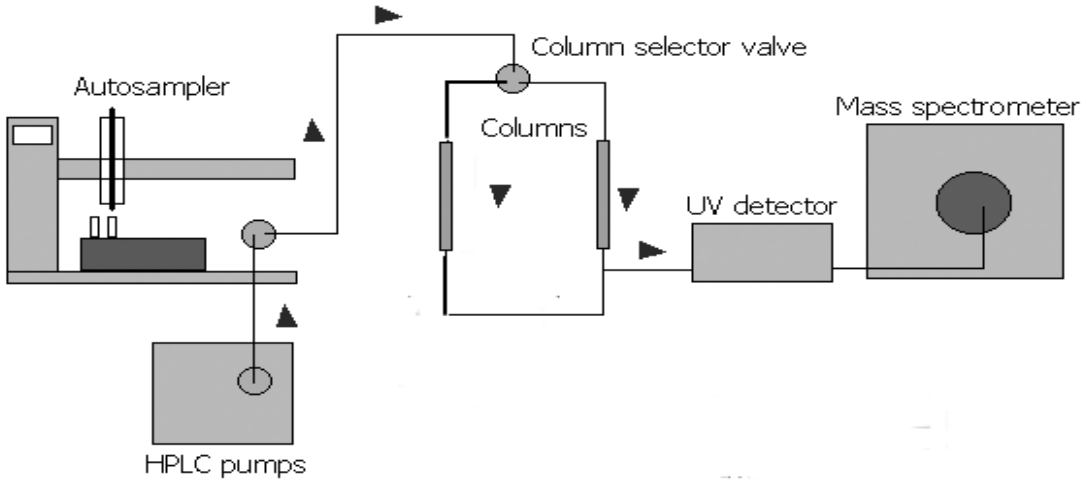

Figure 1.3 Schematic diagram of HPLC/MS machine. Samples are pumped into HPLC by autosampler, separated through columns, and then detected by mass spectrometer.

1.8.1 HPLC optimization for LC/MS analysis

1.8.1.1 HPLC column optimization

The column where the analytes separation occurs is the most important part of the HPLC system. The different types of HPLC columns are listed on Table 1.2.

Types of column	Characters or application
Normal-Phase Columns	They are usually packed in nonhydrated form, with nonpolar mobile phases, enabling the more nonpolar compounds to be washed out of the column first.
Other Bonded-Phase Silica Columns	Enantiomeric–silica and poly columns are designed to resolve mixtures containing optical isomers. Zirconium Bonded-Phase Columns can be used at a wide pH range
Reverse-Phase Column	Reverse-phase column used with a polar mobile phase supplies a nonpolar bound phase. The most polar sample components should come off first from reverse phase column, since the nonpolar compounds retain on the nonpolar column packing.
Ion-Exchange Columns	These columns work under a high salt concentration condition, where a salt gradient elutes the retained ionized material from the column.
Size-Separation Columns	Columns separate analytes based on their size.

Table 1.2 Specific designed columns for different application. Commonly used columns are listed, and their characteristics and application are introduced.

Development of columns accelerates the LC/MS techniques application, since operating a mass spectrometer requires extremely small amounts of material for analysis and at very high vacuum condition. Large volumes of solvent tend to overwhelm and complicate the analysis. It is therefore an incentive to develop

microflow HPLC systems that would use very thin, high-resolution HPLC columns. Nano-LC/MS and ultra-high pressure liquid chromatography (UHPLC) has been developed for molecular-level separation. The use of small particle HPLC packing column and the corresponding UHPLC provides great benefits in reducing chromatographic time with minimum sacrifice in resolution [49]. With these characters, nano-LC/MS has been developed for proteomics study [50].

1. 8.1.2 Pump and mobile phase optimization for LC separation

HPLC pump system is also modified for the purpose of separation. A cheap single isocratic pump system is capable of pumping a constant mobile phase. The complex mixtures of compounds which are poorly separated under single isocratic systems can be resolved by gradient solvent chromatography. Gradient chromatography allows compounds separations that cannot be achieved with a simple mobile phase and allows washing out of late-running peaks.

Acidification of the mobile phase with formic acid gives additional benefit of maintaining a reasonably high retention factor for the analyte [51]. The compounds of a water/acetonitrile mobile phase give only a weak electrospray ionization (ESI) response in the positive ion mode. In contrast, the same compounds in a water/methanol mobile phase can give a significantly higher response, approximately 25-fold, with formic acid and/or ammonium acetate [52].

Automated methods have been developed for molecules separation. A gradient HPLC system under advanced computer control can be equipped with an autosampler, and the system can be programmed to inject the samples under a variety of gradient

conditions.

1.8.2 Mass Spectrometry optimization for LC/MS analysis

1. 8.2.1 Ionization

Mass spectrometry technique is based on the production of ions and detection according to their mass-to-charge (*m/z*) ratio. The target compounds separated by HPLC need to be ionized in an interface between HPLC and MS so that they can be drawn into the mass spectrometer analyzer. Applications and methods are typically defined by the ionization method of choice [53]. For examples, electron ionization (EI) mass spectra derived from EI ionization are highly reproducible. Extensive collections of standardized EI mass spectra are available for on-line computer evaluation. An important limitation of EI is the necessity to present the analyte as vapour, which excludes the use of EI in the study of nonvolatile and thermally labile compounds. MALDI (maser-assisted laser desorption and ionization) is a robotically controlled spotter plate system for collecting samples from the HPLC, and then the collected samples are injected into a time-of-flight mass spectrometer. MALDI is one of the most important ionization techniques in the MS analysis of biomacromolecules. The methods of ionization are classed in Table 1.3.

Types of ionization	Principles of ionization
Electron ionization (EI)	The analyte vapour is subjected to a bombardment by energetic electrons. EI is performed in a high-vacuum ion source; and intermolecular collisions are avoided in this way.
Chemical ionization (CI)	Chemical ionization having positive CI and negative CI is one of the most versatile ionization techniques as it relies on chemical reactions in the gas phase. It is based on ion-molecule reactions between reagent-gas ions and the analyte molecules.
Electron-capture negative ionization (ECNI)	An alternative procedure for the production of negative ions is electron-capture negative ionization.
Energy-sudden or desorption ionization	A wide variety of desorption ionization methods is available: desorption chemical ionization (DCI), secondary-ion mass spectrometry (SIMS), fast-atom bombardment (FAB), liquid-SIMS, plasma desorption (PD), matrix-assisted laser desorption ionization (MALDI), and field desorption (FD).

Table 1.3 Types of LC/MS ionization.

1. 8.2.2 LC/MS interface

The LC/MS interface is the connection between the HPLC and mass spectrometer. The samples are ionized and the solvent removed while entering into the high-vacuum environment of the mass spectrometer analyzer. Generally MS interfaces are classified as either electrospray interface (ESI), atmospheric-pressure chemical ionization spay interface (APCI) or ion spray interface (IS).

The atmospheric pressure chemical ionization (APCI) LC/ MS analysis is usually applied for small drug molecules [53], while the ESI+LC/MS analysis for big biomolecules. Atmospheric pressure photo ionization (APPI) serves as a complement to the more established ESI and APCI techniques by expanding the range of compounds to be analyzed [54]. The electron capture APCI (EC-APCI) technique has been shown to increase ion detection sensitivity by 2 orders of magnitude for a number of compounds, compared with conventional APCI [55, 56].

Electrospray interface is usually used with highly polar and ionized materials. It is a very soft ionization method that results in little fragmentation. The nanospray interface is an electrospray interface optimized for use with microflow HPLC systems.

Ion spray interface is most commonly used to determine the molecular-weight through producing intact molecular ions. However ion repeller can sometimes cause molecule fragmentation which can be used to provide preliminary compound and structural information.

Either ESI or IS interfaces can serve as the start point for tandem mass spectrometers. The tandem mass separates elution ions in the first mass spectrometer, and subsequently the ions fragmented and separated to form daughter ions that are analyzed in the second MS.

An emerging technique called high-field asymmetric waveform ion mobility spectrometry (FAIMS) has been designed to reduce chemical noise. FAIMS separation technique is based on the differences in ion mobility at high versus low

electric fields, and the separation takes place in an atmospheric pressure gas-phase environment. The FAIMS device is located between the ion source and the orifice [57], [58].

1. 8.2.3 LC/MS analyzer

There are four basic types of LC/MS analyzers that are commonly used for molecules identification. The first is the *quadrupole* or the *octapole analyzer.* The quadrupole or octapole are composed of a bundle of oppositely charged rods swept with radio frequencies, which separate and focus ions from the injector on the detector. The second system is either a three-dimensional spherical or a quadrupole *ion trap*. Ion traps contain and release ions from the trap to the ion detector as the radio frequency changes. The third type is the time-of-flight tube (TOF). TOF increases ions separation efficiency by focusing them on its detector. The fourth system is the Fourier Transform mass spectrometry, also called as Fourier transform ion cyclotron resonance mass spectrometry, which is a mass analyzer for determining the mass-to-charge ratio (m/z) of ions based on the cyclotron frequency of the ions in a fixed magnetic field [59]. Fourier Transform mass spectrometry has a trapping volume that is bombarded with a full-frequency radio signal. The full frequency radio promotes ions to a higher-energy state and collapses later, the collapses ions produce modified all-frequency signals that are detected and analyzed by *Fourier transform* software.

MS/MS hybrid analyzers are combinations of one or all of these mass spectrometer analyzers. A combination multiple mass spectrometer analyzers is used

to fragment, separate, and detect the daughter ions of the original molecular ion, by which the compound can be identified.

1. 8.2.4 LC/MS software

For the analysis of LC/MS results, data analysis software is used to interpret and extract information from MS datasets. Molecules corresponding to MS detected masses are next identified after MS database searches to identify peptides or chemicals are performed. The role of software is becoming more important in integrating key analysis, including sample preparation, real-time examination and the distribution of results [60]. At present, the standard libraries of mass spectral data that are commonly used include Swiss-prot, NIST and Wiley et al.

Current limitations of the LC/MS technique lie primarily in the separation speed, peak resolution, data analysis and cost. Simplified library searching for MS/MS fragment library identification will help develop LC/MS technique.

1.9 Application areas for LC/MS

With the development of LC/MS techniques, the requirements on fast analysis and the rapid turn-around of results have generated immense challenges and opportunity [60].

The first main area of LC/MS application is compound discovery and identification in pharmaceutical manufacturing. LC/MS methods are applicable to analyze a wide range of interest compounds having pharmaceutical potential, as these methods have powerful analytical merits (sensitivity, selectivity, speed of analysis and cost effectiveness). LC/MS can be used not only to confirm the structure of the final

product and its impurities, but also to study precursor purity, intermediate compounds in the synthesis pathway, and the completeness of the conversion.

There are a series review and books discuss this area [61]. Some studies used LC/MS techniques for chiral drug investigation, for example, using LC/MS to determine molindone enantiomers [62]. Reddy et al. applied HPLC/LC/MS methods to study enzymatic chiral inversion of compounds which are structurally similar to Ibuprofen [63]. Quantitative LC/APCI-MS/MS method was set up for the stereoselective analysis of torcetrapib (TTB) enantiomers, such as TTB enantiomers [(+)-TTB and (-)-TTB] [64].

The second application area is on macromolecular investigation such as special proteins or protein profile *proteomics*. The pharmacokinetic mechanism of special macromolecular protein can be studied with LC/MS tool applied. Some studies used LC/MS for the analysis of specific proteins from complex biological samples. Chang's group developed a LC–MS/MS method for the quantitation of a large peptide, T-20 and its metabolite in human plasma. The method was developed and used for analyzing pharmacokinetic profiles and metabolite of samples treated by the HIV fusion inhibitor peptide drug [65]. Lin's study described a LC–MS/MS method for the determination of levovirin in rat and Cynomolgus monkey plasma, and the assay was validated and used in pharmacokinetic studies in rats and monkeys [66].

Advances in LC/MS separation and bioinformatics for large scale data analysis in MS-based proteomics have made MS technologies an indispensable research tool for protein profile study. Among two dimensional gel-electrophoresis, antibody-based

protein microarrays and LC/MS based proteomics, LC-MS or tandem MS technologies offers highly sensitive protein detection capabilities [67]. Integrated LC/MS workstations have been developed enabling autosampler injection and providing automated database searching [68]. Among of various LC/MS combinations, the most advanced LC/MS uses ultra-high pressure capillary LC combined with Fourier transform ion cyclotron resonance mass spectrometry (FTICR). The use of FTICR has advantages over conventional MS platforms, including greater confidence in protein identification and enhanced sensitivity for low abundance proteins [69].

The third area of LC/MS application is in metabolite and trace contaminates studies. Application of hybrid LC/MS/MS systems for studying fragmentation can help identify unknown components, making these systems ideal for metabolite analysis.

Metabolomics is the systematic study of their small molecule metabolite profiles. The metabolome is the large scale collection of all the small molecule metabolites including metabolic intermediates, hormones and other signaling molecules, and secondary metabolites, which are found within biological samples [70]. A series reviews have discussed the LC/MS application on metabolomics [71-73].

Various analytical techniques for analyzing global metabolite profiling, such as 1H NMR, MS, HPLC-MS, and GC-MS, have been used in metabolomics study. None of these is the perfect tool for the global metabolite-profiling study.

1.10 Application of mass spectrometry-based proteomics

The term 'proteome' was first introduced by Wilkins et al in 1996 [74], referring to the complete determination of proteins expressed in a given cell, tissue or organism. The study of proteomics is often considered complementary to the genomics studying of biological systems. However, proteomics provides more useful information about an organism than genomics, as cellular functions are more closely related to proteins than to genes.

The study of proteomics first requires the protein be resolved. One of the approaches here is two-dimensional gel electrophoresis (2-DE). Expressed proteins of interest selected from 2-DE results are defined, excised and cleaved into peptides by using proteolytic enzyme such as trypsin. The peptide digests are then identified by MS, for example using MALDI. However, this gel-based separation has limitations in identifying low abundance proteins and low resolution proteins. As a result, an alternative approach involving the use of liquid-based techniques including HPLC and capillary electrophoresis has gradually substituted the gel-based separation to meet the increasing demand for resolving of the high degree of complexity of cellular proteomes and detecting low abundance of many of the proteins. In this LC-based technique, the mixture of the cleaved peptides are bonded, separated sequentially on the multi-dimensional columns based on charge or hydrophobicity of the ionized analytes, and then eluted into the MS for identification [75]. Using C. elegans model, Takahashi et al. showed that most proteins could be detected using the LC/MS technique. The most acidic protein identified has a pI 3.48, while the most basic one

has a pI 12.41. The smallest gene product detected has a MW 6.0 kDa and the largest one has a MW 1369 kDa [76].

LC/MS has become the technique of choice for proteomics study for the separation and identification of the polypeptides. On-line libraries of information and sequence structures of polypeptides are now available to aid in efficient identification of the peptide sequences. Published articles summarize and discuss the LC/MS technique development and applications for proteomics. Shen research group discussed the advances and limitations of LC/MS proteome analysis for biomarker discovery, including quantitative proteomics, deep proteome profiling, and phosphoproteome profiling [77]. Another review summarized recent advances in LC-MS-based proteomics profiling and its applications in clinical proteomics, as well as discussed the challenges of more effective candidate biomarker discovery using these technologies [67]. In a review, Tannu et al. examined techniques using two-dimensional gel electrophoresis as well as multi-dimensional LC followed by MS for subcellular organelle isolation, protein fractionation and separation. Methods including Two-Dimensional Difference Gel Electrophoresis (2D-DIGE), isotope-coded affinity tag (ICAT) and isobaric tag for relative and absolute quantitation (iTRAQ) were compared for quantifying relative protein profiles among samples, and an overview evaluation of these techniques has been published [78].

1.10.1 Quantitative proteomics by LC/MS

Generally two or more unique peptides are usually sufficient to recognize a protein. If quantitative information is provided, the degree of proteins expression

induced by perturbation of a biological system can be detected. Therefore, quantitative proteomics data for modeling is increasingly required in biological investigations. For this purpose the technique of stable-isotope labeling has been widely adopted. The underlying principles are that: due to the mass difference resulted from the introduction of individual stable isotope, the amount ratio for the isotopic analytes can be directly determined.

Several methods have been developed for stable isotope-based quantification in proteomics and these methods are classified based on the ways that stable isotope labels are introduced into the peptide or protein. The classification includes (i) spiking an isotopically labeled peptide by chemically synthesized as internal standards with known quantities [79], (ii) incorporating through an enzyme via transfer of ^{18}O from water to peptides during protein digestion [80, 81], (iii) introducing isotope-tagging chemicals onto peptides or proteins and (iv) metabolic incorporation of the stable isotope to the cells, particularly stable isotope labeling by amino acids in cell culture, in which amino acids containing stable isotopes are supplied in growth media, thereby one cell state is metabolically labeled by, for example, ^{13}C-labelled arginine [82]. Among the developed stable isotope-based quantification methods, iTRAQ has recently gained popularity as its simple iTRAQ labeling procedures and up to four labeled samples examined in a single experiment. The principle of iTRAQ labeling is shown in Figure 1.4, and the quantification of the amount of peptides shown in Figure 1.5. In this thesis, iTRAQ LC/MS was applied on studying biological effects of chiral Ibuprofen.

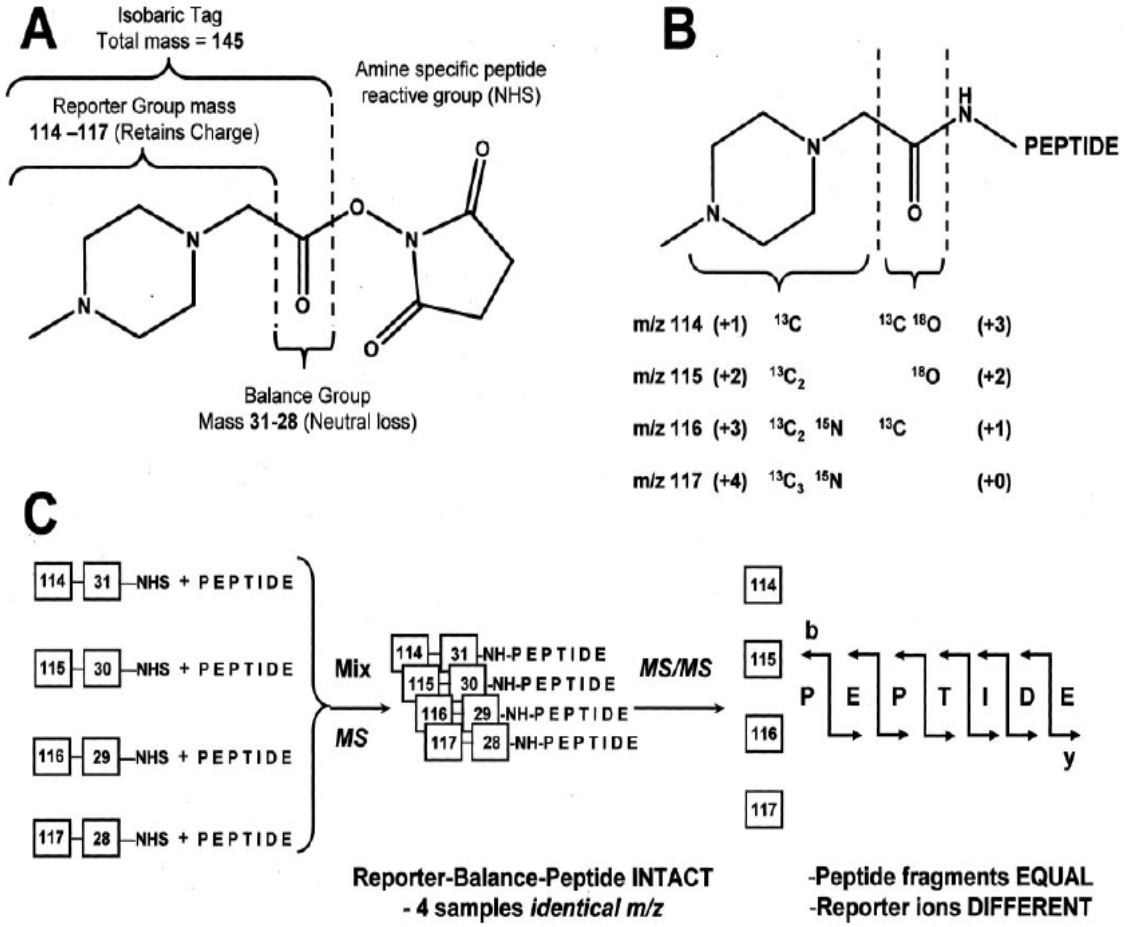

Figure 1.4 Components of the multiplexed isobaric tagging chemistry. Isobaric tag (mass 145) is composed of reporter group (mass 114-117), balance group (mass 31-20) and peptide reaction group. Its chemical structure is shown in A); B) reporter group and balance group have different atom isotope combination so that isobaric tags have same molecular weight with different molecular weight reporter group; C) different isobaric tags labeled peptides have identical m/z in first MS, but in MS/MS broken isobaric tags provide different molecule weight reporter ions. (Adapted from: Ross, P., Huang, Y., et al. (2004) Multiplexed Protein Quantitation in Saccharomyces cerevisiae Using Amine-reactive Isobaric Tagging Reagents. *Mol. Cell.*

Proteomics 3, 1154-1169.)

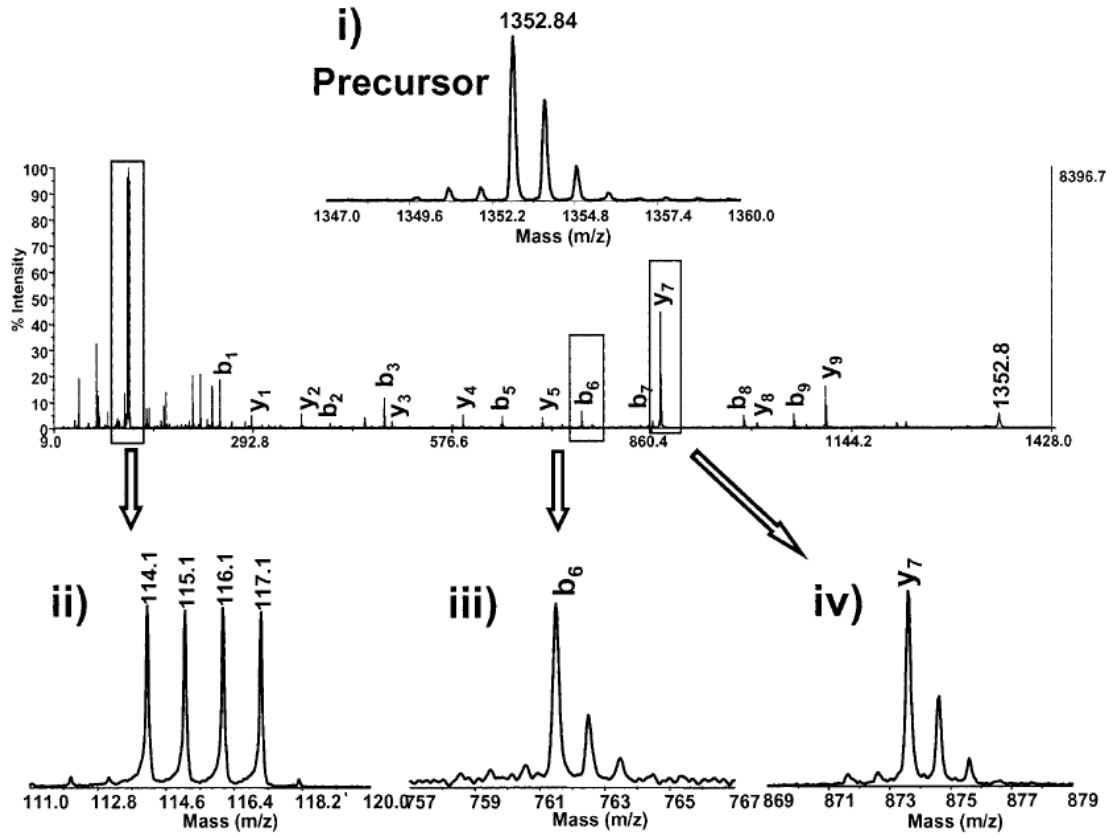

Figure 1.5 An example of MS/MS spectrum of peptide TPHPALTEAK. A peptide digest mixture was prepared by labeling four separate digests with each of the four isobaric reagents and combining the reaction mixtures in a 1:1:1:1 ratio. i) The isotopic precursor m/z 1352.84 was fragmented in MS/MS. (ii) Low mass region of MS/MS spectrums show reporter ions used for quantitation. (iii) Mass region of MS/MS spectrums display isotopic distribution of the b6 fragment, and (iv) isotopic distribution of the y7 fragment ion. (Adapted from: Ross, P., Huang, Y., et al. (2004) Multiplexed Protein Quantitation in Saccharomyces cerevisiae Using Amine-reactive Isobaric Tagging Reagents. *Mol. Cell. Proteomics* 3, 1154-1169.)

1.10.2 Functional studies of proteomics

Stable-isotope labeling and LC-MS/MS are used to identify clinically useful molecular patterns in cancer [83], heart disease [84], and other common ailments, to build up cellular signaling pathways in response to various stimuli through comparing normal and diseased conditions [85-88]. Goufman et al. documented that the thermostable fractions of serum samples from patients with ovarian, uterus, and breast cancers, as well as samples from benign ovarian tumor, were analyzed by mass spectrometry system. Among them, the expression of R-1 acid glycoprotein and clusterin has been found to be down-regulated in breast cancer, whereas that of transthyretin decreases specifically in ovarian cancer [89]. Huang group performed LC/MS proteomics method and reported that ATP synthase is up-regulated in tumor tissues and is present in the plasma membrane of breast cancer cells. When treated with ATP synthase inhibitor, aurovertin B, breast cancer cells exhibit a significant decrease in cell density, indicating that aurovertin B can be used as an antitumorigenic agent and may be exploited in cancer chemotherapy [90].

1.10.3 Protein interactions study of proteomics

Most proteins exert their function by binding to other proteins and these interaction partners may directly implicate the protein in a cellular process. To study this question by LC/MS, the protein itself is used as an affinity reagent. Compared with chip based and two-hybrid approaches, LC/MS-based proteomics strategy has the advantages that the fully processed and modified protein can act as the affinity

reagent to isolate its binding partners, that the interactions occur in the cellular location and native environment, and that multicomponent complexes can be isolated and examined in a single operation [91]. For example, to explore and understand the critical regulatory role of Nedd8 in cell proliferation and development, Jones et al. purified the proteins that are associated with Nedd8 from HEK293 cells stably expressing GST-Nedd8, and performed subsequent protein identification employing LC-MS/MS. A total of 496 proteins modified and associated with GST-Nedd8 were identified, providing clues on the biological role of Nedd8 and thus laying the foundation for an in-depth analysis of the regulation of the Nedd8 pathway [92]. Recently the MS-based approach to identify partners involved in tyrosine kinase receptor (TrkA) signaling in breast cancer cells has been reported. Wild type and modified TrkA constructs with green fluorescent protein were transfected in MCF-7 cells, and co-immunoprecipitated proteins were resolved by sodium dodecyl sulfate polyacrylamide gel electrophoresis (SDS-PAGE) before identification with nano-LC-MS/MS. Several TrkA putative signaling partners were identified among which was the DNA repair protein Ku70, which is increasingly reported for its role in cell survival and carcinogenesis [93].

1.10.4 Analysis of protein modifications with proteomics

Proteins are modified to their mature form through post-transcription modifications, which regulates biological function through a multitude of mechanisms. Specific mass spectrometric methods have been developed that can identify the peptides cleaved from a protein with the presence of a particular modification. Protein

modifications are determined by examining the measured mass and fragmentation spectra, comparing with the original ones via manual or computer-assisted interpretation. Although great efforts have been put to define modifications on a proteome-wide scale, at present it is obvious that scanning for proteome-wide modifications is not comprehensive, considering the fact that identifying all modifications is difficult even in a single protein.

Current research focuses on identifying one type of modification made on all the proteins present in a sample, in particular, phosphorylation. For example, McNulty et al. made full use of the strong hydrophilicity of the phosphate group to selectively trap and made fractionation of phosphopeptides based on their increased binding force under hydrophilic interaction chromatography (HILIC) conditions. The phosphopeptides from HILIC fractions were subsequently enriched on immobilized metal ion affinity chromatography (IMAC), showing better than 99% selectivity. In a 300-μg equivalent of HeLa cell lysate, over 1000 unique phosphorylation sites were identified and more than 700 novel sites have been added to the HeLa phosphoproteome [94].

1.10.5 LC-MS Analysis on protein or proteomics affected by chiral drug

Interaction between chiral drug and protein

Researches on the interactions between chiral drugs and cellular protein start firstly, and then similar researches are done for relationship between chiral drugs and cellular proteomics. Determination and characterizing interactions between chiral drug and biomolecules are important in many new scientific areas, from biochemistry,

pharmacology, to organic chemistry. Chiral recognition including the ubiquitous enzyme–substrate interaction plays a central role in various biological processes. Series methods about enzyme–substrate interactions have been developed.

Akira Kawamura group has demonstrated that it is possible to attain high protein-binding selectivity by the use of simple chemical probes containing benzophenone. The chirality center as well as the neighboring substituent in the vicinity of benzophenone plays a major role in the protein-binding selectivity. They set up a method in which chiral recognition processes can be examined in complex proteomes with a simple chemical strategy using photoactive probes [95].

A surface plasmon resonance (SPR) and HPLC perturbation method (HPLC-PM) have been used for a detailed investigation of enantioselective alprenolol and propranolol drug protein interactions. Arnell et al. studied the interaction of alprenolol and propranolol enantiomers with the protein Cel7a. It was found that the interactions with the enantioselective and nonselective binding sites are highly pH dependent. The chiral mechanism is affinity driven and there are large affinity differences between the two enantiomers, while the binding capacity difference has a smaller influence [96].

Some chiral drugs act on cell receptor, and studying the chiral drugs interaction with cell receptor will help to understand the molecular mechanism of chiral drug therapy. Li group examined the actions of the natural and unnatural forms of neuroactive steroids on the responses of ρ1 receptors using LC/MS. They confirmed that the enantiomers of the natural steroids are much less effective at either potentiating (3α5αP) or inhibiting (3α5βP) the activation of the ρ1 receptor. Their

results indicated that neurosteroids, and probably other steroids, act on the ρ1 receptor by interacting with a chiral site, probably on the receptor protein [97].

Protein profile of bio-organism treated by chiral drug

Chiral medicines can selectively interact with biological macromolecules through strict chiral recognition and demonstrate different pharmacokinetic characteristics and drug effects. Proteomics-based discovery for candidate target of chiral drug should gain significant attention due to the power of these technologies for analyzing complex protein mixtures and their potential for identifying novel therapeutic targets of chiral drugs. However, until now very few references about proteomics and chiral drugs have been published.

Sui et al. used a quadrupleplex iTRAQ to detect and quantify differences in protein expression levels in vascular smooth muscle cells treated with *S*- and *R*-enantiomer propranolol for understanding the reflect pharmacologic action of enantiomers. To identify proteins from a complex mixture, a 2D LC setup was applied. In this approach, a strong cation exchange (SCX) column was used for protein separation in the first dimension, while a reversed-phase (RP) column was used for protein separation in the second dimension, and separated peptides were then analyzed in ESI-MS/MS. The higher protein level of a number of enzymes involved in cellular anabolism and antioxidant activity were revealed by LC-MS/MS proteomics. The identification of anabolic metabolic enzymes in *S*-enantiomer incubated cells is in line with earlier clinical reports on the reversal of catabolism by propranolol treatment after severe burn [98], reduction of metabolic rate in patients

receiving propranolol [99], and increase in body fat which is considered as one of the side effects of propranolol treatment [100]. Furthermore, Sui et al. examined extracellular protein profiles of A7r5 cells in response to individual enantiomers of propranolol. Their results indicated that the *S*-enantiomer of propranolol is able to trigger the secretion of T-kininogen by A7r5 cells more than control cells or *R*-enantiomer of propranolol incubated ones [101].

The above researches demonstrated that proteomics approaches represent new strategies for a deeper investigation of chiral drugs and their biological characteristics, which might be significant to improve the development and rationalization of clinical administration of chiral drugs.

Proteomics, in particular quantitative proteomics, has been proved to probe most of the proteins in a sample, allowing scientists to distinguish pertinent changes from background proteins and therefore provides a better biological understanding of the follow-up of functional experiments. However specific challenges for quantitative proteomics still remain, in particular, the issues of quantitating low-level putative biomarkers in human body fluids and characterizing whole proteomes comprehensively need to be addressed. The issues to be addressed will require the advanced achievement through development of MS instrumentation and more intelligent algorithms and software. In the contemporary era, all scientific fields are developing rapidly; with the improvement on physics, mathematics, electronics and chemistry, the future LC/MS techniques will surely meet the biological scientists' special requirements.

1.11 Objectives of research project

The purpose of this thesis is to work out the protective mechanisms of chiral Ibuprofen on AD patients, and the mechanisms of chiral Ibuprofen inhibiting HCC angiogenesis. With referring literatures, both AD and HCC angiogenesis mechanisms are rather complicate, since many proteins and their interactions are related with these diseases. Proteomics, which has a major advantage of performing a high-throughput, large scale proteins investigation, was applied in this thesis, enabling the relationship between the disease-related proteins and chiral Ibuprofen to be outlined. Efficient therapy methods may be designed upon analyzing target proteins of chiral Ibuprofen. LC/MS proteomics, as noted previously has more desirable features than other proteomics techniques, such as protein detection range, online library database, automatic control system etc. In this thesis, LC/MS proteomics coupled with advanced protein labeling technique (iTRAQ), were applied in two research fields such as AD and HCC angiogenesis.

This thesis is composed of 7 chapters. Background information and current research related with this thesis are outlined in chapter 1. Materials and methods applied in the study are introduced in chapter 2. In chapter 3, we investigated the protein profile of neuroblastoma cells incubated separately with the two enantiomers of Ibuprofen using iTRAQ 2D LC-MS/MS. The results showed changes in expression levels of a number of enzymes in cells incubated with the *S*-enantiomer, involved in fatty acid synthesis and antioxidant activity. The changes suggested that S-Ibuprofen may offer protection for AD through reducing oxidation stress. In chapter 4, the

mechanism of HBV inducing angiogenesis was studied. 2D LC-MS/MS analysis was used to detect differentially expressed proteins in cells supporting HBV replication compared with those transfected with an empty vector. Enzymes associated with angiogenesis, namely fumarate hydratase and tryptophanyl-tRNA synthetase, were identified in HBV replicating RPHs and HepG2 cells. In chapter 5, we found that IL6 and Cox2 mRNA were upregualted in HepG2 cells with HBV replication. Ibuprofen as Cox2 inhibitor was investigated in HBV replication cells and HBx transfected cells. Our results showed that HBx-expressing cells induced Cox2 expression, while HBx-expressing cells inhibited Cox2 expression with Ibuprofen addition. The contrasting effect of HBx on Cox2 was found to be determined by differential dimers formation among the members of the NFκB family of proteins. In chapter 6, the conclusion for the thesis is included. Lastly, in chapter 7, future works is planned out.

Chapter Two

Materials and methods

2.1 Cell culture

All cell lines used for tissue culture were obtained from the American Type Cell Culture Collection (ATCC) unless otherwise specified.

HepG2, a human Hepatocellular carcinoma cell line, was cultured in Dulbecco's Minimum Essential Medium (DMEM) (GibcoBRL) supplemented with 10% heat-inactivated Fetal Bovine Serum (FBS) (GibcoBRL) and 1% Penicillin-Streptomycin (Life technologies). The CRL-2273 neuroblastoma were maintained in monolayer culture in (DMEM-F12) Dulbecco's modified Eagle medium-Ham's nutrient medium mixture with F-12 medium (GibcoBRL) in ratio 1:1, supplemented with 10% FBS.

Human umbilical vein endothelial cells (HUVECs) were cultured in CSC medium (Cell system), supplemented with 10% FBS. The isolated rat primary hepatocytes (RPHs) were culture in HBM medium (Clonetics), supplemented with 10% FBS.

All cells were cultured in a humidified 37^{o}C 5% CO_2 incubator (Shel lab). The cells were maintained through subcultures at a ratio of 1:3. Subculturing of cells was carried out using 0.25% trypsin-EDTA (life technologies). Briefly, at confluence, the medium was discarded and the adherent cell monolayer was gently washed twice with warm sterile phosphate-buffered saline (PBS, 8 g/L NaCL, 1.44 g/L Na_2HPO_4, 0.24 g/L KH_2PO_4, pH 7.4). After aspiration PBS completely, appropriate amounts of 0.25%

trypsin-EDTA was added to the cell monolayer, and cells were incubated in 37^{o}C incubator until most of the cells became detached. Cells were neutralized in 5 ml complete media and centrifuged for 5 minutes at 1000 rpm at 4℃ using a refrigerated bench top centrifuge (Sigma). The cell pellet was then resuspended in appropriate medium and divided into individual tissue culturewares.

For cryopreservation of the cells, cells were trypsinized and pelleted as above. Then resuspended cells were aliquoted into 2 mL plastic cryogenic vial (IWAKI, Japan) and tissue culture grade dimethylsulphoxide (DMSO) (Sigma, USA) was added to a final concentration of 10%. The cryovials were put into freezer overnight at -80℃ and transferred and stored in -150℃ freezer (Sanyo, Japan) on the next day.

2.2 Determination of cell number

2.2.1 Manual counting

Cells were counted in an improved Neubauer hemacytometer (Baxter Scientific, Germany). After trypsinization and centrifugation, the cells were resuspended in medium or PBS to form a uniform suspension. A clean cover glass was centered over the hemacytometer chambers. Appropriate dilutions of the cell suspension were loaded on one chamber using a micropipette. Excess liquid was blotted off and the cells were allowed to settle on the slide for 30 seconds. The number of cells in each of the four corner and central squares was counted under an inverted microscope (Olympus) under a 100X magnification using a hand-held counter. The number of cells per millimeter and total cell number were determined using the following calculations:

$$\text{cells / ml} = \text{cells counted} \times 10^4 \times \text{dilution factor} \div \text{squares counted}$$

$$\text{total cells number} = \text{cells / ml} \times \text{volumn of original cell suspension}$$

2.2.2 Automatic counting

Alternatively, cells can be counted by using NucleoCounter (Chemometec, Denmark). Briefly, as the machine manual instruction, an appropriate volume of cell solution was mixed with equal volume of reagent A. After vortex, same volume of lysis buffer B was added to the solution and mixed well. When the purpose of the measurement was to measure the number of non-viable cells, this step was omitted. Approximately 50 ul of the sample mixture was loaded into the NucleoCassette (Chemometec, Denmark). The NucleoCassette was then analysed in the NucleoCounter Instrument. The estimation of the cell number per ml would appear on the screen after 30 seconds. The actual cell number in the original sample solution was three times the number shown on the screen.

2.3 Routine techniques

2.3.1 Preparation of LB medium and Agar plates

LB (Luria-Bertani) media were prepared by mixing 10 g Bacto-tryptone (Difco, USA); 5 g yeast extract (Difco, USA), 10 g NaCl (Merck, Germany) and the volume was adjusted to 1 liter with distilled H_2O. The media were sterilized by autoclaving.

Super Optimal Broth (SOB) medium was made by mixing 20 g Bacto-tryptone, 5 g yeast extract, 0.5 g NaCl, 2.03 g $MgCl_2 \cdot 6H_2O$ and 2.46 g $MgSO_4 \cdot 7\ H_2O$. SOB medium without Mg^{2+} was prepared and followed by adjusting pH to 6.8-7.0 and

autoclaving. A filtered 2 M stock of Mg^{2+} (1M $MgCl_2$ and 1 M $MgSO_4$) was added to a final Mg^{2+} concentration of 20mM.

To make LB/Amp medium, LB was cooled in a 55℃ water bath after autoclaving and Ampicillin (Sigma, USA) was added to the medium to a final concentration of 100 μg/ml.

The LB/ Amp Agar plate was prepared by adding 1.5% agar to LB medium. After autoclaving, 100 μg/ml Ampicillin was added to the medium. The LB/Agar/AMP plates were poured and stored.

2.3.2 Preparation of *E. coli* competent cells

E. coli competent cells (DH5α, JM109) were prepared as described by biological manual with some modifications. Briefly, frozen stock *E. coli* cells were thawed, streaked on an LB/Agar plate, and cultured overnight at 37°C. About one to two colonies were inoculated into 2 ml SOB medium in culture tube, and grown 10 hours at 37°C with vigorous shaking at 250 rpm. After that, 300 μl cell suspension was inoculated into 100 ml SOB medium in a 1-liter flask, and grown to an A_{600} of 0.6 at room temperature with shaking at 250 rpm. Normally, 15-20 hours was required to reach A_{600} of 0.6. The culture was transferred to two 50 ml Falcon tubes and placed on ice for 10 minutes before centrifugation at 4,000 rpm in a centrifuge (Sigma, USA) for 5 minutes at 4°C. The pellet was then resuspended in 20 ml of ice-cold TB (10 mM Pipe; 55mM $Mncl_2$; 15 mM $Cacl_2$; 250 mM KCl, pH 6.7), incubated on ice for 10 minutes and followed by spinning down as above. The cell pellet was gently resuspended in 4 ml of TB, and DMSO (Sigma, USA) was added with gentle swirling

to a final concentration of 7%. The cell suspension was dispensed by 100µl into freezing microcentrifuge tubes and immediately chilled by immersion in liquid nitrogen. The aliquots were stored at -80^{o}C and could be used for up to one year.

2.3.3 Polymerase chain reaction (PCR)

The PCR was carried out using 0.5 or 0.2 ml thin wall PCR tubes. The samples were prepared in a dedicated vertical laminar airflow cabinet with U. V. sterilization (Syngene) using dedicated pipetors (eppendorf) and filter pipette tips (Axygen). Normally, the PCR reaction was using Taq DNA polymerase and the reaction mix was prepared in a total volume of 50 µl including 1 X reaction buffer (Promega), 0.2 mM of each dNTP, 1.5 mM $MgCl_2$, 0.1 µM each forward and reverse primer, 5 unit Taq polymerase (5 unit/µl, Promega), 1-2 µl cDNA or DNA template (~500ng) and nuclease free water.

The PCR reactions were performed on Biometra® *Tpersonal* thermocycler (Biometra, Germany) by initial heating at 94℃ for 4 minutes. The amplification phase involved heating at 94℃ for 30 sec, annealing for 1 minute at primer specific temperature and extension at 72℃ for 2 minutes for 30 cycles, followed by a final extension of 10 minutes at 72℃. After completion of reaction, the products were either removed for further analysis or held at 4℃ until used.

2.3.4 DNA gel electrophoresis

A 1% analytical grade agarose (Promega, USA) in 1×TAE (40 mM Tris-Acetate and 1mM EDTA) buffer was melted by microwave oven. After the agarose solution completely dissolved, the gel was from microwave oven. When agarose gel cooled

down to around 60℃ in room temperature, Ethidium bromide (Amersham, USA) was added in order to visualize the DNA fragment under UV light. Agarose gel was put into prepared tray to wait gel solidification in room temperature. The molecular makers are 1kb DNA ladder (life Technologies, USA) and 100 bp DNA ladder (Promega, USA). After gel electrophoresis, the gel was placed on UV-transilluminator (Hoefer, USA), and the fluorescent ethidium bromide-stained DNA separation pattern was scanned and recorded by a picture using gel documentation system (Syngene).

2.3.5 Gel extraction

DNA fragments were separated according to DNA size by DNA agarose gel electrophoresis. The interested bands were cut from agarose gel during bands visualized by ethidium bromide staining under UV light. QIAquick Gel purification kit (Qiagen, USA) was used for extraction DNA from agarose gel by the manual introductions. Briefly, agarose slice was added buffer QG at ratio 1:3 (weight: volume), and incubated in 50℃ until gel completely dissolved. 1 volume isopropanol proportion to agarose slice was added to the mixture. The mixture was transferred to QIAquick spin column, and was then centrifuged at 13000 rpm for 1 minute, discarding flow-through. 750 μL buffer PE was added to spin column, and was centrifuged at 13000 rpm for 1 minute, discarding flow-through. 30 μL buffer EB (10mM Tris-Cl, PH 8.5) was added to the spin column, and stayed 1 minute. A new collection tube was added to column, and centrifuge 13000 rpm for 1 minute. The eluted DNA solution was collected and kept at -20℃.

2.3.6 Ligation

Before doing DNA ligation reactions, the size of DNA fragment should be known, and the concentration of DNA fragment should be calculated. The ratio of amount of DNA fragment to vector in ligation reaction is generally 3 to 1. The suitable buffer and T4 ligase was added to reaction mixture, and incubated in 4℃ for overnight.

2.3.7 Transformation

After ligation reaction, the ligation mixture was centrifuged at 14000 rpm for 1 minute. The appropriated amount DNA was mixed with 50 μL competent cell *Ecoli* stain *DH5α* in a microcentrifuge tube. The tube was stored on ice for 15 minutes, and transferred to waterbath of 42℃ for 90 seconds and returned to ice immediately for 2 minutes.450 μL SOC medium was added and incubated at 37℃ with shaking at 250 rpm for 1 hour.

Fresh X-gal/Isopropyl-β-D-thio-galactoside (IPTG) plates were needed to culture the bacterial. For fresh X-gal/IPTG plated preparation, LB/amp agar plate (1% Trytone, 0.5% yeast extract, 171mM NaCL, 1.5% agar, PH 7.0) was added 20 μL of X-gal (50 mg/mL) and 5 μL of IPTG (0.1 mg/mL), and spread by shaking small glass beads on plate. These X-gal/IPTG plates were put into 37℃ incubator to warm up.

100 μL transformed bacterial cell suspension was spread onto a fresh X-gal/IPTG plate. The rest transformed bacterial cell suspension was centrifuged at 1000 g for 1 minute, the supernatant was suck out, leaving around 100 μL supernatant, and then mixed with bacterial pellet. The mixture was spread on another X-gal/IPTG plate. The plates stay for 10 minutes, then the plates was incubated in 37℃ incubator

for 8-12 hours in an invert position.

2.3.8 Colony screening

Appropriate amount colonies were selected for screening. There are two methods for screening, one is PCR screening, and the other is restriction digestion.

2.3.8.1 PCR screening

White colonies were picked as templates to do PCR reaction directly. Cells were transferred to PCR reaction system by a pipette tip. The 25 μL PCR reaction system is composed of 1 unit Taq polymerase (Promega, USA), 2.5 μL 10×reaction buffer, 2.5 μL 25mM $MgCl_2$, 2.5μL 2mMdNTP, 0.2 μL 10 pmol primers, and appropriated water. The PCR program was set to: 94℃ for 3 minutes, 35 cycles of amplification (94℃, 30 sec; 55℃, 30 sec; 72℃, 30 sec), at last extension at 72℃ for 5 minutes. The PCR products were checked by electrophoresis in 1% agarose gel.

2.3.8.2 Restriction digestion

Whether plasmids contained the target DNA fragment was checked by restriction digestion. Restriction digestion was performed as recommended by manufacturer (New England Biolabs, USA). Plasmid DNA was incubated in appropriate amount of restriction enzyme, in its recommended buffer, at the optimal temperature and time. After digestion, the reaction mixture was loaded on 1% agarose gel to check the result by agarose gel electrophoresis.

2.3.9 Mini plasmid preparation

A single colony was incubated in 5mL sterile LB medium with 100ng/mL Amp by 15 mL falcon tube at 37℃ with agitation at 250 rpm overnight. Bacteria were

harvested directly by centrifuge 2500 rpm for 15 minutes (Beckman Allegra 64R, USA). Plasmid extractions were carried out using QIAprep Miniprep plasmid kit (Qiagen, USA). Briefly, 250 μL buffer P1 was used to resuspend the bacterial pellet and to transfer to a microcentrifuge tube. 250 μL buffer P2 was added and mixed gently. Subsequently, 350 μL buffer N3 was added and mixed gently, and then centrifuged at 13000 rpm for 10 minutes. The supernatant was loaded on QIAprep Spin Column, and centrifuged at 13000 rpm for 30 sec, discarding the flow-through. 750 μL buffer PE was added to the column, and then centrifuged at 13000 rpm for 30 sec again, discarding the flow-through. The column was finally centrifuged for additional 1 minute to remove residual buffer PE. The column was placed on a new microcentrifuge tube, 30 μL buffer EB (10mM Tris.Cl, pH 8.5) was added. After a 1 minute stay, the DNA elute was obtained by centrifugation of 1 minute. the DNA elute was kept at -20℃ until used.

2.3.10 DNA sequencing

ABI PRISM ™ BigDye ™ terminator cycle sequencing ready kit (Applied Biosystems Inc., USA) was used for a double-strand DNA sequencing. Following the manual instructions with minor modification, 10 μL sequencing reaction system was set up instead of the recommended 20 μL reaction systems. The sequencing reaction was composed of 4 μL of terminator ready reaction mix (Applied Biosystems Inc., USA), 1.6 mol primer, and 150 ng of plasmid.

The sequencing reaction was done with the following recipe: 25 cycles of 96℃ for 30 sec, 50℃ for 15 sec, 60℃ for 4 minutes in thermocycler. After cycle reaction

finished, the reaction mixture was needed further purified to get clean DNA sequencing samples. The extension samples were purified using ethanol/sodium acetate precipitation method. Briefly, extension products were spinned down and transferred to clean 1.5 mL microcentrifuge tubes. 80μL ethanol/sodium acetate solution (consisting of 3.0 μL 3M sodium acetate, pH 4.6, 62.5 μL of 95% ethanol and 14.5 μL of deionized water) was added, and left on ice for 15 minutes to precipitate the extension products. The extension products were spinned down by centrifugation at 13000 rpm for 20 minutes. The supernatant was aspirated by pipette, and 500 μL of 75% ethanol was added to rinse the pellet. Centrifugation at 13000 rpm for 15 minutes was done again to aspirate the supernatant. The DNA pellet was dried in a 50℃ oven. Before sequencing, 4 μL automatic sequencing loading buffer (10/11 (volume/volume) deionized formamide, 1/11 (volume/volume) 25mM EDTA pH 8.0 with 50 mg/mL dextran blue) was added to the DNA pellet. The sample was denatured by heating to 90℃ for 2 minutes and chilled on ice. The sample was used for sequencing on 377 ABI PRISM automated DNA sequencer (Applied Biosystems Inc., USA). The sequencing results were analyzed by blast searching them in NCBI database.

2.3.11 Diethylpyrocarbonate (DEPC) treatment of solution

In order to prevent RNase contamination, all solutions used in RNA works were treated with DEPC (Sigma, USA). In a fume hood, 0.1% DEPC was added to the solution and mixed well in a bottle which can be autoclaved. The mixture was left for overnight with the cap tightly closed, followed by autoclave with loosened cap.

2.3.12 DNase treatment of RNA sample

Total RNA isolated from culture cells or tumor tissues was pretreated with DNase to remove possible contaminating genomic DNA and diluted to a final concentration of 1 μg/μl. Briefly, 10 μg of total RNA was mixed with 1 μl 10 X DNase buffer (Promega, USA), 1 μl RQ1 RNase free DNase (1 unit/μl) (Promega, USA), 0.25 μl of SUPERase·In RNase inhibitor (20 unit/μl) (Ambion, USA) and appropriate amount of DEPC-treated water was added to a final volume of 9 μl. The mixture was mixed thoroughly and spinned briefly, which was then followed by incubation at 37^{o}C for 10 minutes. After that, the reaction mix was spinned down and 1 μl of 25 mM EDTA was added to stop the reaction and further incubated at 65^{o}C for 15 minutes to inactivate the enzyme. The RNA samples were aliquoted and kept at –80^{o}C until used.

2.3.13 Quantification

Quantification of DNA, RNA, oligonucleotide primer and protein was performed by using BioSpec UV-1601 spectrophotometer (Shimadzu, Japan). The concentration of DNA, RNA and oligonucleotides was measured by reading OD_{260} in spectrophotometer. Briefly, the machine was turned on 15 minutes before measuring and baseline correction was performed once a month. The quartz cuvettes were washed thoroughly and two cuvettes with 100 μl of distilled water were used to autozero the machine at 260 nm wavelength. The water in sample cuvette was aspirated and replaced by 100 μl sample solution. The samples were routinely diluted 1/100 and the readings were taken in duplicate. The readings at both A260 and A280

were shown. The purity of samples was indicated by the ratio between A260 and A280 in the range of 1.8 –2.0. The absorption of 1 OD (A) is equivalent to approximately 50 μg/ml double strand (ds) DNA, 40 μg/ml RNA, respectively. The DNA concentration can be calculated by the following formula:

$$\text{DNA Concentration sample}(\mu g/\mu l) = 50 \times A_{260} \times \text{dilution factor} = OD \times 100 \times 0.05 \mu g/\mu l$$

$$\text{RNA concentration } (\mu g/\mu l) = OD \times 100 \times 0.04\ \mu g/\mu l = OD \times 4$$

The approximate concentration of oligonucleotides was calculated by the following formula:

$$\text{Oligonucleotides concentration}(pM) = OD \times (20 \sim 30) \times \text{dilution time} \times 10^6 pg \times 1pm \div \text{No. of nucleotides} \times 1ug \times 330pg$$

2.3.14 Protein quantification

The Bradford dye-binding assay described by Bradford with modification was used to measure the concentration of total protein in samples. Bovine serum albumin (BSA) (Sigma, USA) at concentration of 1 mg/ml was used to make protein standards. 0, 5, 10, 15, 20, 25 and 30 μl of BSA (1 mg/ml) were pipetted into 1 ml disposable plastic PLASTIBRAND® cuvettes (Brand, Germany). The volume was topped up to 800 μl by adding PBS. After that, 200 μl Bio-Rad protein assay (Bio-rad, USA) was added to the solutions and mixed by pipetting gently. This was followed by incubation at room temperature for 5 minutes and the absorbance at 595 nm was read. The readings were used to make a BSA standard curve.

For measurement of the protein concentration in samples, 1μl of the protein sample was diluted in 799μl of PBS. 200 μl Bio-Rad protein assay was added, and the

samples were incubated at room temperature for 5 minutes. 200 μl of the dye were resuspended in 800 μl of PBS to act as blanks for the measurement. OD was read at 595nm. Concentration was determined against the BSA standard curve.

2.4 Cloning constructions

2.4.1 Viral DNA extraction from serum sample

Serum samples were obtained from HBV-infected patients, from National University of Singapore (NUH). HBV genome genotype shown in Figure 2.1 was confirmed by sequencing cloned HBV DNA fragment. The HBV surface antigen gene (2848bp to 835bp) was amplified by PCR reaction with the P1 and P2 primer. This amplified DNA fragment was sequenced using primer P3 which is prior to the HBV position 155. The DNA fragment sequence was confirmed by comparing it with HBV sequence in NCBI database. Primers P1, P2, and P3 sequences were listed:

P1 5’-TCACCATATTCTTGGGAACAA-3’

P2 5’-GTTTTGTTAGGGTTTAAATG-3’

P3 5’-TCCTGCTGGTGGCTCCAGTTC-3’

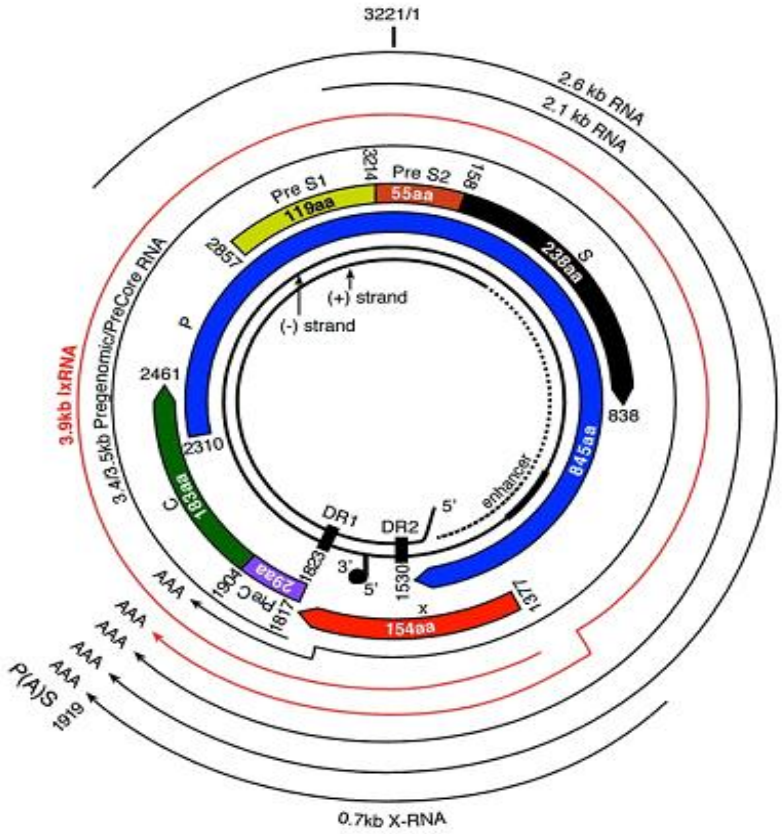

Figure 2.1: Organization of the HBV genome.

Four major viral genes (preC/C, preS1/preS2/S, P and X) are found in HBV genome. The capsid protein encoded by the core (C) gene, the viral polymerase by P gene, X protein by X gene. In addition, three envelope proteins are translated by a single ORF with three start codons in the same open reading frame. http://www.hixonparvo.info/parvovirus.html

2.4.2 Bacterial and mammalian expression vectors applied

Mammalian expression vector pcDNA3.1 (Invitrogen) and pXJ40 (Invitrogen) were used in this study. The pGEM-T vector in HBV clone construction was applied for cloning HBV PCR products. PXJ40 was given by from Dr. Cheng Gee Koh (NTU). The vector PXJ40 (Figure. 2.2) has high expression efficacy in mammalian cells. Between the endogenous restriction sites EcoRI and BamHI, PXJ40 has a HA

tag which can be used for the target protein expression detection. In this work, pXJ40 was used to clone and express HBx.

The pcDNA3.1 (Figure. 2.3) was a used for target gene expression in mammalian cells widely. The vector was used for whole HBV genomes construction. The HBV construction was confirmed by HBV core gene and surface gene's RT-PCR.

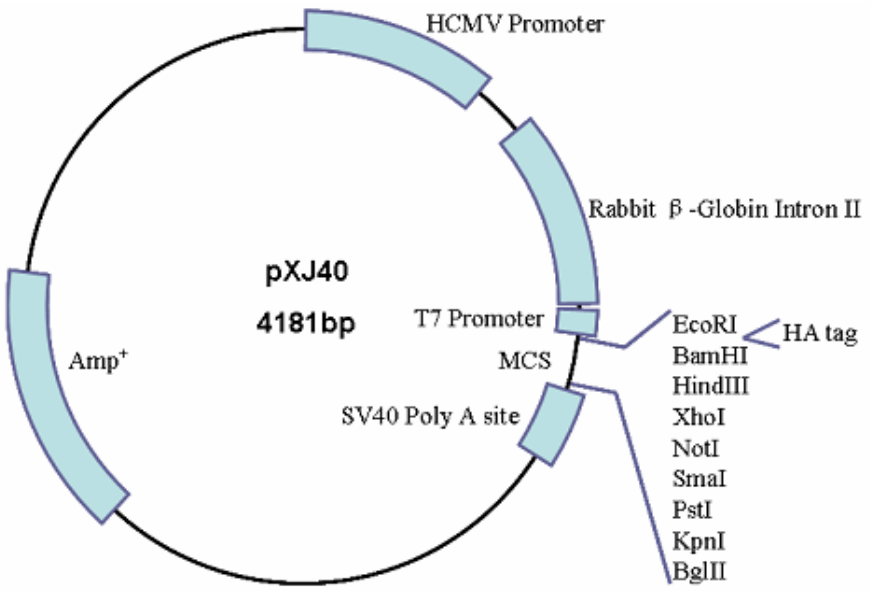

Figure 2.2: Feature map of mammalian expression vector pXJ40.

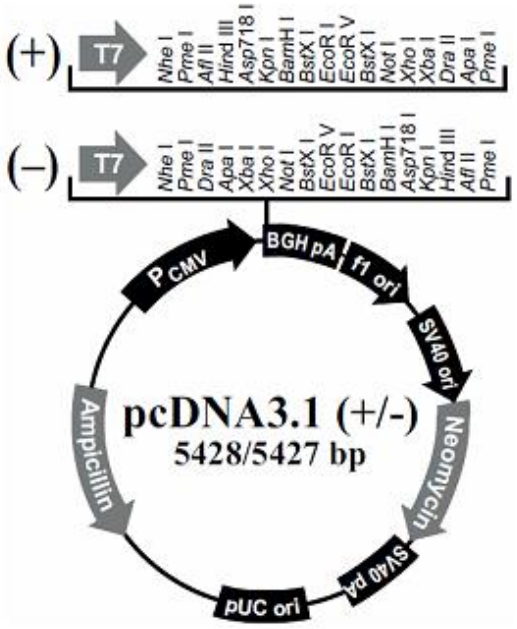

Figure 2.3: Feature map of mammalian expression vector pcDNA3.1+. MluI restriction site, prior to the pCMV promoter was used for cloning of the replicative HBV genome instead of the MCS.

2.4.3 Cloning construction of HBx

HBx clinical samples were given by A/P. Lim Seng Gee (National University Hospital). HBx gene was cloned individually between the HindIII and PstI sites of PXJ40. The oligonucleotide primers for HBx gene PCR amplification were shown in the following.

HBx B Forward: 5'- CCCAAGCTTGCTGCTAGGCTGTGCT-3'

HBx B Reverse: 5'- AACTGCAGTTAGGCAGAGGTGAAA-3'

The sequenced HBx inserts were compared with HBx sequences in NCBI

database to ensure the correct cloning of HBx.

2.5 Cell transfection and drug treatment

The Hepg2 cells were maintained in monolayer culture in DMEM, supplemented with 10% FBS in an incubator containing 5 percent CO_2 at 37^{o}C. RPHs were maintained in monolayer culture in CSC medium. After reaching 70% confluence, cells were transfected by Pxj40 plasmid with HBx gene or PcDNA 3.1 plasmid with HBV whole genome. After that, transfected cells were incubated with *S*-enantiomer and *R*-enantiomer form of Ibuprofen at a concentration of 100 μM, respectively, for 48 hours.

Transient transfection of plasmid DNA was carried out using Effectene Transfection Reagent kit (Qiagen). Briefly, 2x10^{5} HepG2 or RPHs were seeded on 6 well plates, and when 70% confluency was reached, the cells were transfected with plasmids following Effectene manuals. *S*-enantiomer and *R*-enantiomer form of Ibuprofen were added to transfected cells at a final concentration of 100 μM, and the cells were incubated at 37^{o}C and 5% CO_2 for 48 hours. After incubation, transfected cells are detached by trypsinization, pelleted and collected for protein or total RNA extraction.

CRL-2273 cells were grown to reach 70% confluence, and were then incubated with *S*, *R* enantiomer form of Ibuprofen at a concentration of 100 μM respectively for 48 hours. The cell pellet was collected for protein or total RNA extraction.

2.6 Isolation of RNA

2.6.1 RNA extraction and quantitation

Mammalian cells were cultured in Petri-dish for RNA isolation using RNeasy mini kit (Qiagen, USA). Before RNA extraction, the medium was pippetted out, and cells were washed by PBS three times. 350 μL buffer RTL was added to monolayer. Buffer RTL was added β-Mercaptoethanol (β-ME) with 10 μL β-ME per 1 mL buffer RTL before adding to cell monolayer. Cell lysate was collected with policeman, and transferred into a microcentrifuge tube, and then mixed to ensure that no cell clumps were visible. In order to homogenize the sample, the cell lysate was passed through a 20-gange needle (0.9 mm diameter) fitted to an RNase-free syringe, 1 volume 70% ethanol was then added and mixed well by pipetting. Samples were transferred to RNeasy mini column placed in a 2mL collection tube, and then centrifuged at 13000 rpm for 30 seconds using a bench top centrifuge (Sorvall, UK). The flow-through was discarded, and 700 μL buffer RW1 was added to column and centrifuged at 13000 rpm for 30 seconds, discarding the flow-through. 500 μL buffer RPE was added to column and centrifuged at 13000 rpm for 30 seconds, discarding the flow-through. Another 500 μL buffer RPE was added and centrifuged at 13000 rpm for 2 minutes. the column was placed to a new 2 mL tube and centrifuged at 13000 rpm for 1 minute. The columns were transferred to a new 1.5 mL collection tube. 30 μL RNase-free water was directly added onto the membrane of column and centrifuged at 13000 rpm for 1 minute. The flow-out contained RNA sample and was kept at -80℃.

The quality of RNA was checked by electrophoresis in 1% agarose gel. A small aliquot RNA sample was loaded into gel. After gel electrophoresis, the sample should have sharp 28S and 18S bands, indicating better quality RNA. DNase was used to

treat RNA to remove any genomic DNA contamination. The RNA mixture was kept at -80℃ until used.

2.6.2 Reverse Transcript

In order to amplify interested genes or partial genes, it is necessary for mRNA to transcript to DNA by reverse transcript reaction. Briefly, Reverse transcript reaction was the following: appropriate total RNA, 2 μL oligo dT Primer (10 μM) and 6 μL DEPC-treated water were mixed and incubated at 80℃ for 3 minutes, the mixture was then chilled on ice for 2 minutes. The master mixture 4 μL 5×RT buffer, 5 μL 2mM dNTP and 1 μL M-MLV Reverse transcriptase (Promega, USA) were added and incubated at 42℃ for 90 minutes, and then heated at 94℃ for 2 minutes, and chilled on ice for 2 minutes. The mixture was kept at -20℃.

2.6.3 Primer design

After sequencing or searching for homology genes of rat species in database of NCBI, the full-length or partial length of genes sequences were obtained. By primer design software (primer design v4), primers were designed to give a product around 150-200 base pairs to reduce the nonspecific binding of SYBR Green. The sequences of primers were listed in the Appendix.

2.6.4 Real Time PCR

In order to accurately quantity the original amount of target mRNAs in samples, real-time RT-PCR was applied. Real-time RT-PCR can monitor the amplification of a PCR product during cycling rather than analysis accumulated product after a number cycles in the traditional RT-PCR. SYBR Green was used as a dye to emit the signal.

SYBR Green binds double-stranded DNA, and emits fluorescence on excitation. Quantification was performed by calculating the fluorescence density during the amplification cycle. All the reactions were prepared to save reagents with half of the reagent volumes recommended by the manufacturers. A non-template control was always included in the sample preparation. GAPDH or β-actin was chosen as internal controls for these experiments.

iSCRIPT one-step RT-PCR kit (Bio-Rad) was used for the precise real-time quantification of RNA targets. Briefly one half reaction mix was prepared by adding 12.5 μL of 2× SYBR Green RT-PCR Reaction Mix, 0.75 μL of each primer (10 p mol/μL), appropriate amount of RNA template, and appropriate amount of Mili Q water to meet a final 25μL volume. The master mix was transferred to 0.2 ml white strip tubes (Bio-Rad) and covered with optical flat strip caps (Bio-Rad). The real-time PCR was carried out in a IQ 5 multicolor Real-time PCR detection system (Bio-Rad). The cycling program was: 50^{o}C for 10 minutes, 95 ^{o}C 5minutes; repeat 40 times the following: 95 ^{o}C 10 sec, 60 ^{o}C 30 sec.

The disassociation analysis was routinely carried out by acquiring fluorescent reading for one degree increase from 55 ^{o}C to 95 ^{o}C. Microsoft Excel formatted data including amplification analysis, experimental report, melting curve analysis and threshold cycle number were provided automatically by IQ5 optical system software version 2.0 (Bio-Rad). The fold changes were calculated as following formula:

Sample $\Delta Ct = Ct_{sample} - Ct_{\beta\text{-actin;}}$ $\Delta\Delta Ct$= Sample ΔCt-control ΔCt; the fold of sample versus control = $2^{-\Delta\Delta Ct}$

2.7 Protein isolation

2.7.1 Collection of conditioned medium

The conditioned media were collected from cultured cell lines in order to measure the secreted protein levels. Briefly, cells treated were seeded in culturewares (TPP, Switzerland) and culture medium was added to a suitable volume. 48 hours later, the media was removed and filtered through a 0.45 μm filter (Millipore, USA) and protease inhibitors was added (1 μg/ml aprotinin, 1 μg/ml pepstatin, 1 μg/ml leupeptin, 1 mM PMSF and 1 mM EDTA). Media was aliquoted and stored in -80℃.

Alternatively, the media were concentrated with Centricon® Plus-20 (Millipore, USA) following the manufacturer's recommendation. Briefly, the conditioned media were transferred into the sample filter cup and sealed with supplied cap. The filter unit was centrifuged for 10 to 30 minutes at 3000 g at 4°C in a swinging-bucket rotor (Beckman, USA). After the centrifugation step, the concentrated sample was transferred to a suitable container and the sample filter cup was inverted and inserted into a retentate cup and spun for 2 minutes at 1000 g to collect the remaining concentrate. The concentrate was combined and aliquoted and stored at -80°C until used.

2.7.2 Protein isolation from cell lysate

Normal culture cells and cells used to produce the conditioned media were harvested for protein isolation. Briefly, the monolayer cells were rinsed twice with PBS, and trypsin was added, followed by harvesting the cells pellet by centrifugation. The cells were pelleted by centrifugation at 17,000 g for 5 minutes. The pellet was

resuspended in M-PER® Mammalian Protein Extraction Reagent (Thermo Scientific) with or without 2 X Complete, EDTA-free protease inhibitor cocktail (Roche, Germany) for 5 minutes on ice with shaking. The debris was removed by centrifugation at 13,000 g at 4°C for 10 minutes and the supernatant was removed to a clean tube and stored at -80°C until used. When desired, the protein concentration was determined by Bradford method in duplicate before storage.

2.7.3 Nuclear Protein Extraction

Cell nuclear proteins were purified for measuring the amount of NFκB family such as RelA and C-rel. Nuclear protein extraction followed the manuals of NE-PER Nuclear and Cytoplasmic Extraction Kit (Thermo Scientific). Briefly Ibuprofen treated and/or HBx transfected Hepg2 cells were collected as cell pellet. The mixture of CER I:CER II:NER reagents at 200:11:100 µl, respectively, was added to cell pellet, vortexed and incubated the tube on ice for 10 minutes. After that, ice-cold CER II was added to the tube and centrifuged for 5 minutes at 15,000 g. The supernatant (cytoplasmic extract) was stored at -80 ℃, while the insoluble (pellet) fraction which containing nucleus in ice-cold NER was suspended. The suspension was vortexed and incubated for 40 minutes and then centrifuged at 15,000 g for 10 minutes, the supernatant (nuclear extract) fraction was collected and kept at -80 ℃ until use.

2.7.4 Western blotting

Western blotting was carried out to detect and compare proteins and their levels in different sample preparations.

2.7.4.1 SDS-Polyacrylamide gel electrophoresis (SDS-PAGE)

The SDS-PAGE gel was carried out using a Mini-PROTEAN 3 Electrophoresis System (Bio-rad, USA). The gels were prepared depending on different gel concentration. Briefly, after setting up the gel apparatus, separating gels were prepared by mixing appropriate amount of 40% acrylamide/bisacrylamide solution (37.5:1, acrylamide/bis; Bio-rad, USA) (1.875 ml for 7.5% gel, 3.125 ml for 12.5% gel and 3.75 ml for 15 gel) with 2.5 ml of 1.5 M Tris·Cl (pH 8.8), 100 µl of 10% SDS, and 100 µl of 10% fresh ammonium persulfate (APS) (Bio-rad, USA) and water to a total volume of 10 ml. The volume can be adjusted accordingly. 5 µl of N, N, N', N'-tetramethylethylenediamine (TEMED) (Bio-rad, USA) was added just prior to pouring gel. Pure ethanol was overlaid gently on top of the separating gel. After polymerization, the overlay was decanted, and a 5 % stacking gel was poured. 4ml of 5% stacking gel was prepared by mixing 0.5 ml of 40% acrylamide/bisacrylamide solution with 0.5 ml 1.0 M Tris·Cl (pH 6.8), 40 µl of 10% SDS, 40 µl of 10% APS, 4µl TEMED and water. Comb was inserted correctly and allowed to polymerize completely before running.

The protein samples were mixed with 1 x loading buffer (62.5 mM Tris Cl pH6.8, 10% glycerol, 2% SDS, 0.05% bromophenol blue), and 100 mM dithiothreitol (DTT) (Sigma, USA) was added just before boiling in 100 ℃ water bath for 5 minutes. For non-reducing condition, the DTT was omitted. After loading the samples, the gel was run under constant voltage (60 V) till the dye reached the resolving gel and thereafter at 100 V till satisfactory protein separation was observed. All blue or dual color Precision Plus protein standards (Bio-rad, USA) or Benchmark^{TM} pre-stained protein

ladder (Invitrogen, USA) was run as a protein reference.

2.7.4.2 Gel transfer

The separated proteins were electrophoretically transferred onto Hybond-C Extra nitrocellulose membrane (Amersham-Pharmacia, UK) using Mini-PROTEAN 3 Electrophoresis System (Bio-rad, USA). The polyacrylamide gel obtained after electrophoresis was rinsed in water, and placed in-between layers of Whatman paper and membrane, cut to exact size of the gel, and inserted with 8 layer filter papers soaked in transfer buffer (0.3% Tris, 1.45% glycine and 20% methanol). The bubbles were carefully and completely removed by rolling across a glass pipet. The orientation of this assembly was membrane facing the anode. The transfer was performed in 1x transfer buffer at 20 V for 1 hour with constant stirring in 4℃. The blotted membrane was marked and washed with 1 x Tris-buffered saline (TBS) (20mM Tris Cl pH 7.4, 150mM NaCl) buffer and stored at 4°C if not used immediately.

2.7.4.3 Immunoprobing

The antibodies used in this study were as follows: (1) Cox2 mouse monoclonal IgG (sc-52972, Santa Cruz), IL6 mouse monoclonal IgG (AH65, Santa Cruz), RelA mouse monoclonal IgG (sc-8008, Santa Cruz), C-Rel rabbit polyclonal IgG (sc-71, Santa Cruz), β-actin mouse monoclonal IgG (Sigma A5441). Western bands were analyzed and quantified by ImageJ software.

The immunoprobing were carried out following the standard protocol. Briefly, the membrane was wetted with 1X TBS buffer before being blocked with 5% nonfat

milk powder in 0.1% TBST (0.1% Tween-20 in 1 x TBS) 1 hour at room temperature. After milk blocking the membrane was incubated with 1/1000 diluted mouse monoclonal antibody in 5% nonfat milk powder in 0.1% TBST for overnight at 4℃ on an orbital shaker (Bellco, USA). After that, it was washed four times with 0.1% TBST for 10 minutes each with shaking. After the washings, the membrane was incubated in corresponding anti-goat, anti-mouse or anti-rabbit IgG HRP-conjugated secondary antibody (Thermo) in 0.1% TBST for 1.5 h at room temperature on a shaker. The membrane was then washed four times as above before incubating in the SuperSignal West Pico Substrate solution (Thermo)) by mixing equal volumes of the two reagents for 3 minutes and exposed to Hyperfilm X-ray films (Amersham-Pharmacia, UK) at various desired time lengths.

2.7.4.4 Stripping and re-probe

The membrane was stripped after chemiluminescent detection for reprobe with other primary antibodies. Briefly, the membrane was washed in TBST for 5 minutes and incubated in sufficient volume of Restore Western Blot Stripping Buffer (Thermo)) at 37℃ for 15 minutes. After washing in 0.1% TBST twice for 10 minutes each, secondary antibody incubation was performed again, followed by fresh substrate detection.

2.8Animal experiment

2.8.1 Animals

250-300 gram Wistar rats were used in this study. Rats were maintained in Animal Holding Unit of Nanyang Technological University and rats were kept on a

temperature-controlled room under 12 hours day-night rhythm with free access to water and a standard rat diet. All animals received humane care and the study protocols complied with the university's guidelines.

2.8.2 Hepatocytes purification by percoll gradient centrifugation

Wistar rats (250-350g) were sacrificed by carbon oxidizer. 150 units (500units/mL) heparin was given through the vein in the tail to prevent blood coagulating. A laparotomy (surgery that involves opening the abdomen) was then performed. The anatomy map of liver blood vessel was showed in Figure 2.4. A needle (20 G catheter, Japan) was inserted into the portal vein and secured. The superior vena cava should be clamped to increase the efficiency of perfusion. The inferior vena cava (IVC) beneath the liver was inserted by a needle (18 G catheter, Japan), and perfusion was carried out with 37℃ hanks' balanced salt solution (HBSS) without calcium (Gibco, USA) at a rate of 5 mL/minutes for 15 minutes till the liver discolourised. HBSS with calcium containing 0.05% collagenase (Gibco, USA), 5% heat-inactivated fetal bovine serum (FBS-HI) (Gibco, USA) and 1% P/S (Gibco, USA), at 37℃ was then pumped through the liver at 5 mL/minutes for approximately 15 minutes. The liver was removed and minced mechanically with scissors. Glisson's capsule (a membranous capsule) along the vessels was discarded to reduce contamination by other cells. The paste-like liver was then digested by shaking in remaining HBSS with calcium solution for 15 minutes at 37℃. Cell suspension was then filtered through a 200 μm filter to remove the undigested tissue.

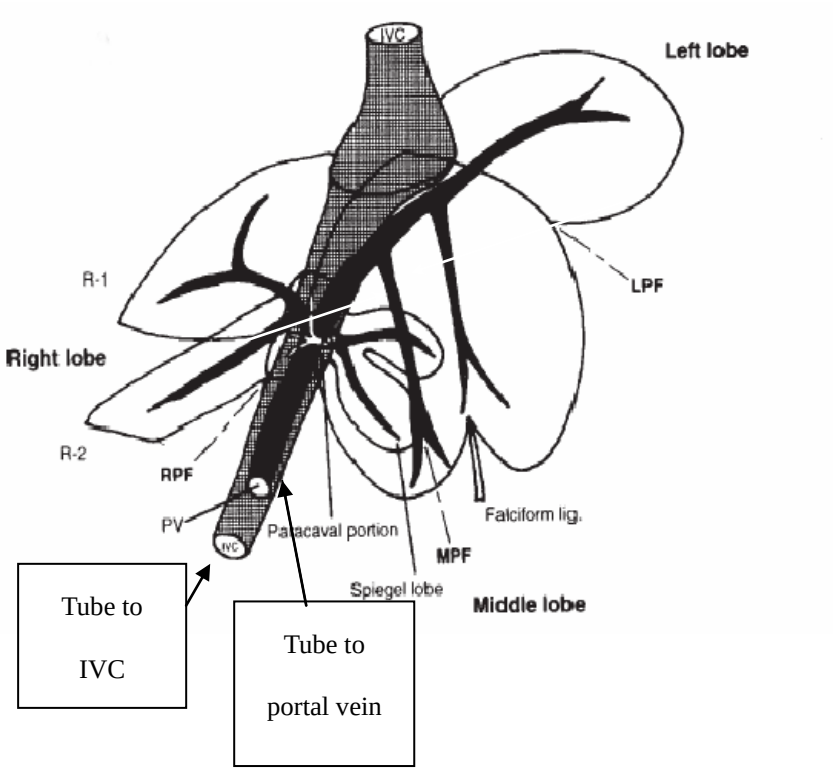

Figure 2.4 Liver perfusion. The tube on the right was inserted into the portal vein while the one on the left was inserted into the inferior vena cava.

Cell suspension after filtered was centrifuged at 500 g for 5 minutes to get cell pellet. The cell pellet was resuspended in 10 mL 1×PBS and this was layered on top of a two-step percoll (Amersham Biosciences, Sweden) gradient. The percoll gradient consisted of 10 mL of 25% Percoll (top) and 10 mL 50% Percoll (bottom). For easier visualization of the enriched cell bands after centrifugation, 50mL Falcon tube which was "glass-clear" was used to make the gradient. The gradient was centrifuged at 800 g for 20 minutes at room temperature. The acceleration/deceleration of the centrifuge was set to zero so as to reduce disturbance to the cell bands. The bottom pellet was

enriched with RPHs. Isolated RPHs isolated were then resuspended and cultured on type I collagen (Sigma)-coated dishes in HBM complete medium (Clonetics).

2.8.3 Hepatocyte identification and Trypan blue staining for cell viability measurement

Hepatocytes are larger than other type cells, usually have multiple nuclear. RPHs purity was examined by optical microscope based on cells special morphological characters. The viability of isolated hepatocytes was examined using trypan blue stock solution (Invitrogen). Briefly, an aliquot of cell suspension (50-100ul) was used to test for viability, 50ul of 0.4% trypan blue was mixed with 50ul cell suspension (dilution of cells), and the mixture was incubated for 3 minutes at room temperature. After that a drop of the trypan blue/cell mixture was applied to a hemacytometer for counting the cells. The cells stained by trypan blue were nonviable, and the cells not stained were viable.

2.9 Dimethylthiazol (MTT) assay

MTT reduction test was used to measure the toxicity of Ibuprofen on CRL-2273 and Hepg2 cells. Briefly, 70% confluency HepG2 and CRL-2273 cells were cultured 96 wells plate with a cell number around $2X10^4$ in each well. 20 ul of MTT solution at final concentration 0.5 mg/ml MTT was added to the each well, then a series of Ibuprofen concentrations (100nM, 1μM, 10μM, 100μM, 1mM) were added respectively to 5 wells. The cells were incubated with Ibuprofen for 5 hours at 37℃ in incubator. After incubation, the culture medium containing Ibuprofen was removed, added 200 μl of pure DMSO and incubated 37 ^oC for 5 minutes. The absorbance of

each well was measured at 550nm using the plate reader (benchmark plus).

2.10 Protein profile preparation and labeling with iTRAQ reagents:

The transfected cells (RPHs and HepG2 cells) and CRL-2273 cells were harvested and lysed in 150 µl of 8 M urea, 0.05% SDS (W/v) and 4% (W/v) CHAPS on ice for 20 minutes with vortexing. Cell lysis was centrifuged at 15,000 g for 1 hour at 4℃, supernatant was stored. 100 µg protein of each sample was added 4 volumes of cold acetone, and incubated for 2 h for protein precipitation. The precipitate protein was dissolved in the solution buffer, denatured and cysteins blocked as following the iTRAQ manual (Applied Biosystems). Each sample was digested with 20 µl of 0.25 µg/ µl sequence grade modified trypsin (Promega) solution at 37℃ overnight. The samples were labeled with the iTRAQ tags 114,115,116 and 117. The labeled samples were pooled before analysis. To verify that sample preparation techniques do not interfere with digestion and labeling procedures. The bovine serum albumin (BSA) standard solution (Pierce) was performed acetone precipitation, enzymatically digested with trypsin and labeled with the iTRAQ reagents as previously stated. These differentially labeled digests were mixed at a ratio of 1: 1: 1: 1 and analyzed by LC-MS/MS. iTRAQ tags 114,115,116 and 117 detected by LC/MS should be at a ratio of 1: 1: 1: 1.

2.10.1 On-line 2D Nano-LC/MS/MS analysis on HP1200 LC system and QSTAR system

Peptides labeled by iTRAQ were firstly separated by 2-D HPLC. Briefly, 3 µl of the peptide mixture was loaded onto a strong cation exchange column (0.32 x 50 mm,

5 µm). The peptide mixture was eluted stepwise by injecting salt plugs of 10 different molar concentrations of 10, 20, 30, 40, 50, 60, 80, 100, 300, and 500 mM KCl solution. The flowthrough with peptides that do not bind to the SCX column was trapped by the ZORBAX 300SB-C18 enrichment column (0.3 x 5 mm, 5µm) and washed isocratically using loading buffer A (5% acetonitrile, 0.1% formic acid) for 100 minutes at 0.5 ml/minutes to remove excess reagent. In the second step, this enrichment column was switched to the solvent path of the nanopump. Peptides were eluted using buffer B (H_2O with 0.1% formic acid) and buffer C (95% acetonitrile, 0.1% formic acid) with a nanoflow gradient starting with 5% buffer C and increasing up to 80% buffer C over 100 minutes at a flow rate of 0.5 ul /minutes in each analysis. An increasing concentration of acetonitrile was used to elute the concentrated sample and further separation was achieved by going through the analytical Zorbax 300SB C-18 reversed-phase column (75 µm x 50 mm, 3.5 µm). The electrospray was interfaced between HP1200 LC system (Agilent Technologies) and QSTAR XL (Applied Biosystems-MDS Sciex) mass spectrometry. Survey scans were acquired from m/z 300-1500 with up to two precursors selected for MS/MS from m/z 100-2000. After the first analysis was completed, the enrichment column was switched again into the solvent path of the cation exchange column. Buffer D was composed of a series of increasing concentration of KCl salt solution from 10 mM to 500 mM used to elute the retained peptides step by step from the SCX column by sequential injection. This was followed by valve switching and reversed phase chromatography, respectively.

Peptide identifications and quantization were performed using Proteinpilot^{TM}

software 2.0 packages (Applied Biosystems, Software Revision 50861). MS/MS spectrum was searched against species of *Homo sapiens* or *Rattus norvegicus* in the UniProt_sprot_20070123 database. The following parameters were set in the searching: fixed modification of methylmethanethiosulfate- labeled cysteine, fixed iTRAQ modification of free amine in the amino terminus and lysine, variable iTRAQ modifications of tyrosine, and allowing serine and threonine residues undergoing side reaction with the iTRAQ reagent. Other parameters such as tryptic cleavage specificity, precursor ion mass accuracy, and fragment ion mass accuracy were built-in functions of ProteinPilot software. Relative quantification of proteins in the case of iTRAQ was performed on the MS/MS scans and was set as the ratio of the areas under the peaks at 114, 115, 116 and 117 Da, which were the masses of the tags corresponding to the iTRAQ reagents. The relative amount of a peptide in each sample was calculated by dividing the peak areas observed at 115.1, 116.1 and 117.1 *m*/*z* by that observed at 114.1 *m*/*z*. The following criteria were required to consider a protein for further statistical analysis: unused protein score was more than 2 (99% confidence) per experiment, one or more high confidence (>95%) unique peptides had to be identified, the *p* value in the Protein Quant was set to be $p < 0.05$, and the fold difference was to be greater than 1.1. The candidate proteins were carefully examined in the Protein ID of the ProteinPilot software. All peptides detected were used in the respective protein quantitation. The peptides without any modification of free amine in the amino terminus or without iTRAQ modification of free amine in the lysine were excluded from calculation of the protein ratios.

2.10.2 On-line 2D Nano-LC-MS/MS analysis on Agilent 1200 nanoflow LC system

The analysis was performed on an Agilent 1200 nanoflow LC system (Agilent Technologies) interfaced with a 6530 Q-TOF mass spectrometer (Agilent Technologies). In the first dimension, 3 µl of the combined peptide mixture was loaded onto the PolySulfoethyl A SCX column (0.3 × 50 mm, 5 µm) and was eluted stepwise by injecting salt plugs of 10 different molar concentrations of 10, 20, 30, 40, 50, 60, 80, 100, 300, and 500 mM KCl solution. The sequentially eluted peptides from the SCX column were trapped onto the enrichment chip (Agilent Technologies) and further eluted with a nanoflow gradient of 5–80% acetonitrile plus 0.1% formic acid at a flow rate of 300 nl/minutes. For MS/MS analysis, survey scans were acquired from *m*/*z* 300 to 1500 with up to two precursors selected for MS/MS from *m*/*z* 100 to 2000 using dynamic exclusion, and the rolling collision energy was used to promote fragmentation. To gain statistical evidence for differential expression of proteins, another two separate experiments were performed as described above.

Relative abundance quantitation and protein identification were performed using Spectrum Mill MS Proteomics Workbench (Agilent Technologies, Software Revision A.03.03.084 SR4). Each MS/MS spectrum was searched for species of *Homo sapients* against the UniProt_sprot_20100123 database. The searches were run using the following parameters: fixed modification of methylmethanethiosulfate-labeled cysteine, fixed iTRAQ modification of free amine in the amino terminus and lysine. Other parameters such as tryptic cleavage specificity, precursor ion mass accuracy,

and fragment ion mass accuracy are built-in functions in the Spectrum Mill software. The protein profile results were filtered with a protein score greater than 11 and peptides score of at least 6, which gives a confidence value of 99%. Relative quantification of proteins in the case of iTRAQ was performed on the MS/MS scans and was the ratio of the areas under the peaks at 114, 115,116 and 117 Da, which were the masses of the tags that correspond to the iTRAQ reagents. The relative amount of a peptide in each sample was calculated by dividing the peak areas observed at 115.1, 116.1 and 117.1 *m*/*z* by that observed at 114.1 *m*/*z*. Sequence coverage was calculated by dividing the number of amino acids observed by the protein amino acid length.

2.11 The ROS level measurement

The ROS level of CRL-2273 neuroblastoma treated by Ibuprofen was measured using The Image-IT™ LIVE Green Reactive Oxygen Species (ROS) Detection Kit (Invitorgen). The assay is based on 5-(and-6)-carboxy-2′,7′-dichlorodihydrofluorescein diacetate (carboxy- H2DCFDA), a reliable fluorogenic marker for ROS in live cells. In the presence of nonspecific ROS, the reduced fluorescein compound is oxidized and emits bright green. Briefly, $2x10^4$ CRL-2273 was seeded to each well of 24 well plates. When the CRL-2273 reach around 70% confluence, *S*-enantiomer and *R*-enantiomer form Ibuprofen were added respectively, incubated 48 hours. For positive control, just before ROS measurement, 0.5ml culture medium with the final concentration 100 μM *tert*-butyl hydroperoxide (TBHP) were applied to the cells, and incubated for 1 hour. 0.5 ml 25 μM carboxy-H2DCFDA for each well was applied and incubated for 30 minutes at

37℃. After washing two times with PBS, the cells were observed under fluorescent microscope (Olympus). The oxidation product of carboxy-H2DCFDA has excitation/ emission maxima of approximately 495/529 nm and can be observed using standard fluorescent filter sets.

2.12 Endothelial cell tube formation assay

2.5 x 10^4 HUVECs were starved with 2% FBS for 4 hours and seeded onto the solidified growth factor reduced Matrigel (Chemicon) in a 96-well plate. After HUVEC were incubated in conditional medium from RPHs and HepG2 cells transfected with or without the replicative HBV genome at 37 ℃ for 4-6 h, HUVEC cells were fixed and tube formation was analyzed by light microscopy. The quantitation of tube formation was done by Branch Point Counting method. Capillary tube branch points formed in 3 wells were counted and the values averaged.

2.13 Statistics

The data were presented in the form of mean ± Structural equation modeling and statistical software from Sigmastat (Version 2.0.3; SPSS, USA) was employed in the statistical analysis. Two-tailed, unpaired student's *t* test was used for comparing experimental data from different groups. A p value < 0.05 was considered as statistically significant.

Chapter 3

Protein profile in neuroblastoma cells incubated with *S*- and *R*-enantiomers of Ibuprofen by iTRAQ-coupled 2D LC-MS/MS analysis: *possible mechanism of action on Alzheimer Disease* [a]

3.1 Introduction

Alzheimer disease (AD) is a kind of neurodegenerative diseases characterized by progressive cognitive deterioration and is normally diagnosed in elderly people. Patients in late stage lose bodily function gradually, eventually leading to death. The cause and progression of Alzheimer's disease are not well understood. Researches indicate that the disease is associated with plaques and tangles in the brain which are caused by accumulation of abnormally folded A-beta (Aβ) and tau proteins. Aβ oligomers bind to a surface receptor on neurons and change the structure of the synapse, thereby disrupting neuronal communication [102]. Abnormal hyperphosphorylated Tau protein causes the microtubules to disintegrate, damaging the neuron's physiological functions. These may result in malfunctions and causing eventual death of the neuron cells [103].

[a] Reproduced in part with permission from [Zhang, J., Sui, J., Ching, C. B., Chen, W. N., Protein profile in neuroblastoma cells incubated with S- and R-enantiomers of Ibuprofen by iTRAQ-coupled 2-D LC-MS/MS analysis: possible action of induced proteins on Alzheimer's disease. *Proteomics* 2008, *8*, 1595-1607.] [104] reference copyright [2009] @ wiley-VCH. Zhang Jianhua designed the experiments, performed most of the experiments, analyzed the data and wrote the paper.

Neuroinflammation can contribute to the pathogenesis of AD that may be via Aβ or Tau pathway [39, 40]. Clinical trial data have shown that NSAIDs may have protective effects against the onset of AD [41-43]. NSAIDs can reduce Aβ plagues related with inflammation that is supported by *in vitro* and *in vivo* investigation [105]. Ibuprofen, as a kind of NSAID drug exists in *S*- and *R*-enantiomer, with the *S* form being more effective than the *R* form on neuron protection [106]. In order to study the mechanism of *S*-enantiomer's effects on AD, *S*-enantiomer and *R*-enantiomer of Ibuprofen were used in this study. This particular protein expression affected by *S*-enantiomer may play an important role for AD therapy.

The rapidly evolved proteomics techniques may be applied to map a comprehensive protein profile in cells incubated with Ibuprofen, which in turn should provide us with a better understanding of these mechanisms. In recent years, various methods have been combined with LC-MS/MS to identify large numbers of protein from a variety of biological samples successfully. In this study, the protein profile of the neuron cells treated by Ibuprofen was compared using iTRAQ method. The results showed that three types of cellular proteins including metabolic enzymes, signaling molecules and cytoskeleton proteins displayed changes. The changes in the level of a number of enzymes were further supported by the real-time RT PCR analysis. The neuroprotective effects of enzymes, involved in antioxidant activity, regulated by S-Ibuprofen were found in this study. Our findings therefore provide molecular evidence on the mechanism of action of Ibuprofen, including its beneficial effects on reducing the development of AD.

3.2 Results

3.2.1 MTT assay

It is critical to determine the suitable Ibuprofen concentration for neuroblastoma treatment. Since the aim of this study was to establish protein profile in response to the NSAID drug, Ibuprofen, the concentration which mostly reproduces *in vivo* condition and minimizes cell death associated with incubation of Ibuprofen was chosen. Whitlam et al. found that the Ibuprofen concentration at serum is 20μg-40μg per ml (around 100μM), when patients uptake Ibuprofen at normal dose [107]. The viability of neuroblastoma was examined by MTT assay, while neuroblastoma CRL-2273 incubated with an increasing concentration of each respective enantiomer of Ibuprofen. Results shown in Figure 3.1 indicated that at 1mM of *S*-Ibuprofen, *R*-Ibuprofen and racemic mixture were toxic to the cells. Our results indicated that no significant effect on cell viability was observed for concentrations below 100μM. In order to simulate the *in vivo* condition at the best, the 100μM Ibuprofen concentration mentioned the previous report was therefore chosen in all the experiments in this study.

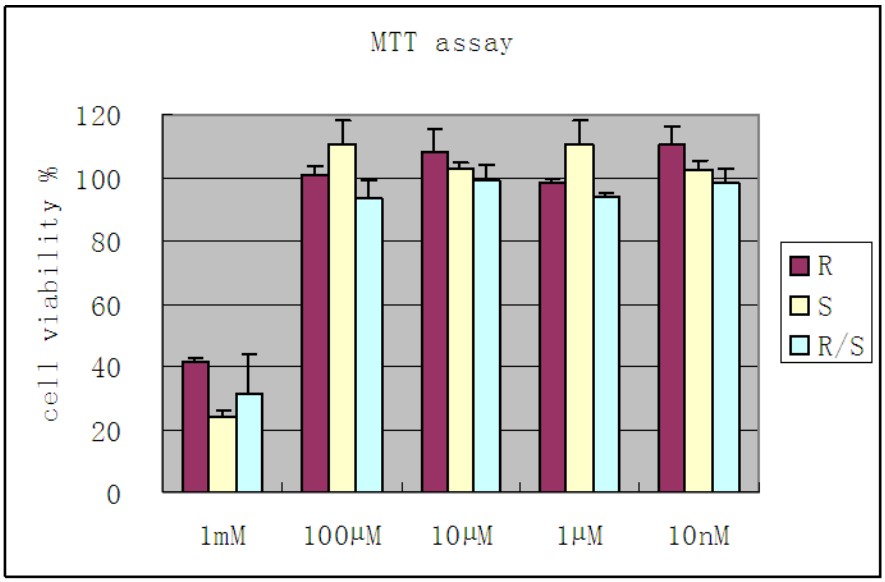

Figure 3.1 Cell viability of neuroblastoma after 48 h of exposure to *R*-, *S*-enantiomer, and R/S racemic form of Ibuprofen respectively. R was representative of R-Ibuprofen; S was representative of S-Ibuprofen; R/S was representative of R and S racemic Ibuprofen. Three independent experiments were carried out for each enantiomer. The viability of control cells only adding DMSO was set 100%.

3.2.2 iTRAQ analysis of differentially expressed proteins

The neuroblastoma CRL-2273 cells with Ibuprofen treatment were lysed to extract the proteins for protein profile study. Three separate experiments were carried out for each enantiomer using different batch cells treated by Ibuprofen. The MS result was analyzed by Proteinpilot software using Uniprot_spot_20070123 database to identify and quantify the different protein expression levels among different samples. Analysis of the first experiment led to the detection of 137 different proteins, 149 proteins were detected in the second experiment and 152 proteins were detected

in the third experiment. A total of 167 unique proteins were identified and analyzed the three repeat MS results together. Identification of protein with significant expression level was based on the ProtScore with a cut-off of 2.0, which means the confidence value of 99%. Among these significant expression proteins, a total of 13 unique proteins which were differentially expressed between the samples incubated with Ibuprofen and normal sample were identified. This was repeated three times and results were consistent, the mass data was shown on Table 3.1 and Table 3.2. These 13 proteins were subsequently categorized into separate categories according to their cellular functions (Table 3.1). The protein function was analyzed through Swiss-Prot database manually. These included five metabolic enzymes, 6 signaling molecules and 2 cytoskeleton proteins. In the cluster of Metabolic Enzymes**,** Triosephosphate isomerase and Phosphoglycerate mutase 1 were upregulated for *S*-enantiomer incubated cells comparing with *R*-enantiomer incubated cells. In contrast, fatty acid synthase was downregulated in *S*-enantiomer incubated cells compared with those incubated with either the *R*-enantiomer or without treatment cell. Proteins in the cluster of Signaling, peroxiredoxin 2 and peroxiredoxin 6 were upregulated for *S*-enantiomer incubated cells compared with *R*-enantiomer incubated cells. The representative peptides MS (Figure. 3.2) of the proteins which function are related with AD were used to show the changes in the expression level: peroxiredoxin 2, fatty acid synthase, triosephosphate isomerase, phosphoglycerate mutase 1, Peptidyl-prolyl cis-trans isomerase A and plectin 1. The changes in protein level, shown in Figure 3.3, were calculated based on the height of the peak on 4 sites of MS diagrams, 114

labeling no treatment sample, 115 labeling R enantiomer Ibuprofen treated sample, 116 labeling S enantiomer Ibuprofen treated sample, 117 labeling R/S enantiomer Ibuprofen mixture treated sample.

Protein cluster	Protein name	R:Control	S:Control	R&S:Control	Function
Metabolic Enzymes	Fatty acid synthase	1.17±0.09	0.87±0.11	0.90±0.08	Catalyzes the formation of long-chain fatty acids from acetyl-CoA, malonyl-CoA and NADPH.
	Enolase	0.80±0.13	0.85±0.05	1.25±0.18	Catalyzes the reversible conversion of 2-phosphoglycerate into phosphoenolpyruvate.
	Triosephosphate isomerase	0.86±0.03	1.29±0.18	0.90±0.08	Catalyzes D-glyceraldehyde 3-phosphate to glycerone phosphate
	Phosphoglycerate mutase 1	0.82±0.07	1.22±0.19	0.85±0.10	Interconversion of 3- and 2-phosphoglycerate with 2,3-bisphosphoglycerate
	L-lactate dehydrogenase B chain	0.85±0.04	0.86±0.12	0.89±0.02	Catalytic activity: (S)-lactate + NAD^+ = pyruvate + NADH.
Signaling regulation protein	Peroxiredoxin 2	0.89±0.14	1.35±0.11	0.86±0.09	Involved in redox regulation of the cell.
	Peroxiredoxin 6	0.72±0.19	1.36±0.33	0.74±0.14	Involved in redox regulation of the cell.
	Galectin-1	1.30±0.06	0.94±0.31	1.33±0.14	Regulate cell apoptosis and cell differentiation.
	ATP-dependent RNA helicase DDX11	1.03±0.14	0.82±0.04	1.13±0.11	Involved in cellular proliferation..
Binding protein	Annexin a2	0.92±0.14	1.19±0.28	1.04±0.14	Calcium-regulated membrane-binding protein
	GTP-binding nuclear protein Ran	0.86±0.12	1.15±0.17	0.79±0.18	Involved in nucleocytoplasmic transport.
Cytoskeleton regulation protein	Peptidyl-prolyl cis trans isomerase A	1.04±0.05	0.79±0.13	1.01±0.08	PPIases accelerate the folding of proteins during protein synthesis
	Plectin-1	0.94±0.30	1.15±0.19	0.89±0.20	Interlinks intermediate filaments with microtubules and microfilaments and anchors intermediate filaments to desmosomes or hemidesmosomes.

Table 3.1 List of differentially expressed cellular proteins. S: C was the ratio of different protein expression level in the S enantiomer incubated cells relative to the unincubated cells; R: C was the ratio of different protein expression level in the R enantiomer incubated cells relative to the unincubated cells; R/S: C was the ratio of different protein expression level in the racemic form incubated cells relative to the unincubated cells

Unused	Total	%Cov	Accessions	Contrib	Conf	Sequence
Fatty acid synthase						
21.89	21.89	17.96	FAS_HUMAN (P49327)	2.00	99.00	DTSFEQHVLWHTGGK
21.89	21.89	17.96	FAS_HUMAN (P49327)	2.00	99.00	ALGLGVEQLPVVFEDVVLHQATILPK
21.89	21.89	17.96	FAS_HUMAN (P49327)	2.00	99.00	HSQDLAFLSMLNDIAAVPATAMPFR
21.89	21.89	17.96	FAS_HUMAN (P49327)	2.00	99.00	LQLNGNLQLELAQVLAQERPK
21.89	21.89	17.96	FAS_HUMAN (P49327)	2.00	99.00	PLFLVHPIEGSTTVFHSLASR
21.89	21.89	17.96	FAS_HUMAN (P49327)	2.00	99.00	SYIIAGGLGGFGLELAQWLIQR
21.89	21.89	17.96	FAS_HUMAN (P49327)	2.00	99.00	VLLSLEHGLWAPNLHFHSPNPEIPALLDGR
21.89	21.89	17.96	FAS_HUMAN (P49327)	2.00	99.00	VTAIHIDPATHR
21.89	21.89	17.96	FAS_HUMAN (P49327)	2.00	99.00	VVEVLAGHGHLYSR
enolase						
13.5	13.5	43.65	ENOA_HUMAN (P06733)	2.00	99.00	HIADLAGNSEVILPVPAFNVINGGSHAGNK
13.5	13.5	43.65	ENOA_HUMAN (P06733)	2.00	99.00	SGETEDTFIADLVVGLCTGQIK
13.5	13.5	43.65	ENOA_HUMAN (P06733)	2.00	99.00	VNQIGSVTESLQACK
13.5	13.5	43.65	ENOA_HUMAN (P06733)	1.70	98.00	GNPTVEVDLFTSK
Triosephosphate isomerase						
8.01	8.01	45.16	TPIS_HUMAN (P60174)	2.00	99.00	DCGATWVVLGHSER
8.01	8.01	45.16	TPIS_HUMAN (P60174)	2.00	99.00	ELASQPDVDGFLVGGASLKPEFVDIINAK
8.01	8.01	45.16	TPIS_HUMAN (P60174)	2.00	99.00	KQSLGELIGTLNAAK
8.01	8.01	45.16	TPIS_HUMAN (P60174)	2.00	99.00	VAHALAEGLGVIACIGEK
Phosphoglycerate mutase 1						
6	6	18.18	PGAM1_HUMAN (P18669)	2.00	99.00	HYGGLTGLNK
6	6	18.18	PGAM1_HUMAN (P18669)	2.00	99.00	NLKPIKPMQFLGDEETVR
6	6	18.18	PGAM1_HUMAN (P18669)	2.00	99.00	TLWTVLDAIDQMWLPVVR
L-lactate dehydrogenase B chain						
4.93	4.93	18.02	LDHB_HUMAN (P07195)	2.00	99.00	GYTNWAIGLSVADLIESMLK
4.93	4.93	18.02	LDHB_HUMAN (P07195)	1.52	97.00	MVVESAYEVIK
Peroxiredoxin 2						
3	3	19.29	PRDX2_HUMAN (P32119)	2.00	99.00	KEGGLGPLNIPLLADVTR
3	3	19.29	PRDX2_HUMAN (P32119)	1.00	90.00	IGKPAPDFK
peroxiredoxin 6						
4.21	4.21	30.94	PRDX6_HUMAN (P30041)	2.00	99.00	ELAILLGMLDPAEKDEK
4.21	4.21	30.94	PRDX6_HUMAN (P30041)	2.00	99.00	LIALSIDSVEDHLAWSK
Galectin-1						
6.89	6.89	58.96	LEG1_HUMAN (P09382)	2.00	99.00	DSNNLCLHFNPR
6.89	6.89	58.96	LEG1_HUMAN (P09382)	2.00	99.00	LNLEAINYMAADGDFK
Annexin a2						

11.21	11.21	36.98	ANXA2_HUMAN (P07355)	2.00	99.00	DIISDTSGDFR
11.21	11.21	36.98	ANXA2_HUMAN (P07355)	2.00	99.00	GDLENAFLNLVQCIQNKPLYFADR
11.21	11.21	36.98	ANXA2_HUMAN (P07355)	2.00	99.00	GLGTDEDSLIEIICSR
11.21	11.21	36.98	ANXA2_HUMAN (P07355)	2.00	99.00	SALSGHLETVILGLLK
GTP-binding nuclear protein Ran						
4.72	4.72	24.07	RAN_HUMAN (P62826)	2.00	99.00	SNYNFEKPFLWLAR
4.72	4.72	24.07	RAN_HUMAN (P62826)	2.00	99.00	YVATLGVEVHPLVFHTNR
ATP-dependent RNA helicase DDX1						
8.74	8.74	17.30	DDX1_HUMAN (Q92499)	2.00	99.00	GHVDILAPTVQELAALEK
8.74	8.74	17.30	DDX1_HUMAN (Q92499)	2.00	99.00	MHNQIPQVTSDGK
8.74	8.74	17.30	DDX1_HUMAN (Q92499)	2.00	99.00	TGAFSIPVIQIVYETLK
Peptidyl-prolyl cis-trans isomerase A						
8.67	8.67	59.76	PPIA_HUMAN (P62937)	2.00	99.00	EGMNIVEAMER
8.67	8.67	59.76	PPIA_HUMAN (P62937)	2.00	99.00	HTGPGILSMANAGPNTNGSQFFICTAK
8.67	8.67	59.76	PPIA_HUMAN (P62937)	2.00	99.00	VNPTVFFDIAVDGEPLGR
8.67	8.67	59.76	PPIA_HUMAN (P62937)	2.00	99.00	VSFELFADK
Plectin 1						
5.58	5.58	14.71	PLEC1_HUMAN (Q15149)	2.00	99.00	AGLVGPEFHEK
5.58	5.58	14.71	PLEC1_HUMAN (Q15149)	2.00	99.00	YLQDLLAWVEENQHR
5.58	5.58	14.71	PLEC1_HUMAN (Q15149)	0.96	89.00	GLVGPELHDR

Table 3.2 The peptide information of the 13 unique proteins

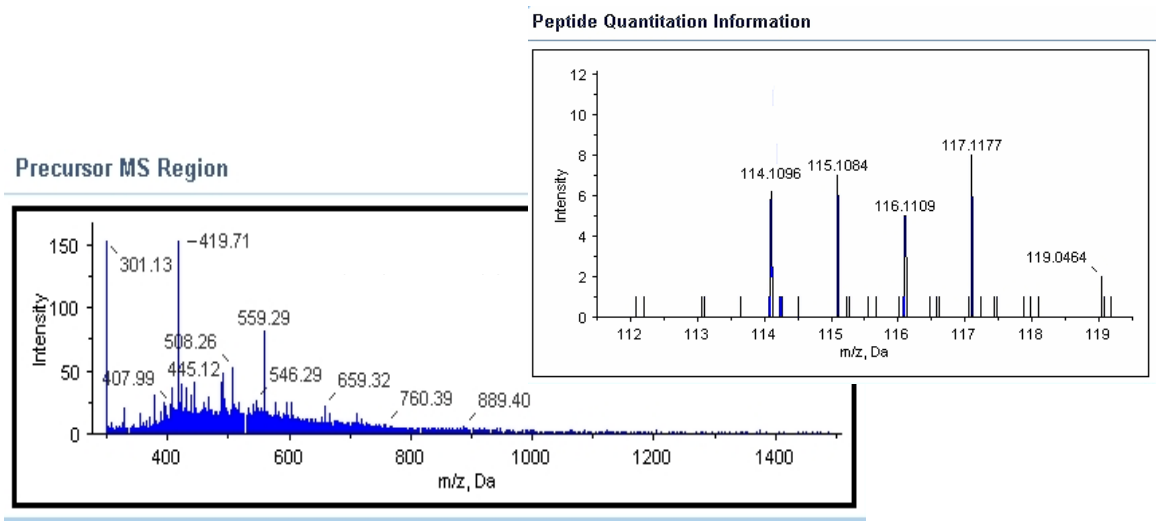

Panel A – Fatty Acid Synthase

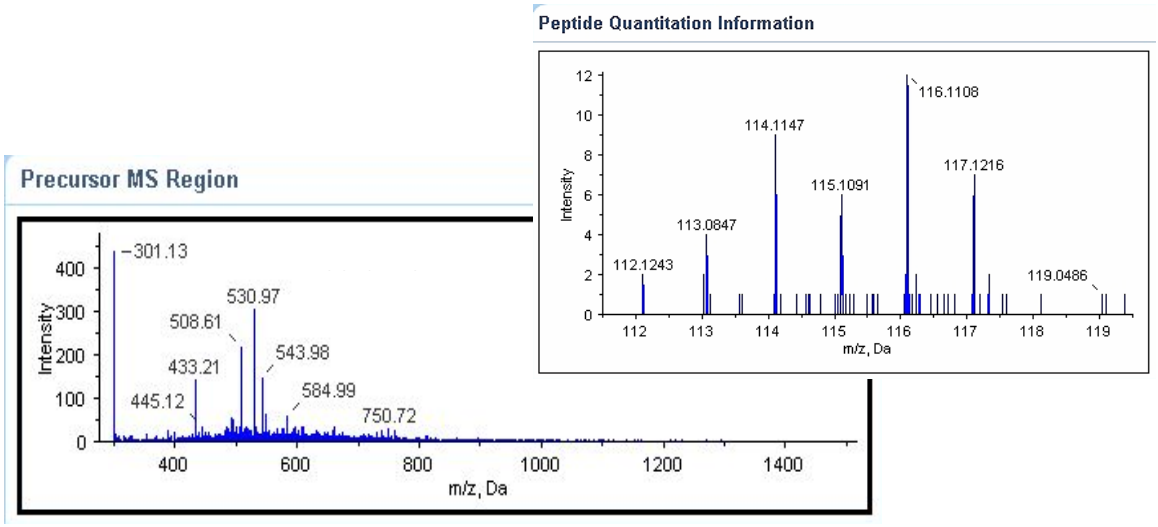

Panel B - Triosephosphate Isomerase

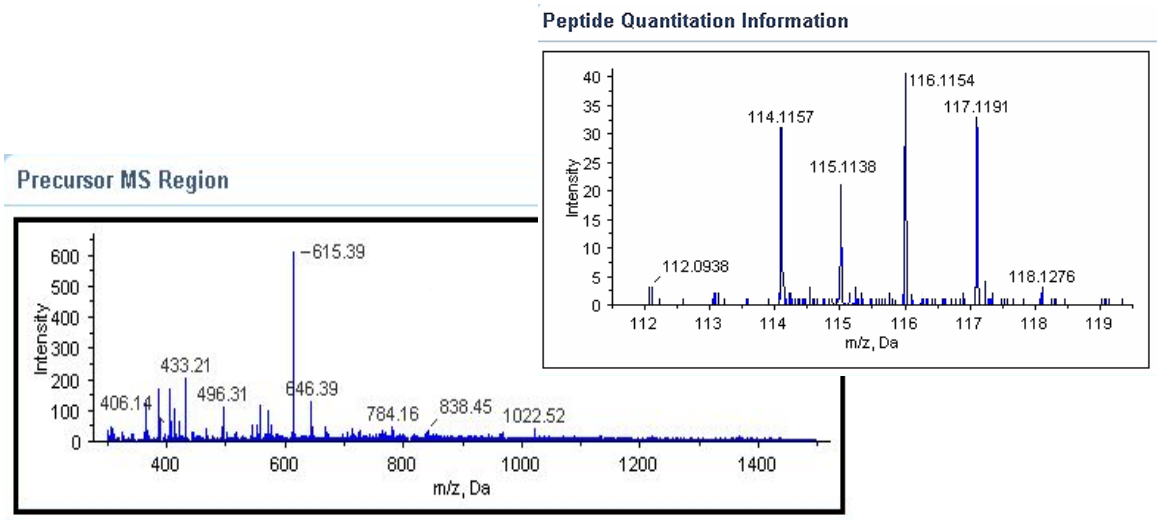

Panel C - Phosphoglycerate mutase 1

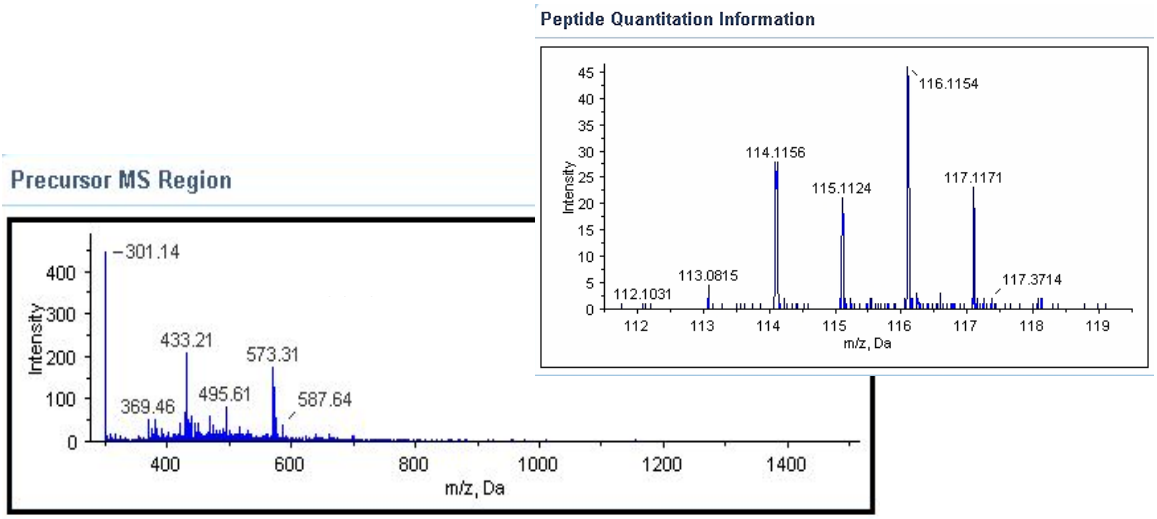

Panel D - Peroxiredoxin 2

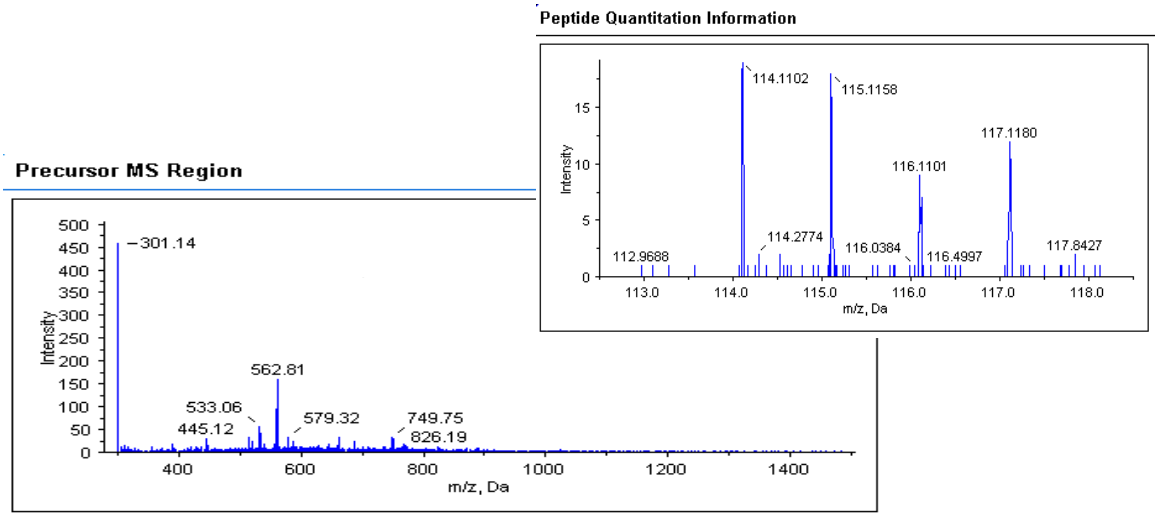

Panel E - peptidyl-prolyl cis trans isomerase A

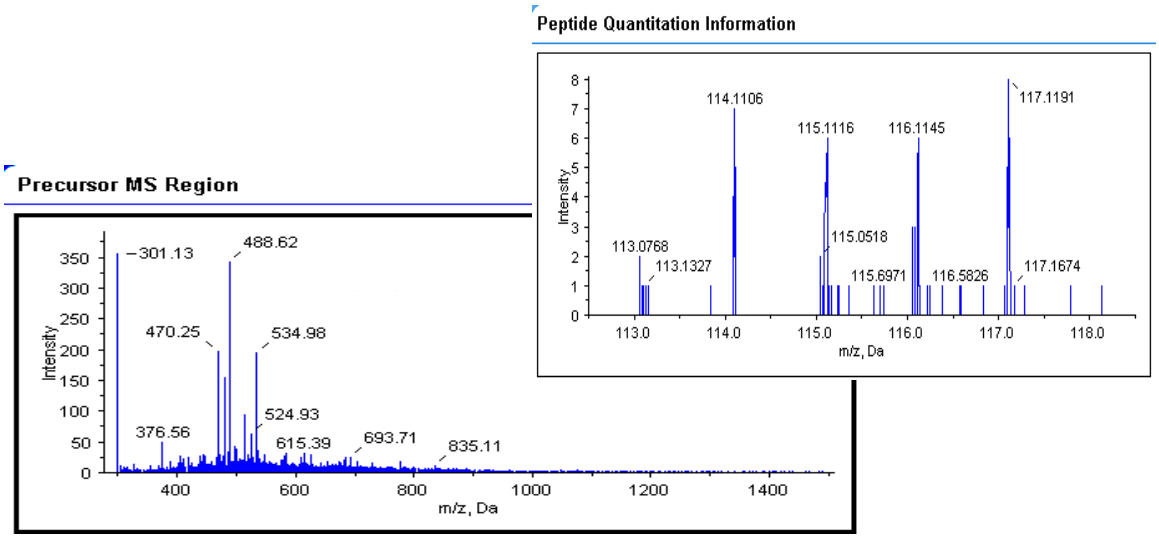

Panel F- Plectin 1

Figure 3.2 A representative MS/MS spectrum showing the peptides. The ion assignments were as follows: 114 non-incubated cells; 115, *R*-Ibuprofen incubated cells; 116, *S*- Ibuprofen incubated cells; 117 *S/R* Ibuprofen incubated cells. The peptides showed that the level changes of 115, 116 and 117 labels compared with control one labeled with 114. Panel A, the spectrum of fatty acid synthase; panel B, the spectrum of triosephosphate isomerase; panel C, the spectrum of phosphoglycerate mutase 1; panel D, the spectrum of Peroxiredoxin2; panel E, the spectrum of Peptidyl-prolyl cis trans isomerase A; and panel F, the spectrum of Plectin-1.

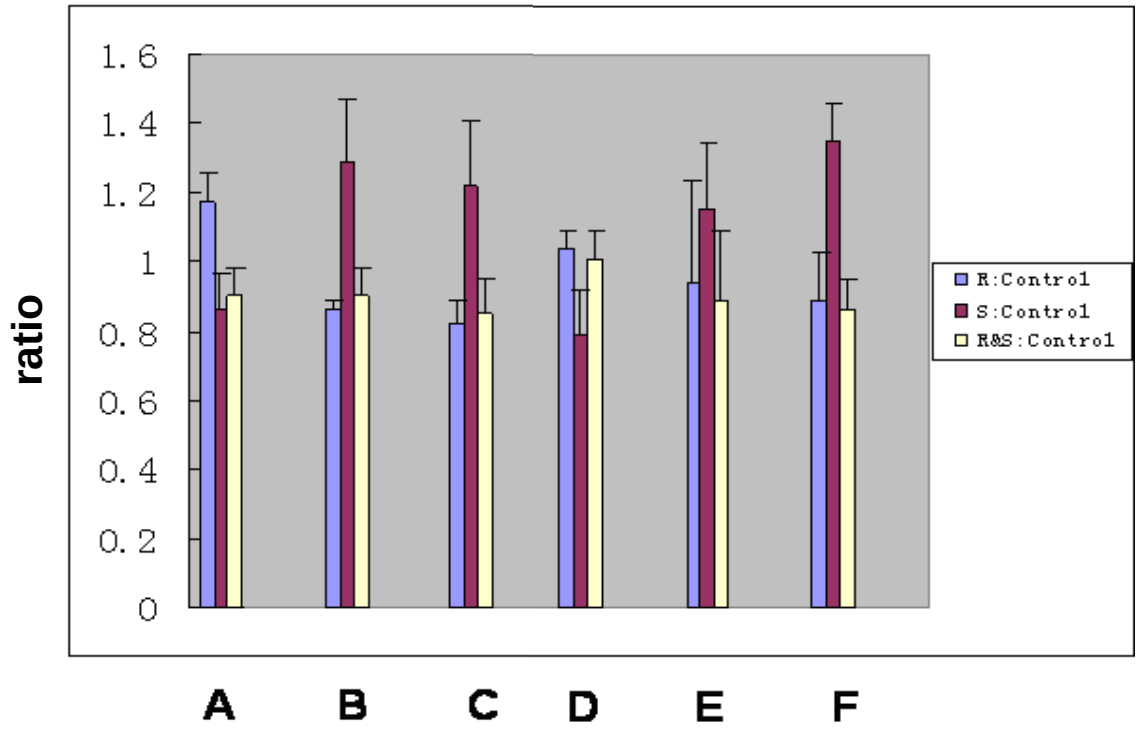

Figure 3.3 Different protein expression level of cellular proteins in *S*-enantiomer and *R*-enantiomer incubated cells. Three independent experiments were carried out for each enantiomer. Ratio between *S*-enantiomer incubated and control (without Ibuprofen incubation) cells (S:C), as well as between *R*-enantiomer incubated and control cells (R:C) was shown. Panel A, Fatty acid synthase; panel B, Triosephosphate Isomerase; panel C, Phosphoglycerate mutase 1; panel D, Peptidyl-prolyl cis trans isomerase A; panel E, Plectin-1; panel F, Peroxiredoxin2.

3.2.3 RT-PCR analysis of genes coding for differentially expressed proteins

To assess if the changes in the protein levels were significant, Real-Time RT PCR analysis was carried out for genes encoding the following proteins:

peroxiredoxin 2, fatty acid synthase, triosephosphate isomerase, phosphoglycerate mutase 1, Peptidyl-prolyl cis-trans isomerase A and plectin 1. For Real-Time RT PCR, the results based on three independent experiments for each enantiomer indicated significant changes ($p < 0.05$) at mRNA level for the 5 genes investigated (Figure 3.4) but not for Peptidyl-prolyl cis-trans isomerase A, whose mRNA level almost showed no changes between S and R enantiomer. The result indicated that Peptidyl-prolyl cis-trans isomerase A expression may not be affected in mRNA transcript level, but in protein modification or subsequent stages.

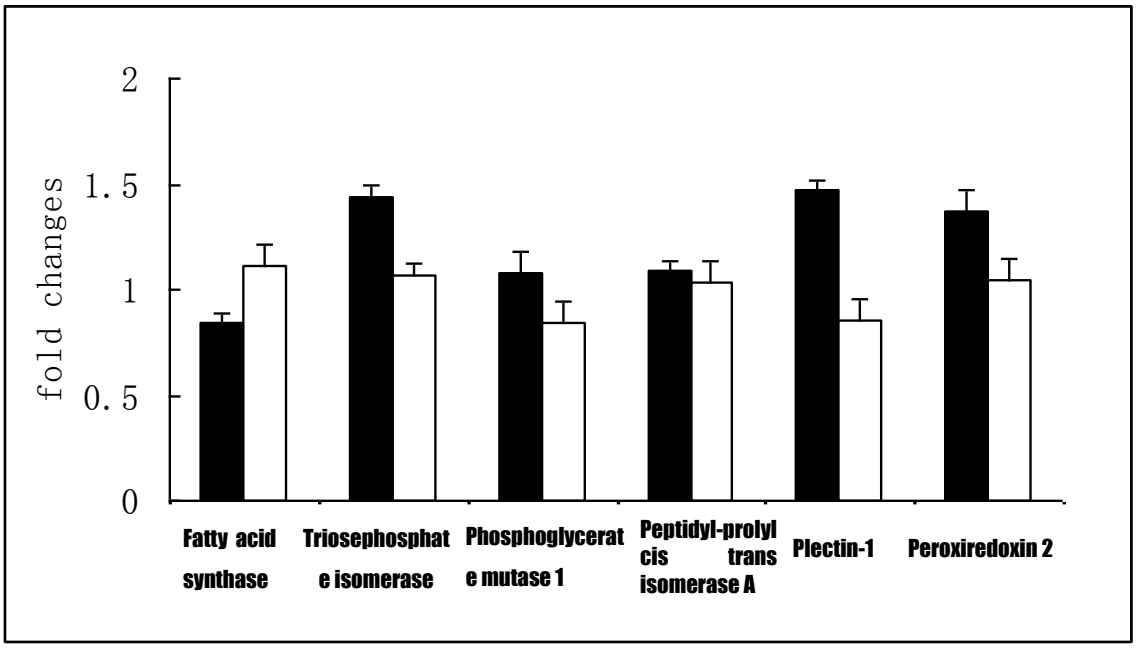

Figure 3.4 Real-Time RT PCR analysis of mRNA levels of genes coding for cellular proteins in *S*- and *R*-enantiomer of Ibuprofen incubated cells. Three independent experiments were carried out for each enantiomer. Ratio between the *S*-enantiomer incubated and control (absence of

Ibuprofen) cells (S:C) was shown as black bar, as well as ratio between the *R*-enantiomer incubated and control cells (R:C) was shown as white bar.

3.2.4 Quantitation of reactive oxygen species (ROS) of Ibuprofen treated neuroblastoma cell

Oxidative stress refers to a state in which oxidant production surpasses the endogenous antioxidant capability, possibly leading to oxidative molecular damage of the tissue [108]. Oxidative stress-associated cell damage has also been described in age-related neurodegenerative disorders, such as Alzheimer's disease [109]. In proteomics study, expression of peroxiredoxin 2, fatty acid synthase, triosephosphate isomerase and phosphoglycerate mutase 1 whose functions are related to ROS regualtion were affected by S enantiomer Ibuprofen treatment. Therefore, ROS of CRL-2273 was measured, shown in Figure 3.5. ROS of cells incubated with carboxy-H2DCFDA will cause green fluorescence, in a concentration dependent manner. The result showed S Ibuprofen can reduce ROS efficiently comparing with controls.

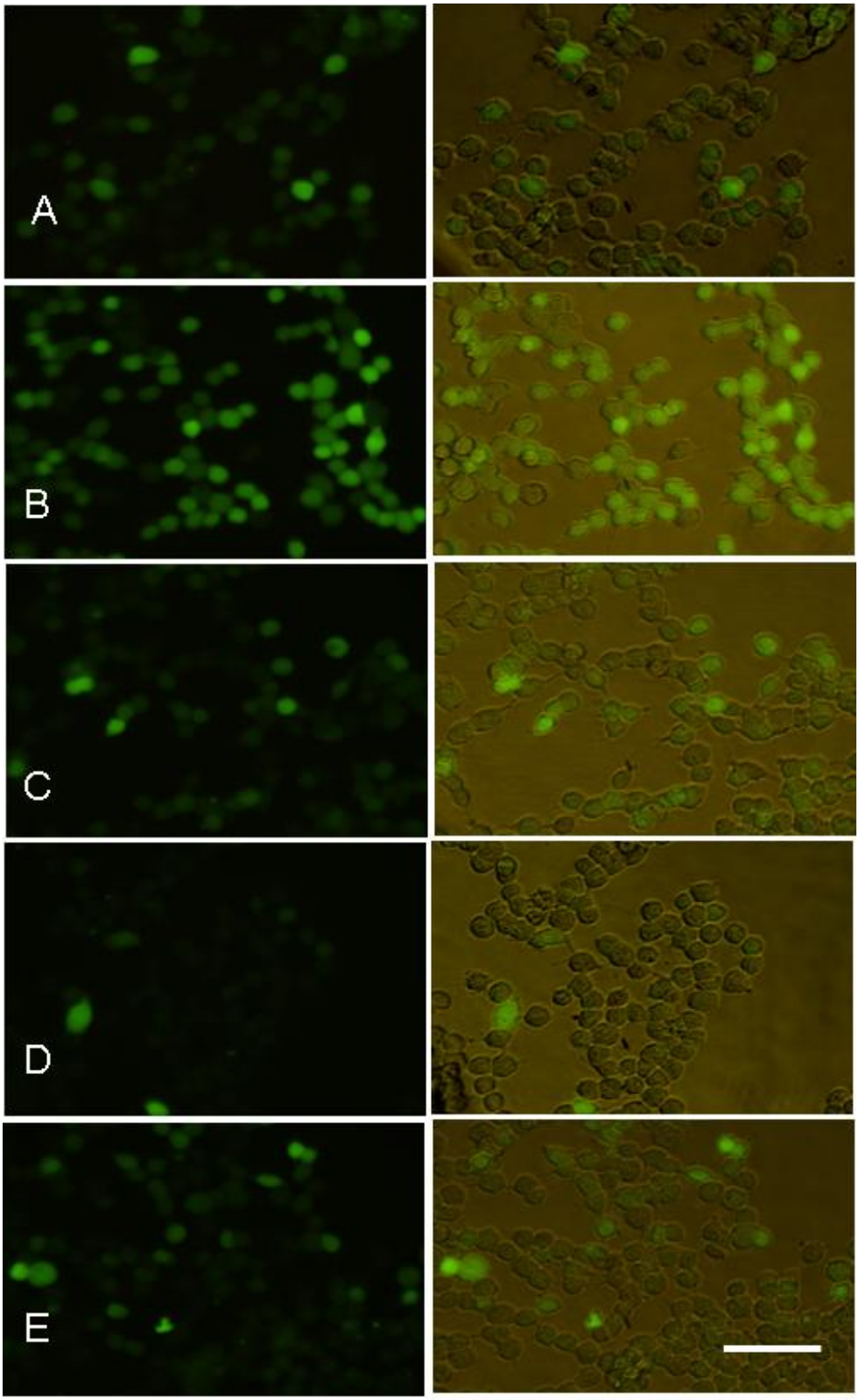
A
B
C
D
E

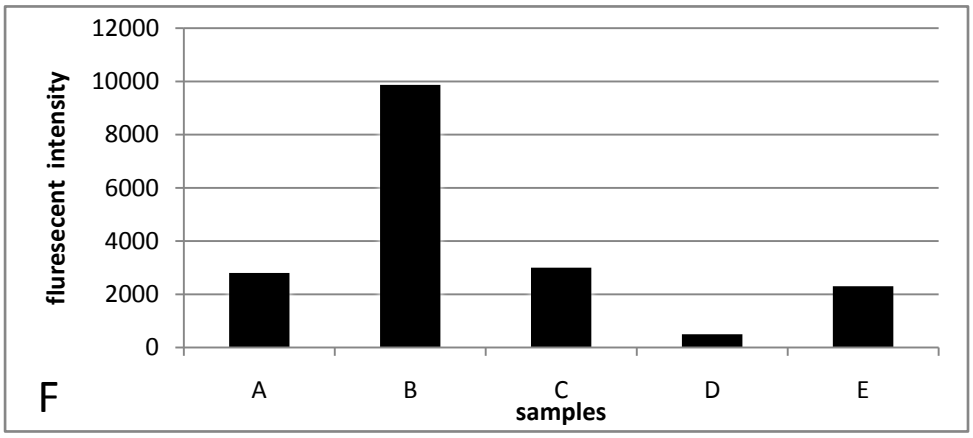

Figure 3.5 ROS level of CRL-2273 cells treated by R, S and racemic form. The pictures (Column 1) were taken under fluorescent filter. ROS of Cells incubated with carboxy- H2DCFDA will cause the green fluorescence; the cells treated by S-Ibuprofen (D) had the least fluorescence labeling cells. The pictures (column2) were taken at phase-contrast setting and overlaid with same images (column1) respectively. The cells without Ibuprofen treatment were shown as the control (A); the cells with TBHP treatment were shown as positive control (B); the cells treated by R-Ibuprofen were shown in (C); the cells treated by S-Ibuprofen were shown in (D); the cells treated by racemic-Ibuprofen were shown in (E); The scale bar is 100μm. The histogram figure showed the average fluorescence intensity/cell in different treatments (F).

3.3 Discussion

In our study, we observed that S-enantiomer Ibuprofen can reduce reactive oxygen species (ROS) of CRL-2273, shown in Figure 3.5. The peroxiredoxin (Prx) are well-known antioxidant enzymes that degrade ROS. The peroxiredoxin plays important roles in eliminating hydrogen peroxide generated. In human brain, Prx II is expressed exclusively in neurons [110]. Previous studies have also reported that Prx II

is upregulated in AD patients. Prx II is not a activate factor for AD, but a compensatory factor. It has been reported that a compensatory mechanism for upregulating Prx II might be initiated by surviving neurons to protect themselves from apoptosis [111]. Our results shown in Table 1 indicated that the peroxiredoxin 2 expression was upregulated on neuroblastoma treated by the *S*-Ibuprofen. It is possible that with increasing activity of Prx II caused by Ibuprofen, oxidant stress was decreased. This may be a reason that long time using Ibuprofen can inhibit AD improvement.

On the other hand, fatty acids are major components in the neuronal structure. About 50% of the neuronal membrane is composed of fatty acids. However, the degree of saturation of fatty acids is critical in determining the risk for the onset of AD. Saturated fatty acids may directly induce aggregation of tau as well as Aβ filaments. Aggregated Aβ filaments have been shown to exert enhanced neurotoxicity and may also induce increased phosphorylation of tau [112]. Based on our result, the *S*-Ibuprofen inhibited the activity of fatty acid synthase in neuroblastoma, thereby reduced the fatty acid production. The low fatty acid can prevent tau protein aggregation and Aβ filaments which are important factors for AD. It is also possible that Ibuprofen may promote fatty acid metabolism to produce fatty acid derivatives by positive feedback signal from inhibition of fatty acid synthase. The peroxisome proliferator-activated receptor a (PPARa) are activated by a range of fatty acid derivatives. Ibuprofen activates PPARa which is neuro-protective and may have a protective role in the neuroinflammatory aspect of AD [113]. Therefore, Ibuprofen

may reduce the severity of AD via the production of fatty acid derivatives to active PPARa receptor. Furthermore, the fatty acid oxidation is the main ROS effect in damaging the neuroplasma causing AD [114]. The reducing fatty acid synthesis can reduce the overall process of fatty acid oxidation. Taken together, Ibuprofen may reduce the oxidative stress effects on neurodegenerative disorder.

Phosphoglycerate mutase 1 (PGM1) is a glycolytic enzyme that catalyzes the interconversion of 3-phosphoglycerate and 2-phosphoglycerate. Glucose metabolism is the basis of cerebral energy under normal conditions. Hence, the necessity for glucose in brain function has been considered solely due to ATP production. These lines of evidence suggest that glycolysis plays an important role in maintaining normal synaptic function [109, 115, 116]. Some study find, PGM1 which participates in the glycolytic pathway is significantly oxidized in AD hippocampus. They observe a significant increase in oxidation of PGM1 and a decrease in protein expression [117]. In our study, S- inbuprofen incubated cells showed higher PGM1 expression comparing with control. Ibuprofen may compensate the PGM1 activity and expression which is found to be decreased in AD; in addition, the increased expression and activity of PGM1 following the exposure to Ibuprofen may also interrupt the pathway for the formation of oxidized PGM1. This may be another target site for Ibuprofen in relieving AD.

Our results were therefore consistent with the published reports in that fatty acid synthase, phosphoglycerate mutase-1 and peroxiredoxin 2 regulate the formation of oxidative stress. The beneficial effects of Ibuprofen in relieving AD seems to

converge through one mechanism, which is to reduce the oxidative stress in cellular generation [118, 119], as our result showed in Figure 3.5.

Our result further indicated that Ibuprofen may regulate other proteins which affect AD not by oxidative stress pathway. For example, peptidyl-prolyl cis trans isomerase A (CyP-A) was found to be at significantly ($p < 0.05$) lower level in cells incubated with the S-enantiomer of Ibuprofen (Table 3.1). CyP-A is a member of the immunophilin family of proteins, which catalyses the interconversion of *cis* and *trans* peptide bonds and is therefore considered to be important for protein folding. Inhibitors of pp-isomerase have recently been shown to be neuroprotective in several experimental models. The N-Me-Val-4-cyclosporin A, inhibitor of CyP-A, inhibits mouse hippocampal neuronal culture death significantly by blocking of mitochondrial permeability transition pore. In addition, the immunophilin ligand FK506, inhibiting the activity of CyP-A, acts as a protective agent against neuronal death of the rat substantia nigra, probably by inhibiting expression of the inducible transcription factor c-Jun and its N-terminal phosphorylation. These reports suggest that the inhibitors of immunophilin family proteins may function as neuroprotective factors and may potentially dampen the initiation and/or progression of neurodegeneration [120]. In our study, a lower CyP-A expression found in *S*-Ibuprofen treated cells suggested a mechanism of neuroprotective action.

Plectin is a high molecular weight protein that serves as a versatile cytoskeletal cross-linker molecule. Mutations of the human plectin gene have recently been implicated in autosomal recessive disorder epidermolysis bullosa simplex with

muscular dystrophy (EBS-MD). A subgroup of EBS-MD patients displays signs of a neurodegenerative disorder suggesting that the expression of defective plectin may also interfere with the structural and functional integrity of the human central nervous system. Extensive plectin immunoreactivity of reactive astrocytes, characterized by cellular hypertrophy, has been noted in areas with neuronal cell loss and concomitant astrogliosis. The upregulation of plectin, therefore, represent a general feature of reactive astrocytes [121]. In our study, the higher expression of plectin in *S*-Ibuprofen incubated cell suggested a neuroprotective role for Ibuprofen.

In conclusion, our results suggested that the *S*-Ibuprofen may offer protection for AD through reducing oxidized stress. Its combined effects through differential regulation of fatty acid synthase, phosphoglycerate mutase 1 and peroxiredoxin 2 may contribute to the decrease in ROS, a pathological factor for the development of AD. The pathways related with ROS were summarized in Figure 3.6. In addition, Ibuprofen may also be neuroprotective through other pathways, for example by decreasing CyP-A expression or increasing plectin expression. Therefore, Ibuprofen seemed to attenuate the cellular phenotypes that resemble AD through a number of cellular pathways. Together with group's recent investigation by similar approach [122], LC-MS/MS analysis holds the promise of effectively depicting cellular protein profile in response to various drugs which in turn should be helpful in our understanding on their mechanisms of actions.

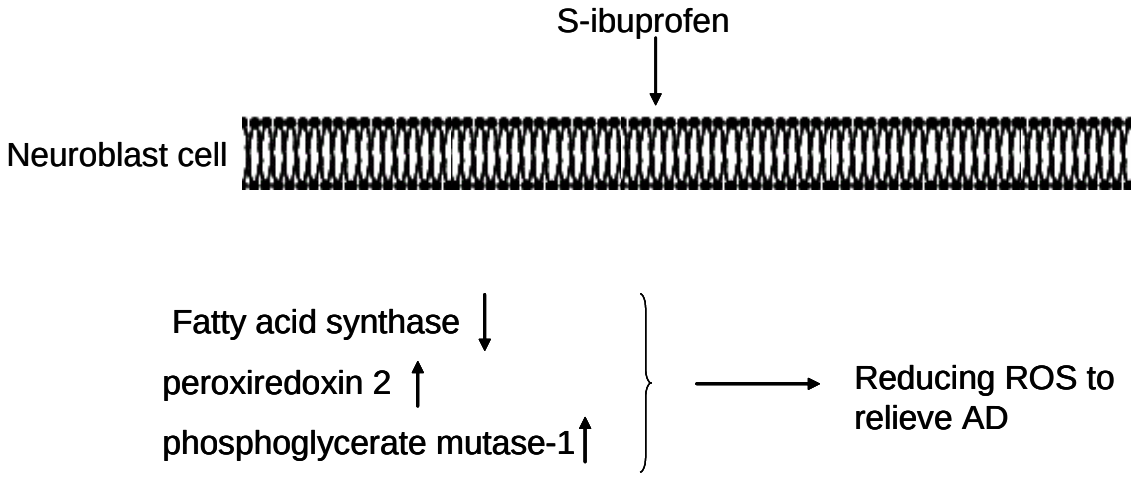

Figure 3.6 S-Ibuprofen regulate ROS pathway to relieve AD. S-Ibuprofen upregulate peroxiredoxin 2 and phosphoglycerate mutase-1 and downregulate fatty acid synthase to relieve AD by ROS reducing.

Chapter 4

ITRAQ-coupled 2D LC-MS/MS proteomics analysis on HCC angiogenesis induced by HBV replication [b]

4.1 Introduction:

More than 350 million people worldwide have been chronically infected by hepatitis B virus resulting in high risk of developing hepatitis, cirrhosis and hepatocellular carcinoma (HCC) which is one of the commonest cancer in the world [123, 124]. A persistent HBV infection is usually implicated the liver cirrhosis that could progress and develop to HCC [125]. Although the relationship between HCC and persistent HBV infection has been well documented, the mechanisms by which HBV infection leads to tumor formation are not clear.

Angiogenesis, formation of new blood vessels, is required for a variety of physiological processes and for the progression of tumor growth. An avascular tumor rarely grows larger than 2 to 3mm^2, but once a tumor becomes vasularized, the progression of tumor growth is rapid [45], as this expansion of the vascular network is essential to provide all the nutrients and oxygen needed for tumor cell proliferation, shown in Figure 4.1. Tumor-induced angiogenesis requires migration and remodeling of endothelial cells derived from pre-existing blood vessels [126].

---

[b] Reproduced in part with permission from [Zhang, J., Niu, D., Sui, J., Ching, C. B., Chen, W. N., Protein profile in hepatitis B virus replicating rat primary hepatocytes and HepG2 cells by iTRAQ-coupled 2-D LC-MS/MS analysis: Insights on liver angiogenesis. *Proteomics* 2009, *9*, 2836-2845.] [127] reference copyright [2009] @ wiley-VCH. Zhang Jianhua designed the experiments, performed most of the experiments, analyzed the data and wrote the paper.

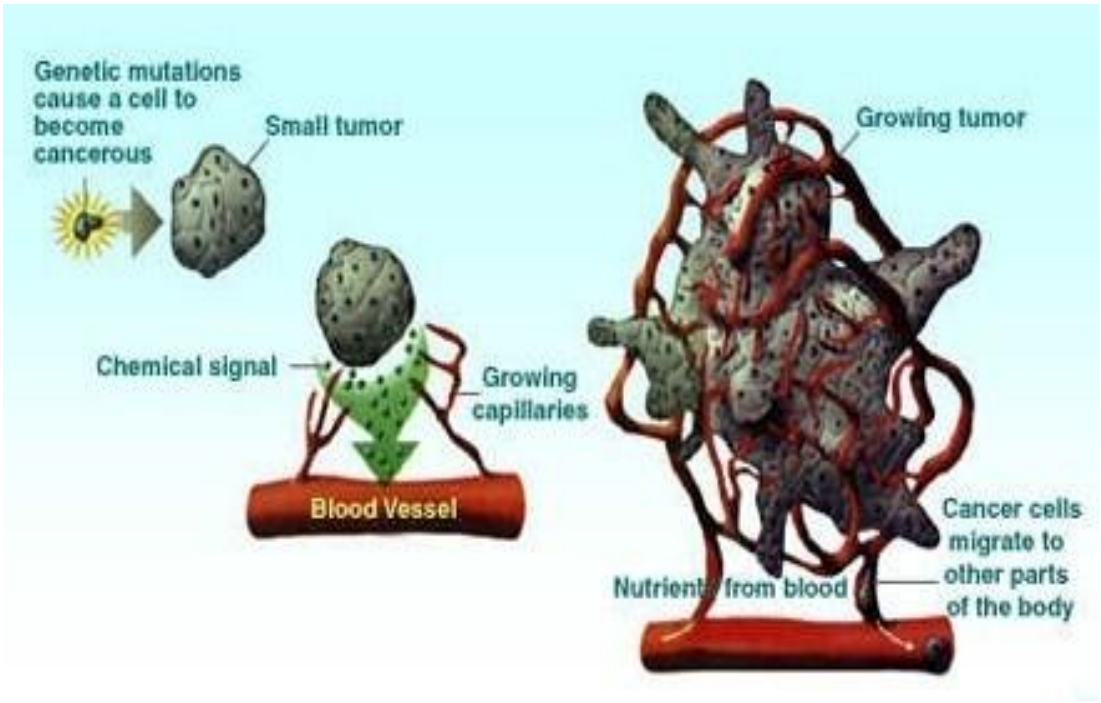

Figure 4.1 Illustration of tumor angiogenesis. (www.dobimedical.com/angio.htm) cancer cells divide and grow with angiogenesis assistance, ultimately become metastasis.

Most chronic liver diseases are characterized by fibrosis and inflammation. During the fibrogenic process, an excessive amount of endothelial cell matrix is synthesized and accumulated. Fibrotic tissues provide resistance to blood flow and oxygen delivery, thus cells become hypoxic. Stimulation of hypoxia-inducible factors leads to an angiogenic switch, causing the upregulation of vascular endothelial growth factor among other proangiogenic factors, and finally results in the formation of new blood vessels [128]. In patients with chronic viral hepatitis, a significant change in the vascular architecture takes place with neovascularization, suggesting that angiogenesis could contribute to the increased risk of HCC in patients with HBV and / or HCV chronic infection. The appearance of endothelial cells (ECs) forming characteristic capillary structures in inflamed portal tracts from chronic viral hepatitis

has been demonstrated. The production of proinflammatory eicosanoids (PEs) by cyclooxygenase-2 (Cox2) plays a role in neovasculature formation as PEs selective antagonists blocks angiogenesis both in experimental animals and in humans. While the mechanism of action is not fully understood, induction of proliferation and reduction of apoptosis in angiogenic ECs have been observed [129]. In addition, local production of nitric oxide (NO) as a result of the over expression of inducible NO synthase in the livers of patients with hepatitis C or B virus infection may also participate in the angiogenic response by inducing vasodilation [130, 131]. Furthermore, the increased expression of VEGF and HGF in chronic viral hepatitis may contribute to the enhancement of vascular permeability [131]. HBV promotes angiopoietin-2 expression in liver tissue, resulting in an enhanced angiogenesis by VEGF pathway [132]. Hepatis B Virus X protein (HBx) has been shown to stabilize the HIF (hypoxia induce factor), leading to an upregulation of the VEGF expression to induce angiogenesis [125, 133].

Despite the recent advances in individual cellular factors and pathways, a comprehensive and coordinated mechanism in the HBV-induced angiogenesis remains to be established. Such an investigation can be carried out in our cell-based HBV replication system, in which a plasmid-based replicative HBV genome can be introduced into various types of cells by transient transfection and the resulting cellular response can be analyzed [88].

In this study, the protein profiles of rat primary hepatocytes and human hepatocellular cell line HepG2 cells treated by HBV genome were compared. To the

best of our knowledge, no proteomic studies have been reported on HCC angiogenesis caused by HBV. Based on our results, Fumarate hydratase was down-regulated on both hepatocyte and HepG2 transfected by HBV, while Tryptophanyl-tRNA synthetase was up-regulated only in HepG2 transfected by HBV. The expression changes of these two enzymes may cause and keep HCC formation by regulating tumor angiogenesis. The variedly-expressed proteins could be used to elucidate the mechanism of HBV on HCC formation and also be used as the target of HCC therapy.

4.2 Results

4.2.1 Rat primary hepatocytes (RPHs) support HBV genome expression:

Although a cell-based HBV replication had been successfully established in HepG2 cells, the use of these cells in investigating angiogenesis-associated hepatocarcinogenesis may not be reflective of the underlying mechanism as these cells were derived from HCC. To overcome this limitation, the possibility of a cell-based HBV expression in rat primary hepatocytes (RPHs) was explored in this study. RPHs were isolated by collagenase perfusion method [134], and displayed typical characteristics such as being binucleated and containing lipid droplets (panel C, Figure 4.2). A closer microscopic examination indicated that the purity of the isolated RPHs was more than 95% and their viability was more than 90% as measured by trypan blue staining experiment (*data not shown*).

To determine whether HBV replication was supported in the isolated RPHs, pcDNA 3.1 plasmid carrying the replicative HBV genome was introduced into these cells by transient transfection. The efficiency of transient transfection was indicated

by co-transfecting plasmid carrying GFP protein coding gene, in either RPHs (panel A, Figure 4.2) or HepG2 cells (panel B, Figure 4.2). Results of the measurement of HBsAg and core gene expressed in transfected RPHs and HepG2 (Section B, Figure 4.2) indicated that HBV replication occurred in RPHs, as those in HepG2 cells.

Section A

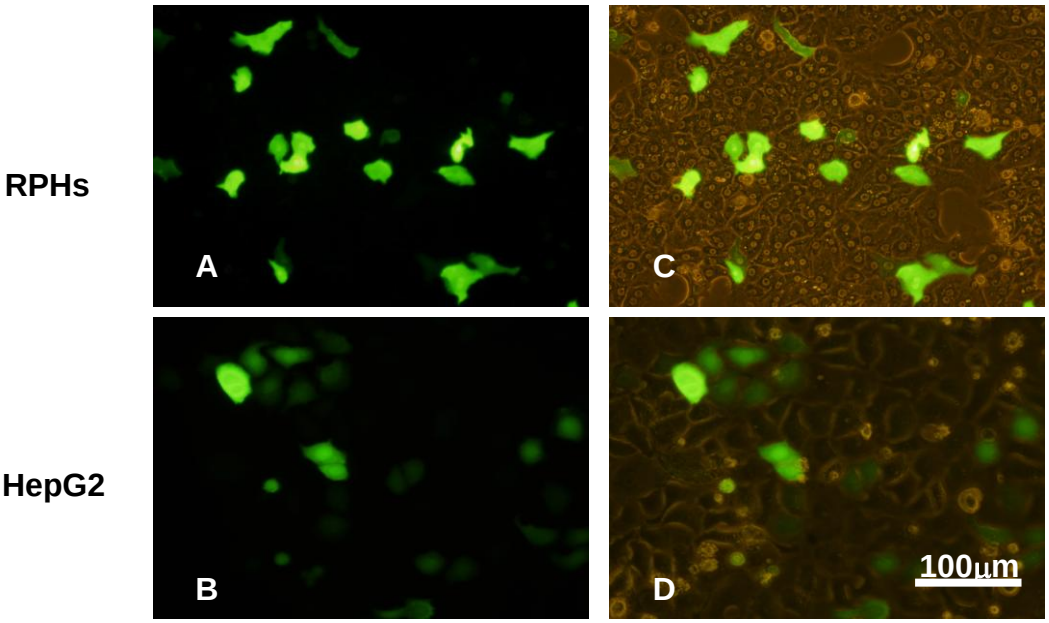

Section B

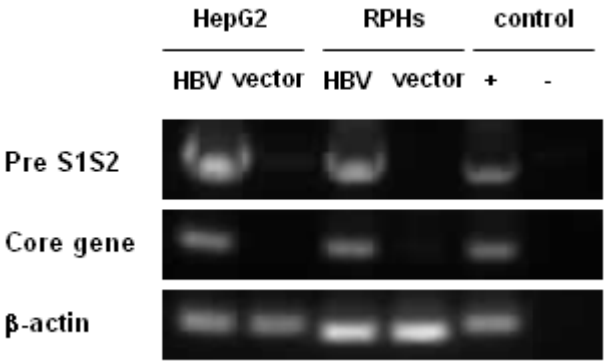

Figure 4.2 HBV genome expressions in RPHs and HepG2 Cells. Section A, transfection efficiency in RPHs and HepG2 cells was evaluated by green fluorescent protein (GFP) expression. Panel A and C represented RPHs and panel B and D for HepG2 cells. Panel A and B were images of fluorescent microscope using FITC filter. Panel C and D were images of fluorescent microscope using both FITC filter and phase-contrast overlaid. The scale bar was 100μm. Section B, RT-PCR analysis of expression of HBsAg and core gene were tested in RPHs and HepG2 cells transfected by either plasmid containing HBV replicative genome or the empty vector pcDNA3.1. Positive control was carried out with HepG2.2.15 RNA. Negative control referred to reaction mixture without RNA.

4.2.2 HBV replication induces angiogenesis

Tube formation is an important characteristic of endothelial cell undergoing angiogenesis [125]. Tube formation assay is widely used to simulate the reorganization stage of angiogenesis. The assay measures capillary-like structures formed by endothelial cells after cells seeded on the extracellular matrix-like reagent. The effects of HBV replication on angiogenesis was investigated by tube formation assay using HUVEC cells. To mimic the *in vivo* close proximity of EC cells with regard to the hepatocytes, the HUVEC cells were cultured in condition mediums of HepG2 and RPHs transfected with the replicative HBV genome. As a control, HUVEC cells were also cultured in medium of RPHs and HepG2 cells transfected with the empty pcDNA3.1 vector. Results indicated that a significantly higher number of EC branch points were observed in condition medium of RPHs (panel A.3, Figure

4.3) and HepG2 cells (panel B.3, Figure 4.3) transfected with the replicative HBV genome, as compared with the branch points in condition medium of the corresponding cells transfected with the empty vector (panel A.2 and panel B.2 respectively, Figure 4.3). Our tube formation assay suggested that HBV replication was able to induce angiogenesis.

1.

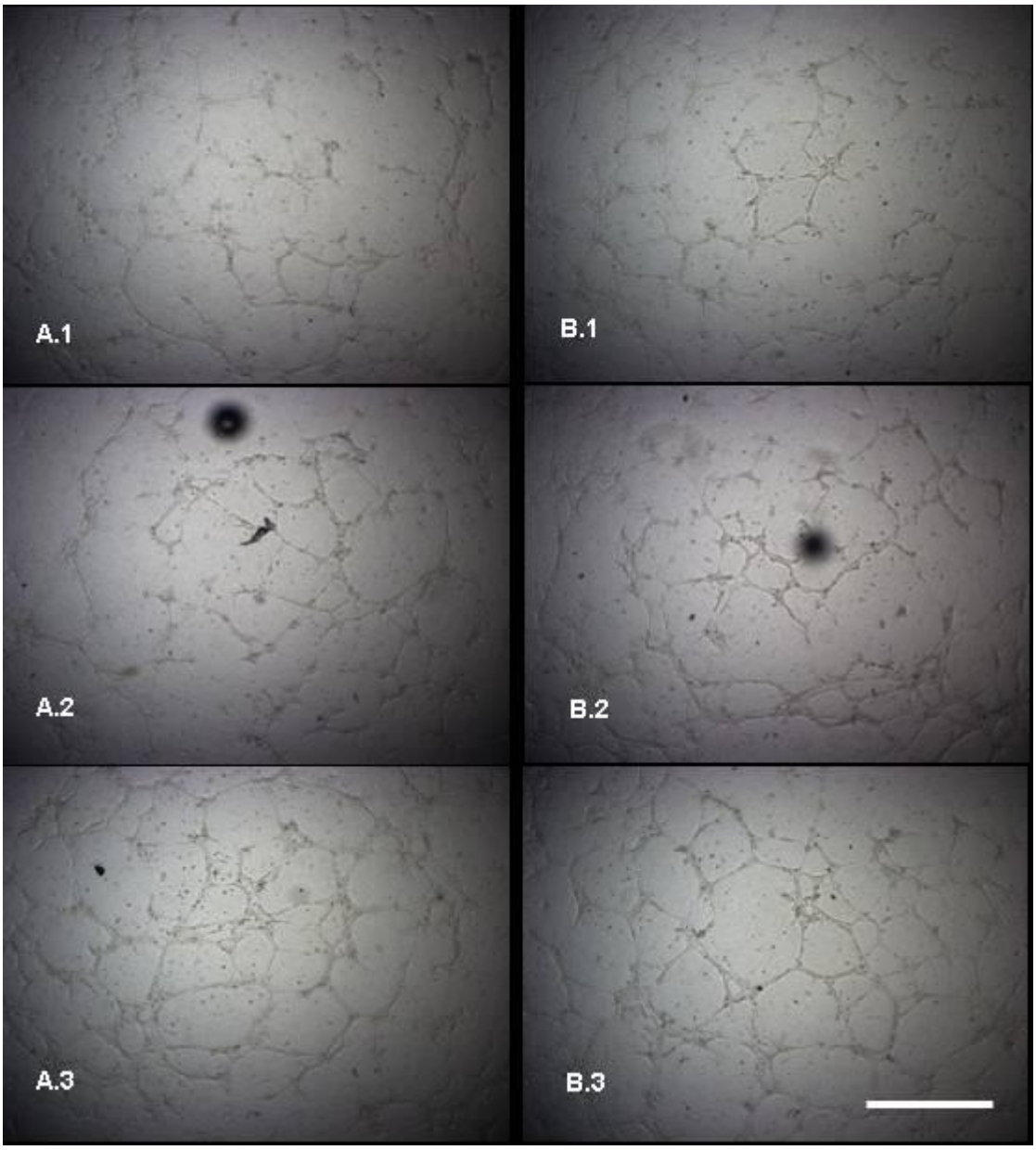

2.

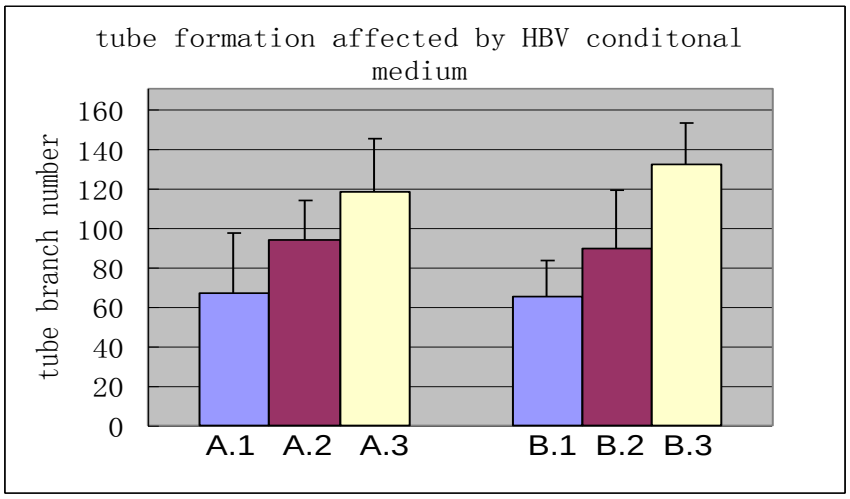

Figure 4.3 HBV replication and HUVEC tube formation in growth factor-reduced Matrigel.

1. Used growth factor-reduced Matrigel, representative photos showed the stimulated effects of two condition medium: HepG2 transfected HBV (A.3) and hepatocyte transfected HBV (B.3) on HUVEC tube formation comparing with 2% FBS CSC medium from HepG2 (A.1) and hepatocyte (B.1), and condition medium: HepG2 (A.2) transfected vector, hepatocyte (B.2) transfected vector. The scale bar was 400 μm. 2. Quantitative of tube formation was showed in histogram figure. The tube formation was quantitative by method of branch point counting. X axis was the number of cell branch points, and Y axis was the samples.

4.2.3 Proteomics analysis identifies enzymes associated with angiogenesis

To establish whether the angiogenesis induced by HBV replication shared the same cellular pathways in RPHs and HepG2 cells, the global protein profile was examined by LC-MS/MS analysis between RPHs transfected with plasmid with or without the replicative HBV genome, as well as between HepG2 cells transfected

with plasmid with or without the replicative HBV genome. The proteins profiles were analyzed in three independent transfections. The number of proteins detected by three independent LC/MS experiment was 107, 99 and 113 respectively for HepG2 cells transfected with the replicative HBV genome; and 165, 229 and 201 respectively for hepatocytes transfected with the replicative HBV genome.

Under the protein selection criteria (seen at Materials and Methods), 14 proteins which displayed differential levels between RPHs transfected with the replicative HBV genome and the control hepatocytes transfected with empty vector were detected (Table 4.1). On the other hand, 18 proteins with differential levels between HepG2 cells transfected the replicative HBV genome and the control HepG2 cells transfected with the empty vector were detected (Table 4.2). The proteins were clustered in 4 categories based on their function: metabolic enzymes, signaling pathway, binding proteins and cytoskeleton. For metabolic enzymes, either increased or decreased levels were observed in both RPHs and HepG2 cells transfected with the replicative genome. While a similar pattern of increased and decreased levels was seen for signaling proteins in HepG2 cells transfected with the replicative HBV genome (Table 4.2), a more consistently increased level in signaling proteins was observed in RPHs transfected with the replicative HBV genome (Table 4.1).

Among the selected proteins, fumarate hydratase (FH) and tryptophanyl-tRNA synthetase (TrpRS) had been implicated in tumor angiogenesis. LC/MS results of the peptides were shown as Table 4.3 and reprehensive peptide was shown in Figure 4.4. The level of FH was lower in both RPHs and HepG2 transfected with the replicative

HBV genome, with a decrease of 0.89 fold and 0.76 fold respectively. In contrast, the level of TrpRS was higher by 1.8 fold in HepG2 cells while it was not detected in RPHs.

To assess if the changes in the protein levels were significant, RT-PCR analysis was carried out for genes encoding both FH and TrpRS. Results based on three independent experiments indicated significant changes ($p < 0.05$) for FH whereas TrpRS mRNA showed no significance changes (Figure 4.5).

Protein cluster	Protein name	Protein ID	HBV:vector	Function
Catalytic Enzymes	3-hydroxyisobutyrate dehydrogenase	P29266|3HIDH_RAT	1.21± 0.17	3-hydroxy-2-methylpropanoate + NAD+ = 2-methyl-3-oxopropanoate + NADH
	Tricarboxylate transport protein	P32089|TXTP_RAT	0.86± 0.13	Involved in citrate-H(+)/malate exchange. it provides a carbon source for fatty acid and sterol biosyntheses, and NAD+ for the glycolytic pathway
	Triosephosphate isomerase	P48500|TPIS_RAT	1.2± 0.09	Catalyzes D-glyceraldehyde 3-phosphate to glycerone phosphate
	Fumarate hydratase	P14408|FUMH_RAT	0.89±0.03	(S)-malate = fumarate + H2O
	Acetyl-CoA acetyltransferase	P17764|THIL_RAT	1.29±0.18	Plays a major role in ketone body metabolism.
	Aldehyde dehydrogenase	Q66HF8|AL1B1_RAT	0.70±0.13	ALDHs play a major role in the detoxification of alcohol-derived acetaldehyde.
	Argininosuccinate lyase	P20673|ARLY_RAT	1.23±0.11	2-(N(omega)-L-arginino)succinate = fumarate + L-arginine.
	Cytochrome P450 2D	P10633|CP2D1_RAT	1.21±0.04	It oxidizes a variety of structurally unrelated compounds, including steroids, fatty acids, and xenobiotics.
	Succinyl-CoA ligase [GDP-forming] subunit alpha	P13086|SUCA_RAT	1.27±0.14	GTP + succinate + CoA = GDP + phosphate + succinyl-CoA.
Signaling protein	ES1 protein homolog	P56571|ES1_RAT	1.26± 0.12	Involved in redox regulation of the cell.
	14-3-3 protein	P62260|1433E_RAT	1.21±0.03	Binds to a large number of partners, usually by recognition of a phosphoserine or phosphothreonine motif.
	Macrophage migration inhibitory factor (MIF)	P30904|MIF_RAT	1.13± 0.005	regulating the function of macrophage in host defense. Also acts as a phenylpyruvate tautomerase.

Binding proteins	T-complex protein 1 subunit	Q68FQ0|TCPE_RAT	0.85±0.23	Molecular chaperone; assist the folding of proteins upon ATP hydrolysis.
Cytoskeletal Proteins	Tubulin	Q6AYZ1|TBA6_RAT	1.14±0.08	Tubulin is the major constituent of microtubules.

Table 4.1 protein cluster in rat primary hepatocyte

Protein cluster	Protein name	Protein ID	HBV:vector	Function
Catalytic Enzymes	Neutral alpha-glucosidase AB precursor	GANAB_HUMAN(Q14697)	1.41±0.22	Cleaves glucose residues from the Glc(2)Man(9)GlcNAc(2) oligosaccharide precursor of immature glycoproteins.
	Tryptophanyl-tRNA synthetase	SYW_HUMAN(P23381)	1.79±0.20	ATP + L-tryptophan + tRNA(Trp) = AMP + diphosphate + L-tryptophyl-tRNA(Trp)
	Delta3,5-delta2,4-dienoyl-CoA isomerase	ECH1_HUMAN (Q13011)	0.75±0.10	Isomerization of 3-trans,5-cis-dienoyl-CoA to 2-trans,4-trans-dienoyl-CoA
	NAD(P)H dehydrogenase	NQO1_HUMAN (P15559)	1.21±0.16	The enzyme apparently serves as a quinone reductase in connection with conjugation reactions of hydroquinons involved in detoxification pathways
	Fumarate hydratase	FUMH_HUMAN (P07954)	0.76±0.08	(S)-malate = fumarate + H2O; Also acts as a tumor suppressor
	Peroxiredoxin 1	PRDX1_HUMAN (Q06830)	0.62±0.23	2 R'-SH + ROOH = R'-S-S-R' + H2O + ROH; Involved in redox regulation of the cell.
	Peroxiredoxin 6	PRDX6_HUMAN (P30041)	1.22±0.12	2 R'-SH + ROOH = R'-S-S-R' + H2O + ROH. May play a role in the regulation of phospholipid turnover as well as in protection against oxidative injury.
	Transitional endoplasmic reticulum ATPase (TER ATPase)	TERA_HUMAN (P55072)	1.20±0.11	Necessary for the fragmentation of Golgi stacks during mitosis and for their reassembly after mitosis. Involved in the formation of the transitional endoplasmic reticulum (tER).
Signaling protein	4F2 cell-surface antigen heavy chain (4F2hc)	4F2_HUMAN(P08195)	1.47±0.01	Involved in sodium-independent, high-affinity transport of large neutral amino acids. Required for normal and neoplastic cell growth.
	Protein NDRG1	NDRG1_HUMAN (Q92597)	0.69±0.17	May have a growth inhibitory role.
	Rab GDP dissociation inhibitor beta (Rab GDI beta)	GDIB_HUMAN (P50395)	1.46±0.25	Regulates the GDP/GTP exchange reaction of most Rab proteins by inhibiting the dissociation of GDP from them, and the subsequent binding of GTP to them.
	Barrier-to-autointegration factor	BAF_HUMAN (O75531)	0.63±0.13	Plays fundamental roles in nuclear assembly, chromatin organization, gene expression and gonad development.
Binding	Calreticulin precursor	CRTC_HUM	0.56±0.05	Molecular calcium binding chaperone

proteins		AN(P27797)		promoting folding, oligomeric assembly and quality control in the ER via the calreticulin/calnexin cycle.
	Collagen-binding protein 2 precursor	SPH2_HUMAN(P50454)	1.78±0.36	Binds specifically to collagen. Could be involved as a chaperone in the biosynthetic pathway of collagen.
	60 kDa heat shock protein, mitochondrial precursor (Hsp60)	CH60_HUMAN (P10809)	0.77±0.11	Implicated in mitochondrial protein import and macromolecular assembly. Interacts with HBV protein X.
	Heterogeneous nuclear ribonucleoprotein (hnRNP)	HNRPD_HUMAN (Q14103)	1.23±0.20	Binds with high affinity to RNA molecules that contain AU-rich elements (AREs). Also binds to double- and single-stranded DNA sequences and functions a transcription factor.

Table 4.2 Protein cluster in HepG2 cells

Unused	Total	%Cov	Accessions	Conf	Sequence
Fumarate hydratase of HepG2 cell					
3.38	3.38	26.08	FUMH_HUMAN (P07954)	99.00	ETAIELGYLTAEQFDEWVKPK
3.38	3.38	26.08	FUMH_HUMAN (P07954)	91.00	IPVHPNDHVNK
3.38	3.38	26.08	FUMH_HUMAN (P07954)	54.00	SQSSNDTFPTAMHIAAAIEVHEVLLPGLQK
Tryptophanyl-tRNA synthetase of HepG2					
3	3	5.31	SYW_HUMAN (P23381)	99.00	ALIEVLQPLIAEHQAR
3	3	5.31	SYW_HUMAN (P23381)	90.00	KPFYLYTGR
Fumarate hydratase of hepatocyte					
2.01	2.01	32.54	P14408|FUMH_RAT	99.00	LHDALSAK
2.01	2.01	32.54	P14408|FUMH_RAT	0.90	VPTDKYYGAQTVRSTMNFK

Table 4.3 Peptide sequences

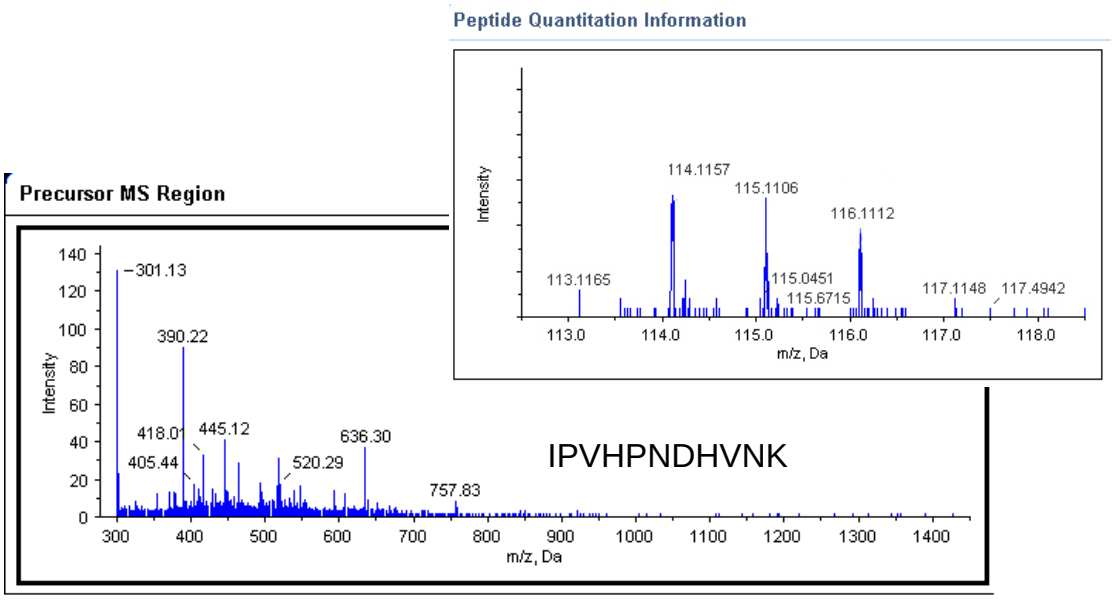

Panel A –Fumarate hydratase in HepG2 cells

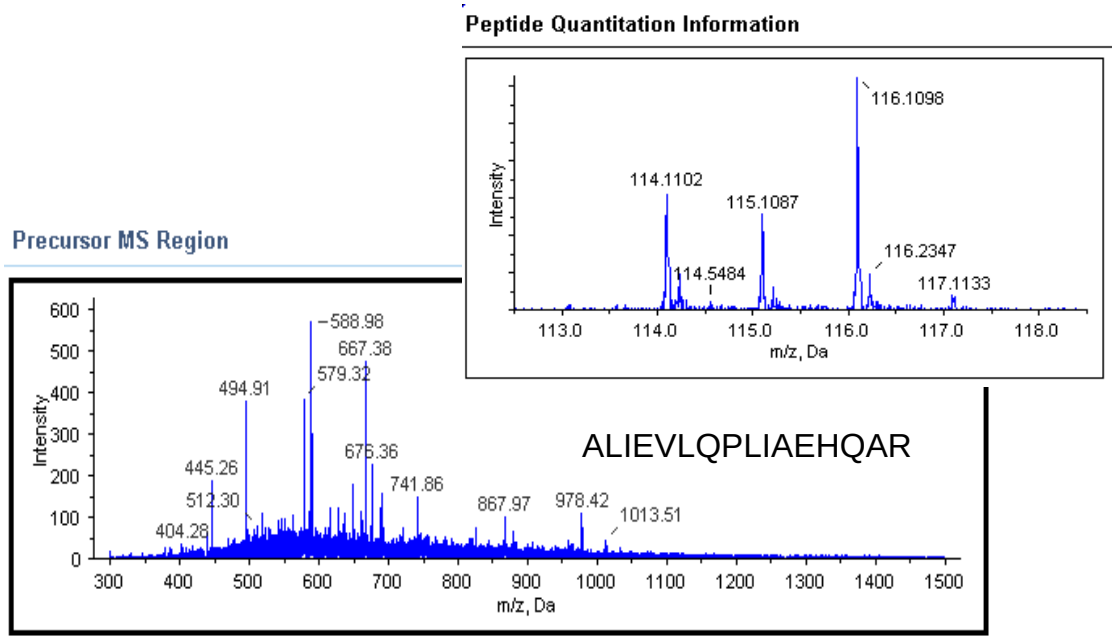

Panel B- Tryptophanyl-tRNA synthetase in HepG2 cells

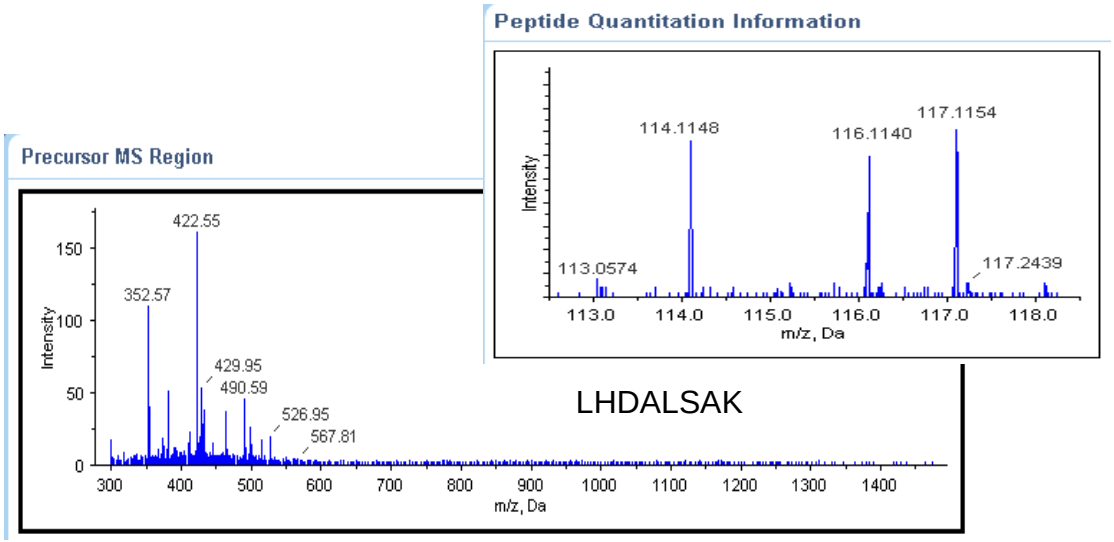

Panel C –Fumarate hydratase in RPHs

Figure 4.4 A representative MS/MS spectrum showing the peptides. The ion assignments for RPHs were as follows: 114, non-transfected cells; 115, HBV transfected cells; 117, empty vector transfected cells. The ion assignments for HepG2 cells were as follows: 114, non-transfected cells; 115, empty vector transfected cells; 116, HBV transfected cells. The peptide showed that the level changes of 114, 115, 116 and 117 labels. Panel A, the spectrum of Fumarate hydratase in HepG2 cells; panel B, the spectrum of Tryptophanyl-tRNA synthetase in HepG2 cells; panel C, the spectrum of Fumarate hydratase in RPHs. The peptide sequences were listed in their respective panel.

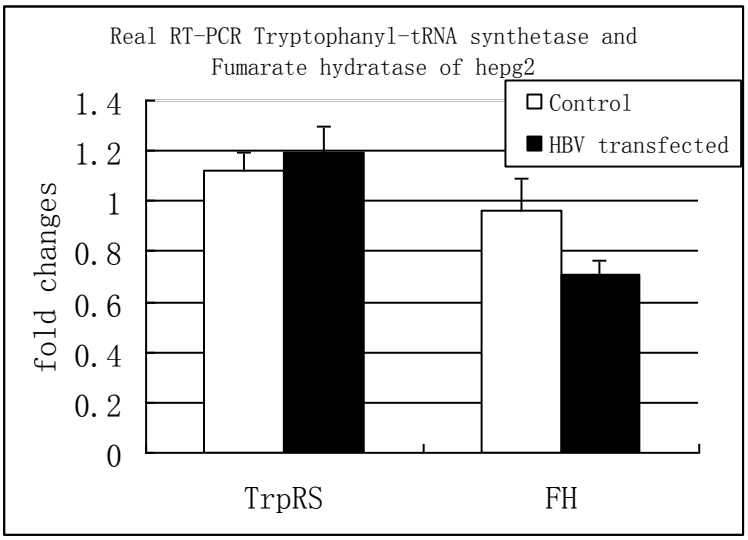

Panel A

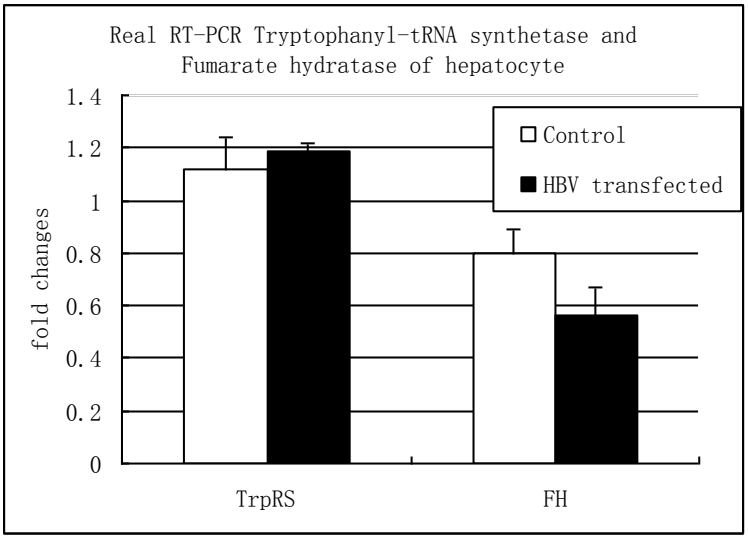

Panel B

Figure 4.5 Real-Time RT-PCR analysis of FH and TrpRS. Real-Time PCR analysis of mRNA levels of genes coding for cellular proteins in HepG2 (A) and hepatocyte (B) transfected HBV. Three independent experiments were carried out. Ratio between the HBV transfected and control (without treatment) cells shown as black bar, as well as between the vector transfected and control (without treatment) cells shown as white bar.

4.3 Discussion

We reported in this study that angiogenesis can be induced in endothelial cells by HBV replication either in RPHs or HepG2 cells. The protein profiles in RPHs and HepG2 cells supporting HBV replication indicated that FH and TrpRS which are associated with angiogenesis displayed changes in their protein levels. Our tube formation assay in HUVEC cells provided the first evidence that HBV replication induced angiogenesis. This may imply that cells supporting HBV replication have an enhanced viability, as new blood vessel formed from angiogenesis can sustain supply of nutrients. These are in line with reported evidence that that HBV replication can cause proliferation of hepatocytes leading to HCC [134]. On the other hand, HBV replication may also trigger angiogenesis in hypoxia condition such as liver cirrhosis with fewer blood vessels [131].

FH and TrpRS, previously linked to angiogenesis, were first identified to involve HCC in our proteomics analysis and represented the first angiogenic factors to be regulated by HBV replication. A decrease in FH as shown in our study would result in cumulation of citric acid cycle intermediates including fumarate, which have been shown to stabilize HIF-1. The stabilized HIF-1 by the lack of FH activity would result in an increased production of a HIF-1 target protein VEGF thus turning on the angiogenic pathways [135]. Although the downregulation of FH has been linked to the development of renal carcinoma, our data constitute the first report on the role of FH in liver angiogenesis. Our results therefore revealed that HBV replication can inhibit FH expression, may lead to fumarate accumulation in either RPHs or HepG2

cells and activation of angiogenesis. TrpRS is a key enzyme of protein biosynthesis catalyzing tRNAtrp aminoacylation [136]. The TrpRS gene is highly induced by interferon which is activated by viral infections including HBV. In this study, the level of TrpRS was found to be higher in HBV replicating HepG2 cells but not in RPHs. Although the increase in TrpRS protein level was not supported by the RT-PCR analysis, it remains possible that HBV replication leads to the stabilization of TrpRS protein and thus higher amount of the enzyme. Although the full-length TrpRS has not shown angiostatic (anti-angiogenic) activity, an angiostatic function has been shown from a natural splice variant of TrpRS which is strongly induced along with other angiostatic factors such as IP-10. Such spliced variants inhibit development of new vessels without affecting pre-established vasculature by binding at the end of developing blood vessels [137, 138]. While normal endothelial cells are remarkably quiescent with one division cycle every 1000 days, cell division is increased to once every 1-2 days during extensive angiogenesis [139]. As HBV replication was shown to induce angiogenesis in our study, it is possible that the level of the angiostatic spliced variant of TrpRS may be reduced, resulting in an increased level of the full length TrpRS in HBV replicating HepG2 cells.

In summary, our results demonstrate that the application of quantitative proteomics based on iTRAQ can be an effective approach to evaluate the effects of HBV replication on liver angiogenesis. The angiogenesis-associated proteins identified in our study may eventually lead to novel anti-angiogenic HCC cancer therapy based on tumor vascular targeting or be the markers for HCC diagnosis.

Chapter 5 Molecular mechanism of chiral NSAID drug (Ibuprofen) inhibition effects on HCC angiogenesis

5.1 Introduction

Hepatitis B Virus X protein (HBx), one of viral proteins that are encoded by HBV, is important in angiogenesis caused by HBV. The HBx expression is positively autoregulated by its own HBx, which exists in both cell cellular and cell nuclear [125]. HBx expression could induce vascular endothelial growth factor (VEGF) transcription and stabilize hypoxia inducible factor HIF-1 [133, 135]. Cells overexpressing Cox2 induce angiogenesis by up-regulating pro-angiogenic factors, including VEGF, basic fibroblast growth factor (bFGF) and transforming growth factor ß (TGF ß) in human HCC tissues. Cheng's group has shown that Cox2 is overexpressed in almost 80% of HBV-associated HCC tissues. Tanaka's group has demonstrated that Cox2 regulates Ang-2 expression in HCC cells *in vitro* and *in vivo*, and that Cox2 inhibitors may serve as anti-tumor agents [140].

Ibuprofen is a Cox2 inhibitor belonging to NSAIDs, existing as S- and R-enantiomer. Recent studies indicated that NSAIDs as Cox2 inhibitors might be an effective approach to colorectal cancer prevention [46]. Rothwell reported that high-dose aspirin (≥500 mg daily) reduces long-term incidence of colorectal cancer [47]. Yao group showed fewer liver cancer metastasis in individuals taking NSAIDs, which presumably reduce the risk of liver cancer at least in part by inhibiting Cox.

There is little evidence on the mechanism of NSAIDs' inhibition of HBV-induced HCC angiogenesis, and even less evidence on the effect of NSAIDs

chirality on angiogenesis. In this thesis, proteomics based on two-dimensional liquid chromatography-tandem mass spectrometry was used to unveil the complicated map of HCC angiogenesis induced by HBx replication. The results showed that Cox2 was up-regulated resulting from HBV replication, and further showed that HBx may make HBV capable to upregulate Cox2 expression. Ibuprofen, as a Cox2 inhibitor, was found to reduce Cox2 expression effectively. Cox2 expression regulation enlightens the possible HCC therapy by HCC angiogenesis inhibition. Since chiral Ibuprofen possesses two enantiomers which demonstrate different pharmacological effects, the chiral effects of different Ibuprofen enantiomers on angiogenesis inhibition were also discussed in this study.

5.2 Results

5.2.1 Concentration of Ibuprofen by MTT Assay

This study was to investigate cellular protein profile of HBx transfected HepG2 incubated with Ibuprofen. The concentration of Ibuprofen mimicking the *in vivo* situation with minimal cell death from the incubation was analyzed. The viability of the HepG2 was examined by MTT assay, with cells incubated with an increasing concentration of individual enantiomers of Ibuprofen.

The results shown in Figure 5.1 indicated that 1 mM of S-Ibuprofen and R-Ibuprofen were toxic to the cells. Our results indicated that no significant effect on cell viability was observed for concentrations below 100 μM. Whitlam's group [107] has found that the Ibuprofen concentration in the serum is 20–40 mg/mL (around 100 μM) for the patients uptake of Ibuprofen at normal dose. In order to best simulate the

in vivo condition, 100 μM was therefore chosen as our working Ibuprofen concentration in all the experiments in this study.

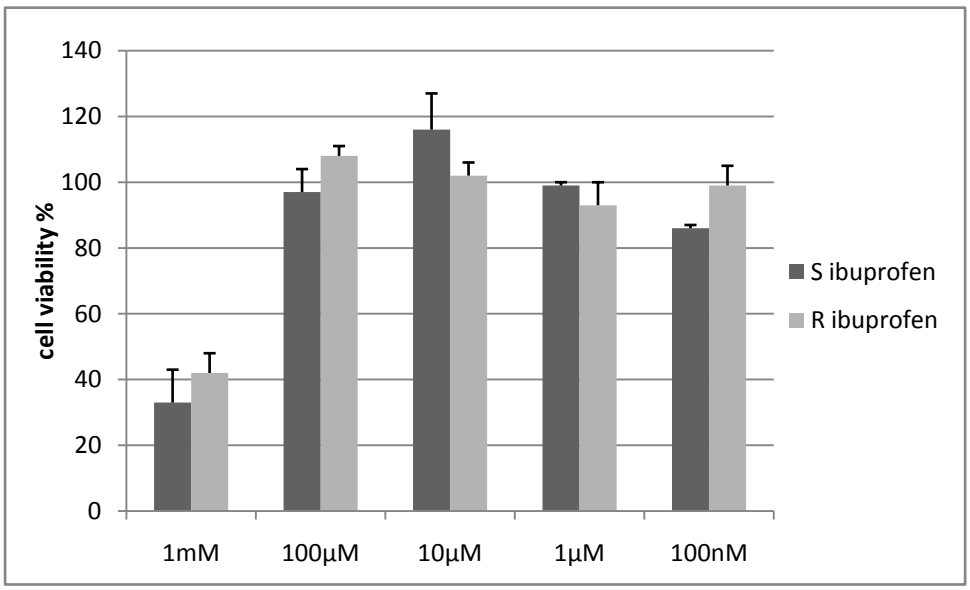

Figure 5.1 Hepg2 cell viability after 48 h of exposure to *R*- and *S*-enantiomer of Ibuprofen respectively. Three independent experiments were carried out for each enantiomer. Y axis was survival rate percent. X axis was the concentration of Ibuprofen treatment. The viability of control cells only adding DMSO was set 100%.

5.2.2 Effect of HBV replication and Ibuprofen on angiogenic proteins IL6 and Cox2

Evidence using LC-MS/MS-based proteomics analysis in the previous chapter has indicated HBV is implicated in HCC angiogenesis. However, not all of the key angiogenic factors had been detected in our earlier study. Therefore, the mRNA level of 38 angiogenic factors was measured by Real-time RT PCR in HBV transfected

HepG2 cell with/without Ibuprofen treatment. The results shown in Figure 5.2 indicated that IL6 and Cox2 genes were affected by both HBV replication and Ibuprofen treatment. Specifically, IL6 mRNA level was induced in HBV replicating HepG2 cells to 7 times higher as compared with the control HepG2 (transfected with empty vector). However, the increase in IL6 mRNA level was less significant in HBV replicating HepG2 cells incubated with Ibuprofen. Specifically, HBV replicating HepG2 cells incubated with R Ibuprofen showed only 3 fold increase in IL6 mRNA. In addition, HBV replicating HepG2 cells incubated with S Ibuprofen showed a 5 fold increase in IL6 mRNA level. Our results therefore suggested that chiral Ibuprofen displayed differential inhibitory effects on IL6 expression induced by HBV replication.

As for Cox2 mRNA level, the RT-PCR analysis (Figure 5.2) indicated that HBV replication in HepG2 cells induced its increase to around 2 fold compared with the control HepG2 cells transfected with empty vector. In contrast to our data on IL6, the addition of Ibuprofen to HBV-replication HepG2 cells resulted in a lower level of Cox2 mRNA. Furthermore, there was no obvious difference in Cox2 mRNA level in cells incubated with R- or S-Ibuprofen (Figure 5.2).

The changes in IL6 and Cox2 mRNA levels were further validated by Western blot analysis. Results shown in Figure 5.3 indicated that IL6 protein level was 2 fold higher in HBV-replicating HepG2 cells compared with the control HepG2 cells transfected with empty vector. Consistent with the RT-PCR analysis, Ibuprofen attenuated the increase of IL6 protein by HBV replication. In addition, S-Ibuprofen

showed greater attenuation of IL6 protein level than R Ibuprofen (Figure 5.3). This is different to the observation in RT-PCR analysis (Figure 5.2). It is possible that chiral Ibuprofen may also involve pathways of IL6 post-transcription. Overall, our Western blot analysis is consistent with RT-PCR analysis indicating that Ibuprofen is able to attenuate the induction of IL6 by HBV replication.

Our Western blotting results on Cox2 were similar to those from RT-PCR. HBV replication in HepG2 cells resulted in higher Cox2 protein level as compared with the control HepG2 cells transfected with empty vector, as shown in Figure 5.3. In addition, the addition of Ibuprofen to HBV-replication HepG2 cells resulted in a lower level of Cox2 protein.

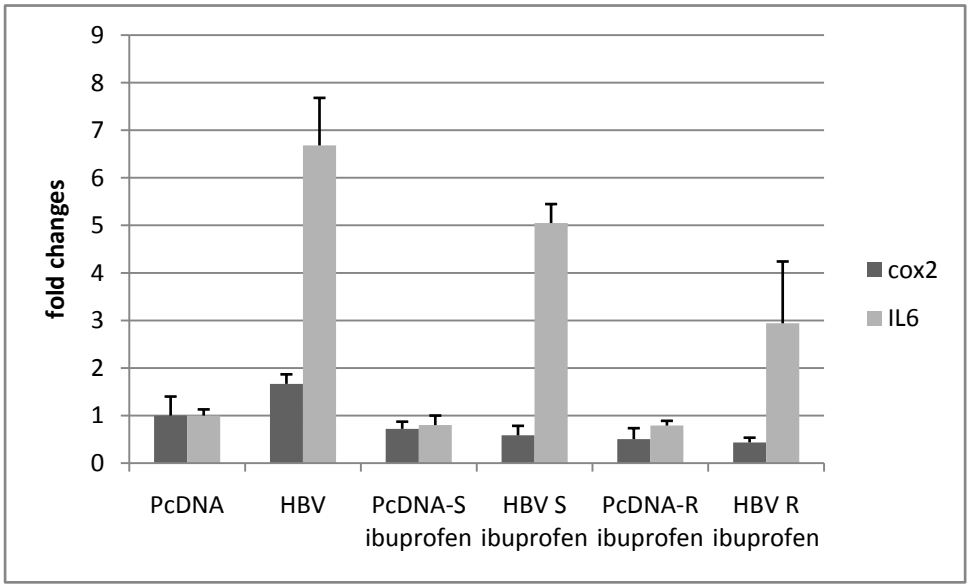

Figure 5.2 Real-Time RT-PCR analysis. Real-Time PCR analysis of mRNA levels of genes coding for cellular proteins, Cox2 (black bar) and IL6 (grey bar). Three independent experiments were carried out. Y axis is the ratio between the Ibuprofen treatment and/or HBV infection cells

and control (empty plasmid) cells. PcDNA represented cells transfected with empty plasmid; HBV represented HBV infection cells versus cell transfected with empty plasmid; PcDNA-S Ibuprofen represented S Ibuprofen treatment cells transfected with empty plasmid versus cells transfected with empty plasmid; HBV S Ibuprofen represented S Ibuprofen treatment cells infected HBV versus cells transfected with empty plasmid; PcDNA-R Ibuprofen represented R Ibuprofen treatment cells transfected with empty plasmid versus cells transfected with empty plasmid; HBV R Ibuprofen represented R Ibuprofen treatment cells infected HBV versus cells transfected with empty plasmid;

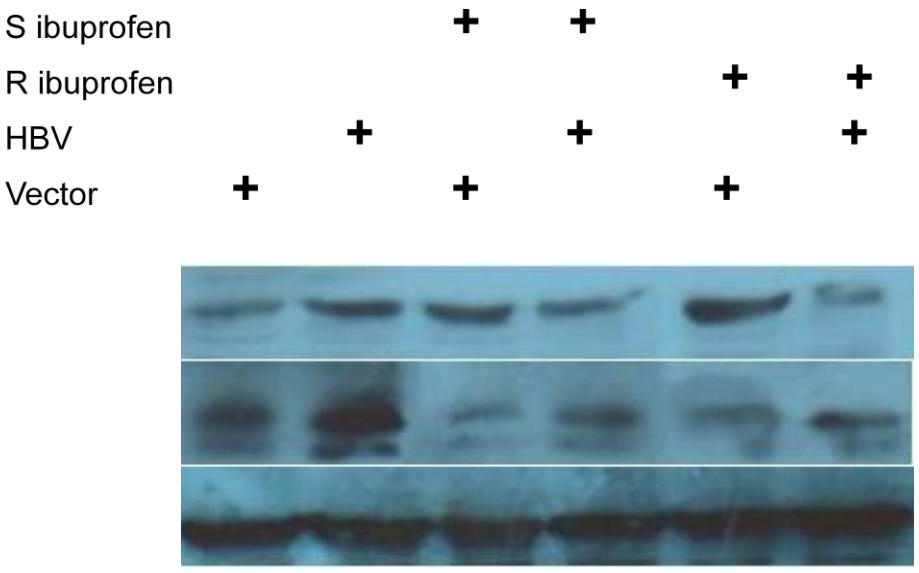

A

Cox2

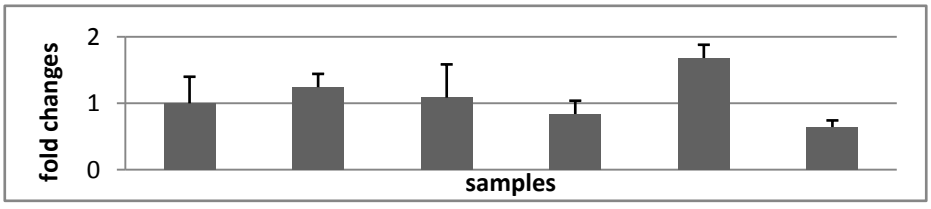

Continue to next page

IL6

β-actin

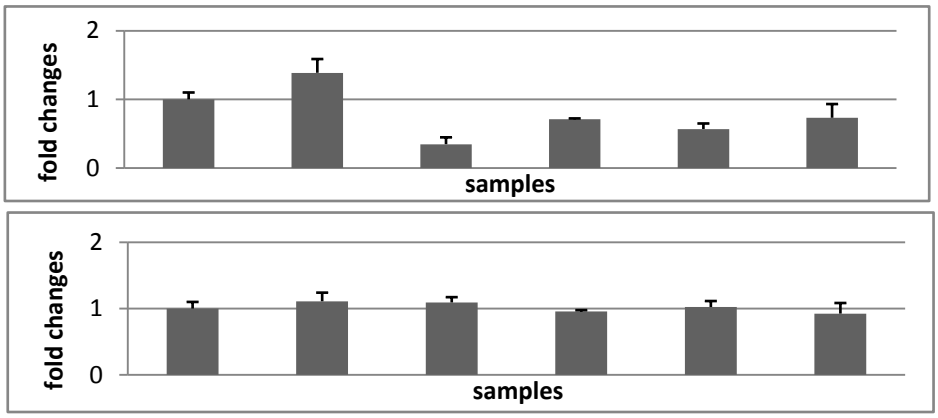

B

Figure 5.3 Western blotting of Cox2 and IL6 in HepG2 cells with HBV infection were measured by western blot. Hepg2 cells were treated under different conditions (+ is at specified condition), and lysed to extract protein for western blot assay. Western blotting results about IL6, Cox2 and β-actin were showed (A). (B) Fold changes of the protein level by Western blot were plotted using Image J software. The results are representative of three separate experiments.

5.2.3 Effect of HBx on angiogenic proteins IL6 and Cox2

HBx is a HBV viral protein and is positively autoregulated. As HBx has been implicated in multiple functions including tumor angiogenesis, its effects on IL6 and Cox2 were further analyzed.

Expression vector PXJ40 containing HBx gene was transfected to HepG2 cells incubated with or without Ibuprofen. RT-PCR results confirmed that HBx gene was transfected into HepG2 cell, as shown in Table 5.1. PXJ-HBx sample from HepG2 cells transfected with HBx gene started specific HBx gene amplification at 26.78 PCR

cycles. The same cells with S and R Ibuprofen treatment started amplification at 27.51 PCR and at 25.18 PCR cycles, respectively. In comparison, their respective controls PXJ, S PXJ and R PXJ transfected cells started amplification after 35 PCR cycles, suggesting nonspecific amplification and thus the absence of HBx. The results indicated that HBx was transfected into HepG2 cells.

IL6 and Cox2 expression at the mRNA level was then analyzed in HBx transfected HepG2 cells. Results shown in Figure 5.4 indicated that HBx induced an increase of IL6 mRNA level to 3 fold when compared with the control HepG2 cells transfected with empty vector. Similarly to our analysis on HBV-replicating cells, Ibuprofen attenuated the increase of IL6 mRNA by HBx. In addition, the attenuating effect was more significant in HBx-expressing cells incubated with R-Ibuprofen than those with S-Ibuprofen.

On the other hand, HBx induced Cox2 mRNA level to a 2-fold increase as compared with that in the control HepG2 cells transfected with empty vector. However, the addition of Ibuprofen to HBx-expressing HepG2 cells resulted in a lower level of Cox2 mRNA. Furthermore, there was no obvious difference in Cox2 mRNA level in cells incubated with R- or S-Ibuprofen (Figure 5.4).

Cox2 protein level was then measured on HBx-expressing HepG2 cells by Western blot analysis. The result shown in Figure 5.5 indicated that HBx was able to regulate Cox2 protein level in a similar way as HBV replication. Specifically, HBx-expressing HepG2 cell showed an increased Cox2 level as compared with HBx untransfected HepG2. In addition, Ibuprofen was able to attenuate the induction by

HBx.

Taken together, our results indicated that HBV replication induced the increase in the level of Cox2 and IL6, possibly mediated by HBx. In addition, Ibuprofen attenuated the induction effect of HBV replication as well as HBx.

Treatment in HepG2 cells	**HBx Cycles number**	**β-actin Cycle number**
Pxj40	38.50±0.71	15.64±0.12
S Ibuprofen and Pxj40	38.36±0.31	15.85±0.32
R Ibuprofen andPxj40	37.21±1.32	14.57±0.34
Pxj40-HBx	26.78±0.37	14.59±0.09
S Ibuprofen and Pxj40-HBx	27.51±0.26	14.61±0.28
R Ibuprofen and Pxj40-HBx	25.18±0.33	14.77±0.32

Table 5.1 Real-Time RT-PCR analysis of HBx mRNA level in HBx transfected HepG2 cells. Pxj40 was empty vector, and Pxj40-HBx was vector containing HBx gene. β actin was used as internal control. Cells with Pxj40-HBx plasmid had significant lower cycle number comparing with control ($P<0.05$).

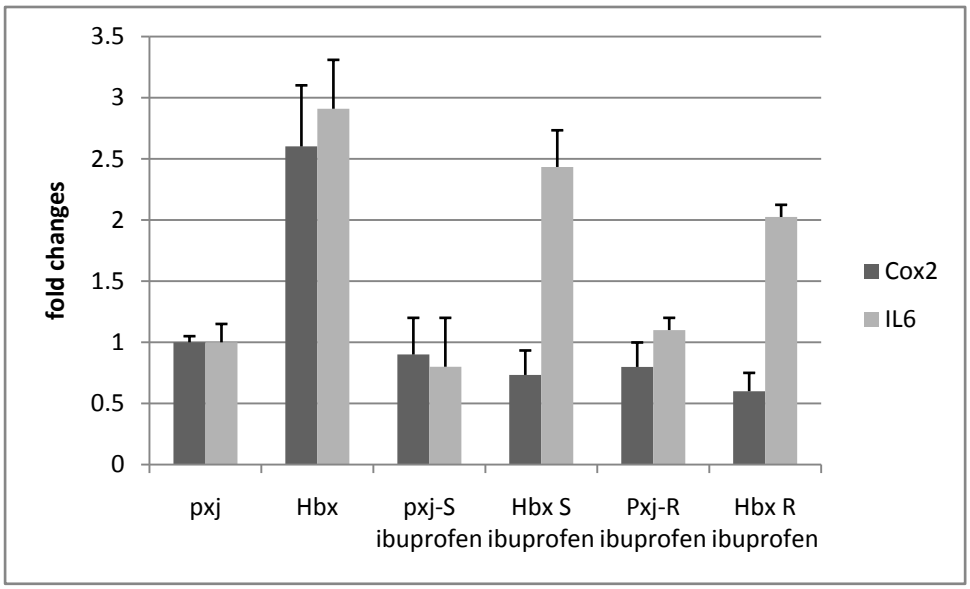

Figure 5.4 Real-Time RT-PCR analysis. Real-Time PCR analysis of mRNA levels of genes coding for cellular proteins, cox2 (black bar) and IL6 (grey bar). Three independent experiments were carried out. Y axis was the ratio between the Ibuprofen treatment and/or HBV infection cells and control (empty plasmid) cells. Pxj (pxj40) represented cells transfected with empty plasmid; HBx represented HBx transfected cells versus cell transfected with empty plasmid; pxj-S Ibuprofen represented S Ibuprofen treatment cells transfected with empty plasmid versus cells transfected with empty plasmid; HBx S Ibuprofen represented S Ibuprofen treatment cells transfected HBx versus cells transfected with empty plasmid; Pxj-R Ibuprofen represented R Ibuprofen treatment cells transfected with empty plasmid versus cells transfected with empty plasmid; HBx R Ibuprofen represented R Ibuprofen treatment cells transfected HBx versus cells transfected with empty plasmid.

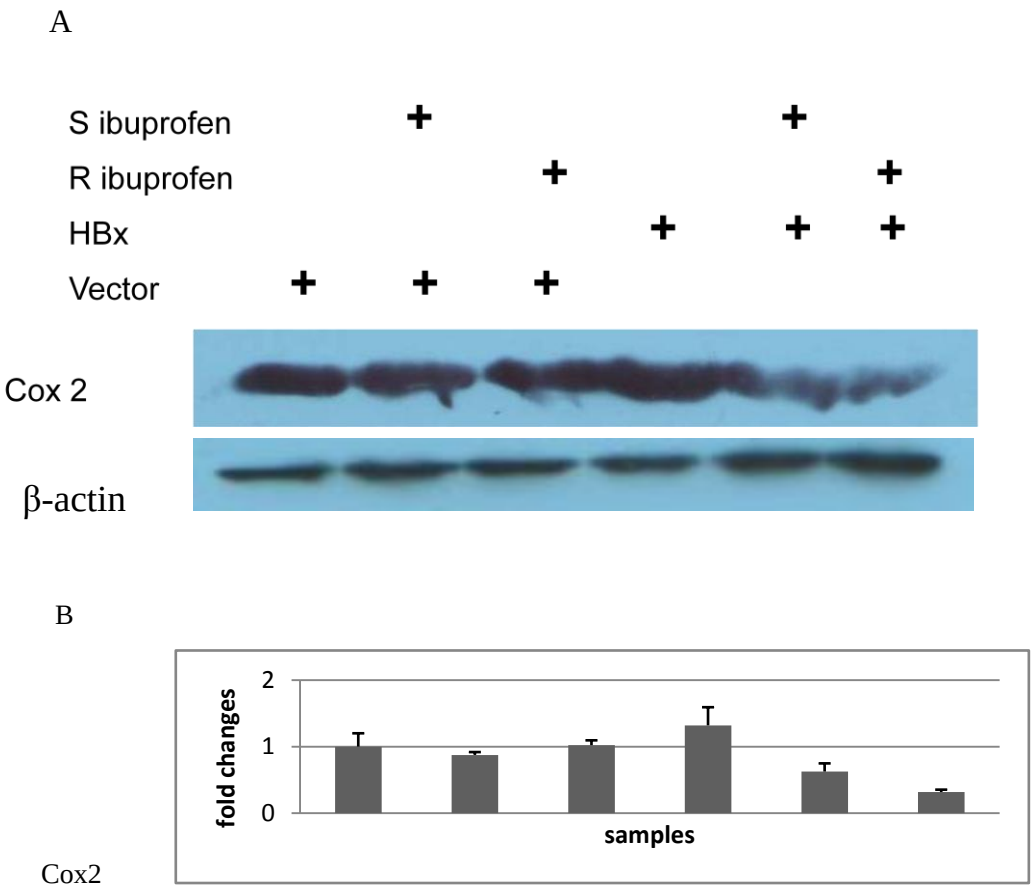

Figure 5.5 The protein level of Cox2 in HBx transfected HepG2 cells was measured by western blot. (A) Under different conditions, the treated cells were lysed to extract protein for western blot assay. "+" represented of the treatment. (B) Fold changes of the protein level by Western blot were plotted using Image J software after normalization with control β-actin. The results were representative of three separate experiments.

5.2.4 iTRAQ analysis of differentially expressed proteins

In order to further study the mechanism by which HBx induces angiogenesis and how HBx and Ibuprofen treatment reduce Cox2 expression from originally HBx increasing Cox2 expression, a proteomics study was done to check the whole protein

profile changes under Ibuprofen treatment and HBx transfection. The HepG2 cells transfected HBx with Ibuprofen treatment were lysed to extract the proteins for protein profile study. Three separate experiments were carried out for using different batch cells treated by Ibuprofen and transfected by HBx. The MS result was analyzed by Spectrum Mill MS Proteomics Workbench software using UniProt_sprot_20100123 database to identify and quantify the different protein expression levels among different samples. Analysis of the first time experiment led to the detection of 393 proteins, while 549 proteins and 516 proteins were detected at the second and third experiment, respectively. Identification of protein with significant expression level was done using the software filter setting. Eighteen proteins which expression levels had variation between the Ibuprofen treatment samples and normal samples were identified based on these criteria and consistent with three times repeats. The protein function was analyzed through Swiss-Prot database manually. Among the 18 differentially expressed proteins, 8 proteins had functions related to NFκB pathways (Table 5.2). The proteins were Cofilin-1, GTP-binding nuclear protein Ran, Interferon-induced transmembrane protein 1, Nucleophosmin, Peptidyl-prolyl cis-trans isomerase, Plasminogen activator inhibitor 1 RNA-binding protein, Stress-70 protein and Thioredoxin. Since Cox2 expression is downstream of NFκB pathway, the 8 proteins found by proteomics suggested that Ibuprofen may involve in regulating Cox2 expression by NFκB pathways besides binding Cox2 directly. The NFκB represents a ubiquitously expressed family of transcription factor participating in various biological effects ranging from immune,

inflammatory, and stress-induced responses to cell fate decisions such as proliferation, differentiation, apoptosis, and tumorigenesis. The mammalian NFκB family is composed of five members: RelA (p65), RelB, c-Rel, NFκB1 (p50 and its precursor p105), and NFκB2 (p52 and its precursor p100).

Overexpression of cofilin-1 destabilizing the actin cytoskeleton inhibits NF-B-dependent reporter activity in response to thrombin. Cofilin-1 functions as impairing nuclear translocation of RelA/p65 [141]. The GTP-binding nuclear protein Ran protein is involved in the control of DNA synthesis and cell cycle progression and also in the signal transduction pathway determining NF-kB-inducing kinase (NIK)-mediated NF-kB activation [142]. Interferon-induced transmembrane protein 1 (IFITM1) is one of the pro-inflammatory mediators that are induced by signaling initiated by the activation of CD147 in macrophages and activation of ERK, PI3K, and NFκB [143]. Nucleophosmin is an NFκB co-activator for the induction [144]. NFκB function is regulated by Peptidyl-prolyl cis-trans isomerase A (Pin1) mediated prolyl isomerization and ubiquitin-mediated proteolysis of its p65/RelA subunit [145]. The prolyl isomerase, Pin1, has been found to bind directly to the NFκB protein, p65, and cause increases in NFκB promoter activity in a breast cancer model [146]. Plasminogen activator inhibitor type 1 (PAI-1) is induced by many proinflammatory and pro-oxidant factors. NFκB regulate PAI-1 expression by PAI-1 promoter which can directly interact with NF-KB [147]. Stress-70 protein (Hsp70) is known to be involved in cellular defense mechanisms. Mild heat shock caused a substantial increase of the intracellular Hsp70 content with the concomitant

suppression of NF-kB complexes, via stress protein Hsp70 interacting with NF-kB regulatory complex in human T-lymphoma cells [148]. Finally, thioredoxin can efficiently block NF-KB activation. As the decreased levels of thioredoxin observed in HIV-infected persons may be directly responsible for disease progression [149], HBx may cause disease progression through a similar mechanism.

The changes in protein levels observed in our analysis suggested that HBx may affect NFκB pathways, and Ibuprofen attenuated the effect of HBx on Cox2 through the same NFκB pathway. Interestingly, HBx has been shown to activate the RelA/NFκB and C-rel/NFκB respectively under different conditions, leading to two contradicting outcomes, namely the cell proliferation and apoptosis [150, 151]. It is possible that Ibuprofen may shift HBx regulated pathways from RelA/NFκB to C-rel/ NFκB. To investigate this possibility, C-rel and RelA transcription factors were extracted from the nucleus of HepG2 cells and measured by Western blot analysis. The results (Figure 5.6) showed that C-rel was reduced and RelA was increased in HBx-expressing cells, in the absence of Ibuprofen. This suggested that HBx may have a role in cell proliferation through the RelA pathway. On the other hand, the results (Figure 5.6) also showed that C-rel was increased and RelA was reduced in HBx-expressing cells, in the presence of Ibuprofen. This suggested that HBx was now involved in apoptosis through the C-rel/NFκB pathway. A proposed pathway was summarized in Figure 5.7. In addition, our results also showed that R Ibuprofen was more potent than S Ibuprofen in regulating the expression of NFκB transcript factors.

Protein name	Protein ID	HBx/Control	S-Ibuprofen /Control	R-Ibuprofen /Control	Function
Cofilin-1	P23528	0.78±0.09	1.63±0.13	1.28±0.11	anti apoptosis related angiogenesis
GTP-binding nuclear protein Ran	P62826	1.98±0.26	2.02±0.06	2.34±0.31	Host-virus interaction
Interferon-induced transmembrane protein	P13164	1.84±0.14	0.75±0.16	0.65±0.07	IFN-induced antiviral protein that mediate cellular innate immunity
Nucleophosmin	P06748	1.54±0.16	0.9±0.02	0.83±0.06	cell proliferation, and regulation of tumor suppressors
Peptidyl-prolyl cis-trans isomerase A	P62937	1.32±0.21	0.72±0.11	0.83±0.17	initiation of viral infection
Plasminogen activator inhibitor 1 RNA-binding protein	Q8NC51	1.21±0.13	0.91±0.15	0.85±0.06	play a role in the regulation of mRNA stability.
Stress-70 protein, mitochondrial	P38646	0.92±0.13	1.83±0.21	1.74±0.16	anti-apoptosis
Thioredoxin	P10599	0.69±0.18	1.75±0.14	1.68±0.26	contribute to the response to intracellular nitric oxide.

Table 5.2 proteins involved in NFκB pathway. The value was the ratio of different protein expression level between the HBx transfected cells and empty plasmid transfected control cells (HBx/control), the ratio of different protein expression level between S-Ibuprofen treated and HBx transfected cells and control cells (S-Ibuprofen/control) and the ratio of different protein expression level between R-Ibuprofen treated and HBx transfected cells and control cells (R-Ibuprofen/control).

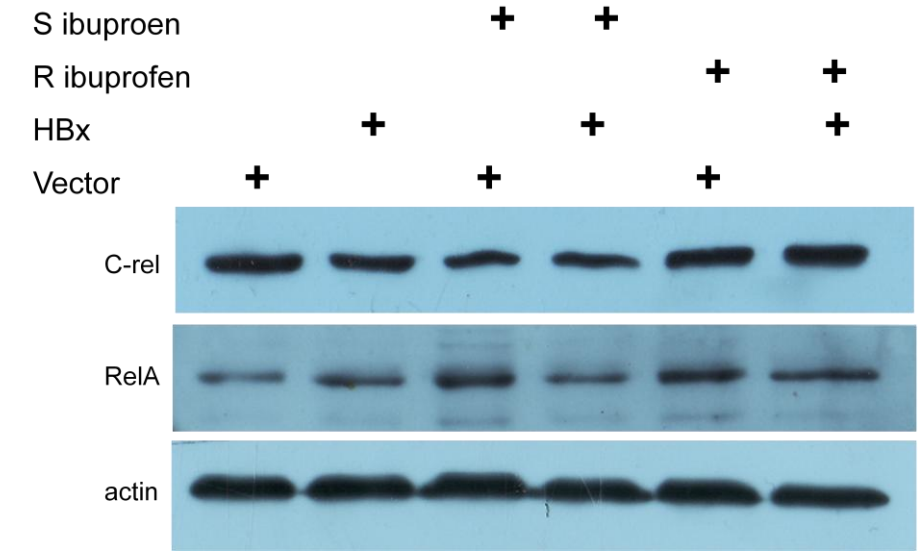

A

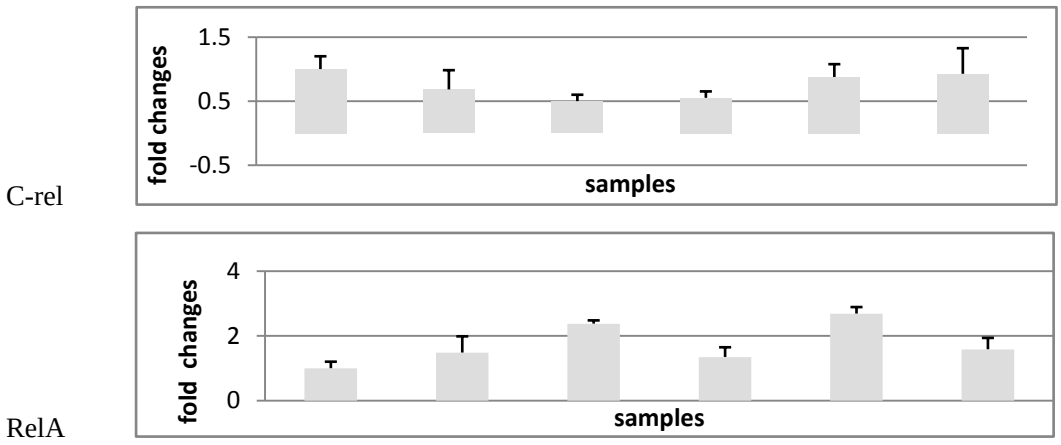

C-rel

RelA

B

Figure 5.6 The protein level of c-rel and RelA in HBx transfected HepG2 cells were measured by western blot. (A) Under different conditions, the treated cells were lysed to extract protein for western blot assay. "+" represented of the treatment. (B) Fold changes of the protein level by Western blot were plotted using Image J software after normalization with control β-actin. The results were representative of three separate experiments.

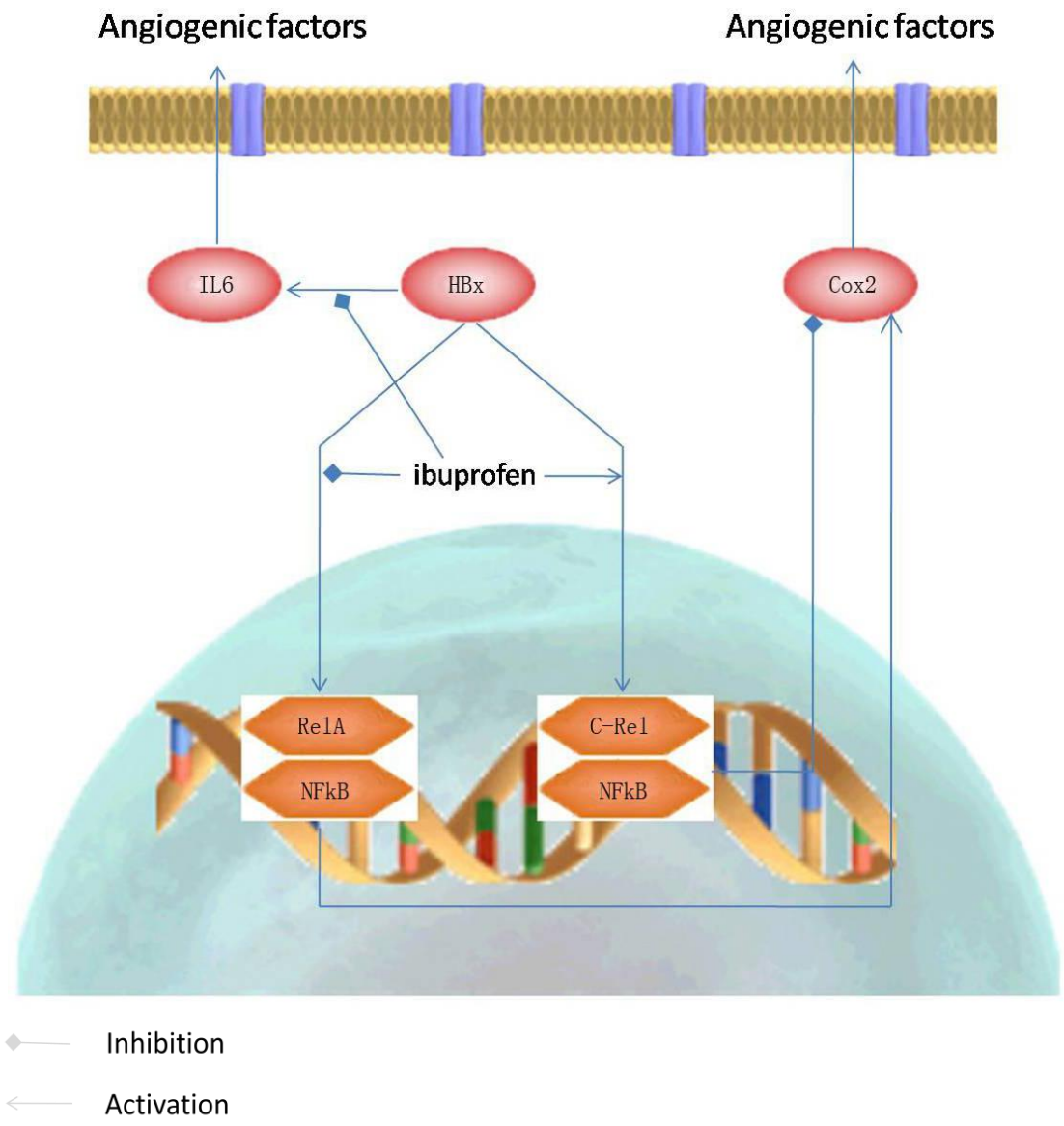

Figure 5.7 the proposed map of HBx and Ibuprofen regulating angiogenesis.

5.2.5 Additional angiogenic pathways regulated by Ibuprofen and HBx

Other proteins associated with angiogenesis were also identified by our proteomics analysis (Table 5.3). These proteins may help unveil other pathways regulating angiogenesis in addition to Cox2-NFκB pathways.

For example, carbamoyl-phosphate synthase (CPS1) was found to have been increased by 1.29 fold in HBx-expressing HepG2 cells. The presence of S or R Ibuprofen moderately attenuated the effect of HBx, with an increase of CPS1 at 1.21 fold and 1.07 fold in HBx-expressing HepG2 cells respectively. It has been shown that genetic variations in CPS1 influence the availability of precursors for nitric oxide (NO) synthesis and play a role in situations where endogenous NO production is critically important, such as angiogenesis [152]. NO induces VEGF expression and the increased expression of VEGF and HGF in chronic viral hepatitis may contribute to the enhancement of vascular permeability.

Another protein, fumarate hydratase (FH) was found to be reduced in HBx-expressing HepG2 cells (Table 5.3). Particularly, these cells had a reduced FH level to 0.65 fold as compared with control HepG2 cells. Interestingly, the presence of Ibuprofen reversed the effect of HBx, with the level of FH at 1.62 fold and 1.34 fold over control HepG2 for S- and R-Ibuprofen, respectively. The reduction of this enzyme has been reported to lead to an accumulation of citric acid cycle intermediates including fumarate, which have been shown to stabilize HIF-1. The stabilized HIF-1 by the lack of FH activity would result in an increased production of a HIF-1 target protein VEGF, thus turning on the angiogenic pathway [127]. Our results therefore suggested that HBx may induce angiogenesis by HIF pathways via FH decrease, and Ibuprofen inhibits angiogenesis by reducing fumarate.

Another enzyme, Glucose-6-phosphate isomerase (GPI) is reportedly induced by hypoxia and promotes angiogenesis [153]. Mammalian GPI can function as a

tumor-secreted cytokine and as an angiogenic factor that stimulates endothelial cell motility. The proteomics analysis in this study showed that HBx had no obvious effects on GPI expression (Table 5.3). Interestingly, S-Ibuprofen reduced the level of GPI to 0.61 fold in HBx-expressing HepG2 cells as compared with control HepG2 cells, while R-Ibuprofen reduced the level of GPI to 0.82 fold (Table 5.3). These results therefore suggested that Ibuprofen may inhibit angiogenesis by reducing the level of GPI.

In addition, the polypyrimidine tract binding protein (PTB) can specifically interact with the HIF-1α internal ribosome entry site (IRES), and that this interaction is enhanced in hypoxic conditions [154]. Overexpression of PTB enhanced HIF-1α IRES activity which induce angiogenesis. Our proteomics results showed that PTB expression increased by 1.18 fold in HepG2 cells with HBx transfection, while S or R Ibuprofen treatment inhibited the expected PTB increase by HBx. Instead, the PTB level was decreased to 0.91 fold and 0.95 fold respectively in HepG2 cell with S and R Ibuprofen treatment. Therefore, Ibuprofen may inhibit angiogenesis through its negative regulation of PTB level.

Protein name	Protein ID	HBx/Control	S-Ibuprofen /Control	R-Ibuprofen /Control	Function
Carbamoyl-phosphate synthase [ammonia], mitochondrial	P31327	1.29±0.12	1.21±0.09	1.07±0.17	related with NO pathway
Fumarate hydratase, mitochondrial	P06744	0.65±0.07	1.62±0.31	1.34±0.32	acts as a tumor suppressor
Glucose-6-phosphate isomerase	P06744	0.99±0.11	0.61±0.17	0.82±0.08	mammalian GPI can function as a tumor-secreted cytokine and an angiogenic factor
Polypyrimidine tract-binding protein 1	P26599	1.18±0.13	0.91±0.04	0.95±0.08	Plays a role in pre-mRNA splicing and in the regulation of alternative splicing events

Table 5.3 proteins involved angiogenesis pathways. The value was the ratio of different protein expression level between the HBx transfected cells and empty plasmid transfected control cells (HBx/control), the ratio of different protein expression level between S-Ibuprofen treated and HBx transfected cells and control cells (S-Ibuprofen/control) and the ratio of different protein expression level between R-Ibuprofen treated and HBx transfected cells and control cells (R-Ibuprofen/control).

5.3 Discussion

HBV chronic infections associated with angiogenesis usually progress to HCC. Understanding the molecular mechanism of HBV-associated angiogenesis should shed new lights on better prevention of HCC onset. To this end, we investigated the expression level of a number of key angiogenic genes in HBV-replicating HepG2 cells. IL6 and Cox2 were found to be regulated by HBV replication.

The multi-functional viral protein HBx was shown to be involved in the regulation of Cox2 and IL6 expression, suggesting its role in inducing HCC angiogenesis, while Ibuprofen attenuated HBx induction effect. Our results suggested that the Cox2 inhibitor Ibuprofen may act through IL6 or other proteins, instead of exclusively regulating Cox2. The expression of IL-6 occurs at sites of angiogenesis *in vivo* and is stimulated by TNF in human endothelial cells [155]. IL6 promotes angiogenesis through regulating VEGF expression which is a key angiogenic factor. The down-regulation of IL6 by Ibuprofen (which was induced by HBx) suggested that this Cox2 inhibitor may reduce the HBx-associated angiogenesis by inhibiting VEGF.

Cox2 was identified to be involved in tumor promotion during colorectal cancer progression. Recent studies in humans indicate that therapy with specific Cox2 inhibitors might be an effective approach to colorectal cancer prevention and treatment [46]. Consistently, population-based studies have established that long-term intake of NSAIDs reduces the relative risk for developing colorectal cancer. In our study, Ibuprofen was found to reduce the level of Cox2 which was stimulated by either HBV replication or HBx expression. Our results suggested that Ibuprofen could be used to reduce or prevent HCC angiogenesis induced by HBV replication.

In addition to Cox2 and IL6, a number of proteins associated with the NFκB pathway were identified in our LC-MS/MS proteomics analysis in the context of HBx expression and presence of Ibuprofen. The results showed that Cox2 has higher expression in HBx transfected cells as compared to control cells with empty vector, but Cox2 has lower expression in Ibuprofen treated HBx transfected cells as compared to

control cells with empty vector. Since RelA/NFκB and C-rel/ NFκB pathways lead to proliferation and apoptosis via Cox2 expression respectively, we further proved that Ibuprofen addition affects NFκB dimers composition, changing from RelA/NFκB to C-rel/ NFκB in HBx expression cells.

New proteins involved in angiogenesis were also identified in our proteomics analysis. These included CPS1, FH, GPI and PTB which participate in the angiogenic responses, for example in inducing vasodilatation by influencing nitric oxide (NO) synthesis. Further characterization of these proteins may help unveil other pathways regulating angiogenesis. These results suggested that Ibuprofen may inhibit angiogenesis by engaging other pathways, in addition to the Cox2 pathway.

In summary, the results showed that Ibuprofen was able to attenuate the induction of angiogenic proteins by HBV replication or HBx expression. In addition, the NFκB pathway implicated in HBx activities was found to be modulated by Ibuprofen. RelA and C-Rel belongs to NFκB families which are regulated by Ibuprofen and HBx. The Rel/NFκB or C-rel/ NFκB heterodimer formation at different conditions such as Ibuprofen treatment or not causes HBx having opposite functions on Cox2 expression. Furthermore, the effects of chiral enantiomers of Ibuprofen on attenuating the induction of angiogenic proteins by HBx were analyzed. Our results demonstrated that the application of quantitative proteomics based on iTRAQ can be an effective approach to depict underlying mechanism of protein-protein interactions, and in this case determine the effect of HBV replication and Ibuprofen on angiogenesis. The angiogenesis-associated proteins identified in our study may well be new targets of

anti-angiogenic therapy based on tumor vascular targeting, or the prognostic markers for HCC onset.

Chapter 6

Conclusion

Abundant evidences show that neuroinflammation contributes to the pathogenesis of several neurodegenerative disorders, including AD. Mass spectrometry interfaced with 2D (strong cation exchange/reversed phase) chromatographic separations coupled with iTRAQ reagents was applied in investigating the mechanism of Ibuprofen inhibiting AD occurrence. LC/MS Proteomics results suggested that the anti inflammatory drug *S*-Ibuprofen offers protection for AD by reducing oxidized stress. Its combined effects through that differential regulation of fatty acid synthase, phosphoglycerate mutase 1 and peroxiredoxin 2 may contribute to the decrease in ROS, a pathological factor for the development of AD. In addition, Ibuprofen may also be neuroprotective through other pathways, for example by decreasing CyP-A expression or increasing plectin expression.

LC-MS/MS Proteomics was also used to study the mechanism of HBV replication inducing liver angiogenesis. HBV replication induced angiogenesis was indicated by tube formation of endothelial cells cultured in condition medium from RPHs or HepG2 cells supporting HBV replication. Enzymes associated with angiogenesis, namely fumarate hydratase and tryptophanyl-tRNA synthetase, were identified by 2D LC-MS/MS analysis in HBV replicating RPHs and HepG2 cells.

The analysis of known angiogenic proteins IL6 and Cox2 regulated by both HBV and Ibuprofen indicated that Ibuprofen may effectively reversed HBV angiogenic

effects at least partially through regulating these two proteins. The multifunctional viral protein HBx gave HBV the role on regulating Cox2 and IL6. The mechanism of chiral Ibuprofen inhibitory effects on angiogenesis was studied. With LC/MS proteomics study aids, NFκB pathways which involving in HBx function were found under Ibuprofen regulation. Our study further showed that RelA and C-Rel belonging to the NFκB families regulated by Ibuprofen causes HBx reverse effects on Cox2 expression. HBx transfection induces Cox2 expression of host cells, while HBx transfection and Ibuprofen treatment inhibits Cox2 expression of host cells. Furthermore, the chiral Ibuprofen inhibition effects on HBx-related HCC angiogenesis were comprehensively studied by proteomics study. The proteomics results showed that Ibuprofen can affect angiogenesis by other pathways besides the Cox2 pathway. By analysing proteomics study, the proteins CPS1, FH, GPI and PTB expression variation showed that HBx and Ibuprofen take part in these angiogenesis pathways. CPS1 participate in the angiogenic response by influencing nitric oxide (NO) synthesis. The stabilized HIF-1 by the lack of FH activity would result in turning on the angiogenic pathway. GPI can function as a tumor-secreted cytokine and an angiogenic factor. Overexpression of PTB enhanced HIF-1α IRES activity which induce angiogenesis. HBx transfection can change these proteins expression towards to angiogenesis direction, while R and S Ibuprofen had similar degree effects regulating these proteins expression towards to anti-angiogenesis.

In this thesis, the MS/MS-based quantitation method was applied on the sophisticated platform of ESI LC/MS/MS system to simultaneously detect and

quantify the differentially expressed proteins in untreated cells and those incubated with the *S*- and *R*-enantiomers of Ibuprofen, respectively, which reflects the pharmacologic action of these enantiomers. LC-MS/MS Proteomics analysis holds the promise of effectively depicting cellular protein profile in response to various drugs which in turn should be helpful in our understanding on their mechanisms of actions. Working on this sophisticated approach, up to 4 samples were investigated at the same time, and hundreds cellular proteins were detected. With powerful software analysis, the candidate proteins that may play important role in disease were identified. In our study, the expression of proteins identified by LC/MS was subsequently confirmed by other techniques such as RT PCR or Western blot, which suggested that LC/MS coupled iTRAQ labelling is a reliable approach in unravelling the important protein interactions involved in AD and HCC angiogenesis.

ROS reduction by Ibuprofen regulating fatty acid synthase, phosphoglycerate mutase-1 and peroxiredoxin 2 expressions, neuroprotective action by Ibuprofen inhibiting CyP-A expression and preventing neuron dystrophy by ibuprofen inducing plectin expression were found in LC/MS proteomics study. These results showed that S Ibuprofen's neuroprotective function is via various different mechanisms at the same time, and suggested that it is promising in clinical AD therapy.

The angiogenesis-associated proteins identified in LC/MS such as fumarate hydratase and tryptophanyl-tRNA synthetase are reported for the first time in liver cancer. Angiogenesis correlating with loss of fumarate hydratase was previously introduced in renal cancer [136], while no publication have been introduced on the

effects of tryptophanyl-tRNA synthetase on tumor angiogenesis of liver organ. Our results may eventually lead to novel anti-angiogenic HCC cancer therapy based on tumor vascular targeting or establish the markers for HCC diagnosis.

In this thesis, there are two novel features on the original study about Ibuprofen inhibition function on HCC angiogenesis, one is NSAIDs inhibition effects on tumor growth of liver, and the other is NSAIDs chirality inhibition effects on angiogenesis. Our results showed that both S and R Ibuprofen inhibit angiogenic factors generation. However R Ibuprofen is more potent in decreasing Cox2 protein expression than S Ibuprofen. All these results on the chiral mechanism Ibuprofen inhibiting angiogenesis may provide new insights on HCC therapy or drug design.

Chapter 7

Future works

In this thesis, a platform of proteomics study was set up by using 2D (strong cation exchange/reversed phase) LC separation coupled with ESI LC/MS and iTRAQ labeling method. The thesis work displayed significant insights for NSAID therapy on AD and HCC research. A series of proteins which may play important roles in AD and tumor angiogenesis were identified by LC/MS, and subsequently confirmed by RT-PCR or Western blot. Fatty acid synthase, phosphoglycerate mutase-1, peroxiredoxin 2, CyP-A and plectin take part in Ibuprofen neuroprotective effects, and hydratase, tryptophanyl-tRNA synthetase, IL6 and Cox2 correlated with HBV affect HCC angiogenesis. All of these proteins may be effective targets for disease therapy. The expression of these proteins may be further studied using cell, animal model and even in clinical test.

For example, these protein expression levels can be modified using the respective siRNAs. siRNA transfected cells may be tested in cell assays; such as cell migration, cell apoptosis, cell proliferation and so on to evaluate whether these proteins affects HCC development. Proteins that significantly affect HCC development may then be used as targets for HCC therapy.

Our results showed that Ibuprofen may effectively regulate the proteins with functions that are related to AD and angiogenesis. This suggested that other NSAIDs may also be good candidates for AD and HCC therapy. With reference to our results, more potent NSAIDs with effects related to our identified pathways may be selected

with priority. Chiral and therapeutic effects on AD and HCC of selected drugs can be measured first in a cell model, and eventually in a clinical test. For example, HBV replication induced angiogenesis was indicated by tube formation of endothelial cells cultured in condition medium from RPHs or HepG2 cells supporting HBV replication. HBV transfection may change some proteins' expression levels to increase angiogenesis. Whether chiral NSAIDs have effects regulating these proteins expression towards anti-angiogenesis can be evaluated by EC tube formation or similar methods. The chiral NSAIDs inhibition on HCC can also be tested out *in vivo*. Cells with HBV replication can be injected into nude mice with NSAIDs orally taken at the same time. The growth of the tumor can be monitored over a time course and tumor volume recorded by carefully measuring the tumor volume. Based on the animal study, the inhibitory effects of chiral Ibuprofen on HCC may provide promising information for cancer therapy.

As introduced earlier, most enantiomers of racemic drugs have biologically different effects such as their pharmacology, pharmacokinetics, toxicology and metabolism in the body. Most new chiral drugs for specific disease therapy are developed in single-enantiomer form. In this thesis, chiral ibuprofen showed chirality in AD neuroprotective effects, and had different regulation effects on expressions of proteins such as Cox2. Further studies can be carried out on the chirality of other NSAIDs on AD or HCC therapy, and hopefully more valuable unichiral NSAIDs that are more potent and with lower drug toxicity can be discovered.

Overall, in this thesis, other than anti-inflammatory activities, chiral Ibuprofen

affects other physiological process such as reducing ROS for AD development and inhibiting angiogenesis induced by HBV replication. This study opens a wide field for chiral drug application research on AD and HCC therapy.

References

[1] Wsol, V., Skalova, L., Szotakova, B., Chiral inversion of drugs: coincidence or principle? *Curr Drug Metab* 2004, *5*, 517-533.

[2] Ariens, E. J., Wuis, E. W., Bias in pharmacokinetics and clinical pharmacology. *Clin Pharmacol Ther* 1987, *42*, 361-363.

[3] Easson, L. H., Stedman, E., Studies on the relationship between chemical constitution and physiological action: Molecular dissymmetry and physiological activity. *Biochem J* 1933, *27*, 1257-1266.

[4] Francotte, E., Lindner, W., *Chirality in Drug Research*, 2006.

[5] Evans, E. A., Problems and wonders of chiral molecules. Edited by Miklos Simonyi. Pub: Akad 閘 iai Kiad? Budpaest 1990, pp. 440. ISBN 963 05 5881 5 Pirce: ?5. *Journal of Labelled Compounds and Radiopharmaceuticals* 1991, *29*, 491-492.

[6] Portoghese, P. S., Relationships between stereostructure and pharmacological activities. *Annu Rev Pharmacol* 1970, *10*, 51-76.

[7] Sastry, B. V., Stereoisomerism and drug action in the nervous system. *Annu Rev Pharmacol* 1973, *13*, 253-267.

[8] Ariens, E. J., Stereochemistry: a source of problems in medicinal chemistry. *Med Res Rev* 1986, *6*, 451-466.

[9] Hutt, A. J., Tan, S. C., Drug chirality and its clinical significance. *Drugs* 1996, *52 Suppl 5*, 1-12.

[10] Jenner, P., Testa, B., The influence of stereochemical factors on drug disposition. *Drug Metab Rev* 1973, *2*, 117-184.

[11] Grinberg, N., Thompson, R., Chiral Separations by HPLC. *Encyclopedia of Chromatography* 2005, 321 - 326.

[12] Nusser, E., Banerjee, A., Gal, J., Excavations in drug chirality: 1. Cyclothiazide. *Chirality* 1991, *3*, 2-13.

[13] Drayer, D. E., Pharmacodynamic and pharmacokinetic differences between drug enantiomers in humans: an overview. *Clin Pharmacol Ther* 1986, *40*, 125-133.

[14] Waldeck, B., Three-dimensional pharmacology, a subject ranging from ignorance to overstatements. *Pharmacol Toxicol* 2003, *93*, 203-210.

[15] Landoni, M. F., Soraci, A., Pharmacology of chiral compounds: 2-arylpropionic acid derivatives. *Curr Drug Metab* 2001, *2*, 37-51.

[16] Marzo, A., Heftmann, E., Enantioselective analytical methods in pharmacokinetics with specific reference to genetic polymorphic metabolism. *J Biochem Biophys Methods* 2002, *54*, 57-70.

[17] V. Wsol, Skalova, L., Szotakova, B., Chiral Inversion of Drugs: Coincidence or Principle? *Current Drug Metabolism* 2004, *5*, 517-533.

[18] Adams, S. S., Bresloff, P., Mason, C. G., Pharmacological differences between the optical isomers of ibuprofen: evidence for metabolic inversion of the (-)-isomer. *J Pharm Pharmacol* 1976, *28*, 256-257.

[19] Hersh, E. V., Lally, E. T., Moore, P. A., Update on cyclooxygenase inhibitors: has a third COX isoform entered the fray? *Curr Med Res Opin* 2005, *21*, 1217-1226.

[20] Flower, R. J., The development of COX2 inhibitors. *Nat Rev Drug Discov* 2003, *2*, 179-191.

[21] Lim, G. P., Yang, F., Chu, T., Chen, P.-p., *et al.*, Ibuprofen reduces inflammation and plaque pathology in a mouse model for Alzheimer's disease. *Neurobiology of Aging* 2000, *21*, 17.

[22] Herndon, D. N., Dasu, M. R., Wolfe, R. R., Barrow, R. E., Gene expression profiles and protein balance in skeletal muscle of burned children after beta-adrenergic blockade. *Am J Physiol Endocrinol Metab* 2003, *285*, E783-789.
[23] Stapleton, M. P., Sir James Black and propranolol. The role of the basic sciences in the history of cardiovascular pharmacology. *Tex Heart Inst J* 1997, *24*, 336-342.
[24] Wu, A., Should beta-blockers still be used as initial antihypertensive agents in uncomplicated hypertension? *Ann Acad Med Singapore* 2007, *36*, 962-964.
[25] Agon, P., Goethals, P., Van Haver, D., Kaufman, J. M., Permeability of the blood-brain barrier for atenolol studied by positron emission tomography. *J Pharm Pharmacol* 1991, *43*, 597-600.
[26] Jamali, F., Mehvar, R., Pasutto, F. M., Enantioselective aspects of drug action and disposition: therapeutic pitfalls. *J Pharm Sci* 1989, *78*, 695-715.
[27] Scott, A. K., Stereoisomers and drug toxicity. The value of single stereoisomer therapy. *Drug Saf* 1993, *8*, 149-159.
[28] Eichelbaum, M., Side effects and toxic reactions of chiral drugs: a clinical perspective. *Arch Toxicol Suppl* 1995, *17*, 514-521.
[29] Cotzias, G. C., Papavasiliou, P. S., Gellene, R., Modification of Parkinsonism--chronic treatment with L-dopa. *N Engl J Med* 1969, *280*, 337-345.
[30] Volosin, K., Greenberg, R. M., Greenspon, A. J., Tocainide associated agranulocytosis. *Am Heart J* 1985, *109*, 1392-1393.
[31] Riva, E., Mennini, T., Latini, R., The alpha- and beta-adrenoceptor blocking activities of labetalol and its RR-SR (50:50) stereoisomers. *Br J Pharmacol* 1991, *104*, 823-828.
[32] Gal, J., New single-isomer compounds on the horizon. *CNS Spectr* 2002, *7*, 45-54.
[33] Burke, D., Henderson, D. J., Chirality: a blueprint for the future. *Br J Anaesth* 2002, *88*, 563-576.
[34] Lin, J. H., Lu, A. Y., Role of pharmacokinetics and metabolism in drug discovery and development. *Pharmacol Rev* 1997, *49*, 403-449.
[35] Stoschitzky K, Lindner W, G., Z., Racemic beta-blockers-fixed combinations of different drugs. *Journal of Clinical and Basic Cardiology* 1998, *1*, 15-19.
[36] Pham-Huy, C., Sahui-Gnassi, A., Saada, V., Gramond, J. P., *et al.*, Microassay of propranolol enantiomers and conjugates in human plasma and urine by high-performance liquid chromatography after chiral derivatization for pharmacokinetic study. *J Pharm Biomed Anal* 1994, *12*, 1189-1198.
[37] Lien Ai Nguyen, Hua He, Pham-Huy, C., Chiral Drugs. An Overview. *Int J Biomed Sci* 2006, *2*, 85-100.
[38] Szelenyi, I., Geisslinger, G., Polymeropoulos, E., Paul, W., *et al.*, The real gordian knot: racemic mixtures versus pure enantiomers. *Drug News Perspect* 1998, *11*, 139-160.
[39] Townsend, K. P., Pratico, D., Novel therapeutic opportunities for Alzheimer's disease: focus on nonsteroidal anti-inflammatory drugs. *Faseb J* 2005, *19*, 1592-1601.
[40] Yan, Q., Zhang, J., Liu, H., Babu-Khan, S., *et al.*, Anti-inflammatory drug therapy alters beta-amyloid processing and deposition in an animal model of Alzheimer's disease. *J Neurosci* 2003, *23*, 7504-7509.
[41] Scharf, S., Mander, A., Ugoni, A., Vajda, F., Christophidis, N., A double-blind, placebo-controlled trial of diclofenac/misoprostol in Alzheimer's disease. *Neurology* 1999, *53*, 197-201.
[42] Jantzen, P. T., Connor, K. E., DiCarlo, G., Wenk, G. L., *et al.*, Microglial activation and beta -amyloid deposit reduction caused by a nitric oxide-releasing nonsteroidal anti-inflammatory drug in amyloid precursor protein plus presenilin-1 transgenic mice. *J Neurosci* 2002, *22*, 2246-2254.

[43] McGeer, P. L., McGeer, E. G., Polymorphisms in inflammatory genes and the risk of Alzheimer disease. *Arch Neurol* 2001, *58*, 1790-1792.
[44] Brigitte Vollmar, S. S., Michael D. Menger,, An intravital fluorescence microscopic study of hepatic microvascular and cellular derangements in developing cirrhosis in rats. *Hepatology* 1998, *27*, 1544-1553.
[45] Sugimachi, K., Tanaka, S., Terashi, T., Taguchi, K., Rikimaru, T., The mechanisms of angiogenesis in hepatocellular carcinoma: angiogenic switch during tumor progression. *Surgery* 2002, *131*, S135-141.
[46] Dormond, O., Foletti, A., Paroz, C., Ruegg, C., NSAIDs inhibit alpha V beta 3 integrin-mediated and Cdc42/Rac-dependent endothelial-cell spreading, migration and angiogenesis. *Nat Med* 2001, *7*, 1041-1047.
[47] Rothwell, P. M., Wilson, M., Elwin, C. E., Norrving, B., *et al.*, Long-term effect of aspirin on colorectal cancer incidence and mortality: 20-year follow-up of five randomised trials. *Lancet* 2010, *376*, 1741-1750.
[48] Yao, M., Zhou, W., Sangha, S., Albert, A., *et al.*, Effects of nonselective cyclooxygenase inhibition with low-dose ibuprofen on tumor growth, angiogenesis, metastasis, and survival in a mouse model of colorectal cancer. *Clin Cancer Res* 2005, *11*, 1618-1628.
[49] Wu, N., Causen, A., Recent development of ultra - high pressure liquid chromatography. *CACS Communications* 2008, *2*, 15-21.
[50] Kromidas, S., HPLC Made to Measure 2006, 627-641.
[51] Wu, Z., Gao, W., Phelps, M. A., Wu, D., *et al.*, Favorable effects of weak acids on negative-ion electrospray ionization mass spectrometry. *Anal Chem* 2004, *76*, 839-847.
[52] Jemal, M., Huang, M., Jiang, X., Mao, Y., Powell, M. L., Direct injection versus liquid-liquid extraction for plasma sample analysis by high performance liquid chromatography with tandem mass spectrometry. *Rapid Commun Mass Spectrom* 1999, *13*, 2125-2132.
[53] Bruins, A. P., Mechanistic aspects of electrospray ionization. *Journal of Chromatography A* 1998, *794*, 345-357.
[54] Wang, G., Hsieh, Y., Korfmacher, W. A., Comparison of atmospheric pressure chemical ionization, electrospray ionization, and atmospheric pressure photoionization for the determination of cyclosporin A in rat plasma. *Anal Chem* 2005, *77*, 541-548.
[55] Singh, G., Gutierrez, A., Xu, K., Blair, I. A., Liquid chromatography/electron capture atmospheric pressure chemical ionization/mass spectrometry: analysis of pentafluorobenzyl derivatives of biomolecules and drugs in the attomole range. *Anal Chem* 2000, *72*, 3007-3013.
[56] Jemal, M., Xia, Y. Q., LC-MS Development strategies for quantitative bioanalysis. *Curr Drug Metab* 2006, *7*, 491-502.
[57] Guevremont, R., High-field asymmetric waveform ion mobility spectrometry: a new tool for mass spectrometry. *J Chromatogr A* 2004, *1058*, 3-19.
[58] Shvartsburg, A. A., Tang, K., Smith, R. D., Optimization of the design and operation of FAIMS analyzers. *J Am Soc Mass Spectrom* 2005, *16*, 2-12.
[59] Marshall, A. G., Hendrickson, C. L., Jackson, G. S., Fourier transform ion cyclotron resonance mass spectrometry: a primer. *Mass Spectrom Rev* 1998, *17*, 1-35.
[60] Lee, M. S., Kerns, E. H., LC/MS applications in drug development. *Mass Spectrom Rev* 1999, *18*, 187-279.
[61] Chen, C., Gonzalez, F. J., Idle, J. R., LC-MS-based metabolomics in drug metabolism. *Drug*

Metab Rev 2007, *39*, 581-597.
[62] Jiang, H., Li, Y., Pelzer, M., Cannon, M. J., *et al.*, Determination of molindone enantiomers in human plasma by high-performance liquid chromatography-tandem mass spectrometry using macrocyclic antibiotic chiral stationary phases. *J Chromatogr A* 2008, *1192*, 230-238.
[63] Reddy, A., Hashim, M., Wang, Z., Penn, L., *et al.*, A novel method for assessing inhibition of ibuprofen chiral inversion and its application in drug discovery. *Int J Pharm* 2007, *335*, 63-69.
[64] Trivedi, R. K., Layek, B., Kumar, T. S., Vittal, S., *et al.*, Chiral bioanalysis of torcetrapib enantiomers in hamster plasma by normal-phase liquid chromatography and detection by atmospheric pressure chemical ionization tandem mass spectrometry. *J Chromatogr B Analyt Technol Biomed Life Sci* 2007, *860*, 227-234.
[65] Chang, D., Kolis, S. J., Linderholm, K. H., Julian, T. F., *et al.*, Bioanalytical method development and validation for a large peptide HIV fusion inhibitor (Enfuvirtide, T-20) and its metabolite in human plasma using LC-MS/MS. *J Pharm Biomed Anal* 2005, *38*, 487-496.
[66] Lin, C. C., Lau, J. Y., Specific, sensitive and accurate LC-MS/MS method for the measurement of levovirin in rat and monkey plasma. *J Pharm Biomed Anal* 2002, *30*, 239-246.
[67] Qian, W. J., Jacobs, J. M., Liu, T., Camp, D. G., 2nd, Smith, R. D., Advances and challenges in liquid chromatography-mass spectrometry-based proteomics profiling for clinical applications. *Mol Cell Proteomics* 2006, *5*, 1727-1744.
[68] Ducret, A., Van Oostveen, I., Eng, J. K., Yates, J. R., 3rd, Aebersold, R., High throughput protein characterization by automated reverse-phase chromatography/electrospray tandem mass spectrometry. *Protein Sci* 1998, *7*, 706-719.
[69] Jon M. Jacobs, Matthew E. Monroe, Wei-Jun Qian, Yufeng Shen, *et al.*, Ultra-sensitive, high throughput and quantitative proteomics measurements. *International Journal of Mass SpectrometryVolume* 2005, *38*, 195-212.
[70] Daviss, B., Growing pains for metabolomics. *Scientist* 2005, *19*, 25-28.
[71] Katajamaa, M., Oresic, M., Data processing for mass spectrometry-based metabolomics. *J Chromatogr A* 2007, *1158*, 318-328.
[72] Lenz, E. M., Wilson, I. D., Analytical strategies in metabonomics. *J Proteome Res* 2007, *6*, 443-458.
[73] Georgios T., Helen G. Gika, Wilson, I. D., LC-MS-based methodology for global metabolite profiling in metabonomics/metabolomics. *Trends Analyt Chem* 2008, *27*, 251-260.
[74] Wilkins, M. R., Sanchez, J. C., Gooley, A. A., Appel, R. D., *et al.*, Progress with proteome projects: why all proteins expressed by a genome should be identified and how to do it. *Biotechnol Genet Eng Rev* 1996, *13*, 19-50.
[75] Aebersold, R., Mann, M., Mass spectrometry-based proteomics. *Nature* 2003, *422*, 198-207.
[76] Takahashi, N., Kaji, H., Yanagida, M., Hayano, T., Isobe, T., Proteomics: advanced technology for the analysis of cellular function. *J Nutr* 2003, *133*, 2090S-2096S.
[77] Shen, Z., Wang, M., Briggs, S. P., Use of high-throughput LC–MS/MS proteomics technologies in drug discovery *Drug Discovery Today: Technologies* 2006, *3*, 301-306.
[78] Tannu, N. S., Hemby, S. E., Methods for proteomics in neuroscience. *Prog Brain Res* 2006, *158*, 41-82.
[79] Kusmierz, J. J., Sumrada, R., Desiderio, D. M., Fast atom bombardment mass spectrometric quantitative analysis of methionine-enkephalin in human pituitary tissues. *Anal Chem* 1990, *62*, 2395-2400.

[80] Mirgorodskaya, O. A., Kozmin, Y. P., Titov, M. I., Korner, R., *et al.*, Quantitation of peptides and proteins by matrix-assisted laser desorption/ionization mass spectrometry using (18)O-labeled internal standards. *Rapid Commun Mass Spectrom* 2000, *14*, 1226-1232.
[81] Yao, X., Freas, A., Ramirez, J., Demirev, P. A., Fenselau, C., Proteolytic 18O labeling for comparative proteomics: model studies with two serotypes of adenovirus. *Anal Chem* 2001, *73*, 2836-2842.
[82] Ong, S. E., Blagoev, B., Kratchmarova, I., Kristensen, D. B., *et al.*, Stable isotope labeling by amino acids in cell culture, SILAC, as a simple and accurate approach to expression proteomics. *Mol Cell Proteomics* 2002, *1*, 376-386.
[83] Hanash, S., Integrated global profiling of cancer. *Nat Rev Cancer* 2004, *4*, 638-644.
[84] Stanley, B. A., Gundry, R. L., Cotter, R. J., Van Eyk, J. E., Heart disease, clinical proteomics and mass spectrometry. *Dis Markers* 2004, *20*, 167-178.
[85] Griffin, T. J., Gygi, S. P., Ideker, T., Rist, B., *et al.*, Complementary profiling of gene expression at the transcriptome and proteome levels in Saccharomyces cerevisiae. *Mol Cell Proteomics* 2002, *1*, 323-333.
[86] Katz-Jaffe, M. G., Schoolcraft, W. B., Gardner, D. K., Analysis of protein expression (secretome) by human and mouse preimplantation embryos. *Fertil Steril* 2006, *86*, 678-685.
[87] Shiio, Y., Donohoe, S., Yi, E. C., Goodlett, D. R., *et al.*, Quantitative proteomic analysis of Myc oncoprotein function. *EMBO J* 2002, *21*, 5088-5096.
[88] Tan, T. L., Chen, W. N., A proteomics analysis of cellular proteins associated with HBV genotype-specific HBX: potential in identification of early diagnostic markers for HCC. *J Clin Virol* 2005, *33*, 293-298.
[89] Goufman, E. I., Moshkovskii, S. A., Tikhonova, O. V., Lokhov, P. G., *et al.*, Two-dimensional electrophoretic proteome study of serum thermostable fraction from patients with various tumor conditions. *Biochemistry (Mosc)* 2006, *71*, 354-360.
[90] Huang, T. C., Chang, H. Y., Hsu, C. H., Kuo, W. H., *et al.*, Targeting therapy for breast carcinoma by ATP synthase inhibitor aurovertin B. *J Proteome Res* 2008, *7*, 1433-1444.
[91] Ashman, K., Moran, M. F., Sicheri, F., Pawson, T., Tyers, M., Cell signalling - the proteomics of it all. *Sci STKE* 2001, *2001*, PE33.
[92] Jones, J., Wu, K., Yang, Y., Guerrero, C., *et al.*, A targeted proteomic analysis of the ubiquitin-like modifier nedd8 and associated proteins. *J Proteome Res* 2008, *7*, 1274-1287.
[93] Com, E., Lagadec, C., Page, A., El Yazidi-Belkoura, I., *et al.*, Nerve growth factor receptor TrkA signaling in breast cancer cells involves Ku70 to prevent apoptosis. *Mol Cell Proteomics* 2007, *6*, 1842-1854.
[94] McNulty, D. E., Annan, R. S., Hydrophilic interaction chromatography reduces the complexity of the phosphoproteome and improves global phosphopeptide isolation and detection. *Mol Cell Proteomics* 2008, *7*, 971-980.
[95] Kawamura, A., Hindi, S., Protein fishing with chiral molecular baits. *Chirality* 2005, *17*, 332-337.
[96] Arnell, R., Ferraz, N., Fornstedt, T., Analytical characterization of chiral drug-protein interactions: comparison between the optical biosensor (surface plasmon resonance) assay and the HPLC perturbation method. *Anal Chem* 2006, *78*, 1682-1689.
[97] Li, W., Covey, D. F., Alakoskela, J. M., Kinnunen, P. K., Steinbach, J. H., Enantiomers of neuroactive steroids support a specific interaction with the GABA-C receptor as the mechanism of steroid action. *Mol Pharmacol* 2006, *69*, 1779-1782.

[98] Herndon, D. N., Hart, D. W., Wolf, S. E., Chinkes, D. L., Wolfe, R. R., Reversal of catabolism by beta-blockade after severe burns. *N Engl J Med* 2001, *345*, 1223-1229.
[99] Lamont, L. S., Brown, T., Riebe, D., Caldwell, M., The major components of human energy balance during chronic beta-adrenergic blockade. *J Cardiopulm Rehabil* 2000, *20*, 247-250.
[100] Lamont, L. S., Beta-blockers and their effects on protein metabolism and resting energy expenditure. *J Cardiopulm Rehabil* 1995, *15*, 183-185.
[101] Sui, J., Zhang, J., Ching, C. B., Chen, W. N., Comparative proteomic analysis of extracellular proteins reveals secretion of T-kininogen from vascular smooth muscle cells in response to incubation with s-enantiomer of propranolol. *Mol Pharm* 2008, *5*, 885-890.
[102] Lacor, P. N., Buniel, M. C., Furlow, P. W., Clemente, A. S., *et al.*, Abeta oligomer-induced aberrations in synapse composition, shape, and density provide a molecular basis for loss of connectivity in Alzheimer's disease. *J Neurosci* 2007, *27*, 796-807.
[103] Goedert, M., Spillantini, M. G., Crowther, R. A., Tau proteins and neurofibrillary degeneration. *Brain Pathol* 1991, *1*, 279-286.
[104] Zhang, J., Sui, J., Ching, C. B., Chen, W. N., Protein profile in neuroblastoma cells incubated with S- and R-enantiomers of ibuprofen by iTRAQ-coupled 2-D LC-MS/MS analysis: possible action of induced proteins on Alzheimer's disease. *Proteomics* 2008, *8*, 1595-1607.
[105] Szekely, C. A., Town, T., Zandi, P. P., NSAIDs for the chemoprevention of Alzheimer's disease. *Subcell Biochem* 2007, *42*, 229-248.
[106] Adams S S, B. P., Mason G C., Pharmacological difference between the optical isomers of Ibuprofen: evidence for metabolic inversion of the (-) isomer. . *J Pharm Pharmacol* 1976, *28*, 256.
[107] Whitlam, J. B., Brown, K. F., Crooks, M. J., Room, G. F., Transsynovial distribution of ibuprofen in arthritic patients. *Clin Pharmacol Ther* 1981, *29*, 487-492.
[108] Bates, K. A., Martins, R. N., Harvey, A. R., Oxidative stress in a rat model of chronic gliosis. *Neurobiology of Aging* 2007, *28*, 995-1008.
[109] Lambert, J.-C., Bensemain, F., Chapuis, J., Cottel, D., Amouyel, P., Association study of the PIN1 gene with Alzheimer's disease. *Neuroscience Letters* 2006, *402*, 259-261.
[110] Krapfenbauer, K., Engidawork, E., Cairns, N., Fountoulakis, M., Lubec, G., Aberrant expression of peroxiredoxin subtypes in neurodegenerative disorders. *Brain Research* 2003, *967*, 152-160.
[111] Yao, J., Taylor, M., Davey, F., Ren, Y., *et al.*, Interaction of amyloid binding alcohol dehydrogenase/A[beta] mediates up-regulation of peroxiredoxin II in the brains of Alzheimer's disease patients and a transgenic Alzheimer's disease mouse model. *Molecular and Cellular Neuroscience, In Press, Corrected Proof*.
[112] Butterfield, D. A., Poon, H. F., St. Clair, D., Keller, J. N., *et al.*, Redox proteomics identification of oxidatively modified hippocampal proteins in mild cognitive impairment: Insights into the development of Alzheimer's disease. *Neurobiology of Disease* 2006, *22*, 223-232.
[113] Cullingford, T. E., The ketogenic diet; fatty acids, fatty acid-activated receptors and neurological disorders. *Prostaglandins, Leukotrienes and Essential Fatty Acids*
Metabolic and Health Implications of Moderate Ketosis and the Ket ogenic Diet 2004, *70*, 253-264.
[114] Patil, S., Chan, C., Palmitic and stearic fatty acids induce Alzheimer-like hyperphosphorylation of tau in primary rat cortical neurons. *Neuroscience Letters* 2005, *384*, 288-293.
[115] Meier-Ruge, W., Iwangoff, P., Reichlmeier, K., Neurochemical enzyme changes in Alzheimer's and Pick's disease. *Archives of Gerontology and Geriatrics* 1984, *3*, 161-165.
[116] Neve, R. L., McPhie, D. L., The cell cycle as a therapeutic target for Alzheimer's disease.

Pharmacology & Therapeutics 2006, *111*, 99-113.
[117] Sultana, R., Boyd-Kimball, D., Poon, H. F., Cai, J., *et al.*, Redox proteomics identification of oxidized proteins in Alzheimer's disease hippocampus and cerebellum: An approach to understand pathological and biochemical alterations in AD. *Neurobiology of Aging* 2006, *27*, 1564-1576.
[118] Zapolska-Downar, D., Naruszewicz, M., Zapolski-Downar, A., Markiewski, M., *et al.*, Ibuprofen inhibits adhesiveness of monocytes to endothelium and reduces cellular oxidative stress in smokers and non-smokers. *Eur J Clin Invest* 2000, *30*, 1002-1010.
[119] Boyd-Kimball, D., Sultana, R., Fai Poon, H., Lynn, B. C., *et al.*, Proteomic identification of proteins specifically oxidized by intracerebral injection of amyloid [beta]-peptide (1-42) into rat brain: Implications for Alzheimer's disease. *Neuroscience* 2005, *132*, 313-324.
[120] Nahreini, P., Hovland, A. R., Kumar, B., Andreatta, C., *et al.*, Effects of altered cyclophilin A expression on growth and differentiation of human and mouse neuronal cells. *Cell Mol Neurobiol* 2001, *21*, 65-79.
[121] Lie, A. A., Schroder, R., Blumcke, I., Magin, T. M., *et al.*, Plectin in the human central nervous system: predominant expression at pia/glia and endothelia/glia interfaces. *Acta Neuropathol (Berl)* 1998, *96*, 215-221.
[122] Sui, J., Tan, T. L., Zhang, J., Ching, C. B., Chen, W. N., iTRAQ-coupled 2D LC-MS/MS analysis on protein profile in vascular smooth muscle cells incubated with S- and R-enantiomers of propranolol: possible role of metabolic enzymes involved in cellular anabolism and antioxidant activity. *J Proteome Res* 2007, *6*, 1643-1651.
[123] Avila, M. A., Lu, K. P., Hepatitis B virus x protein and pin1 in liver cancer: "les liaisons dangereuses". *Gastroenterology* 2007, *132*, 1180-1183.
[124] Feitelson, M. A., Lee, J., Hepatitis B virus integration, fragile sites, and hepatocarcinogenesis. *Cancer Lett* 2007, *252*, 157-170.
[125] Lee, S. W., Lee, Y. M., Bae, S. K., Murakami, S., *et al.*, Human hepatitis B virus X protein is a possible mediator of hypoxia-induced angiogenesis in hepatocarcinogenesis. *Biochem Biophys Res Commun* 2000, *268*, 456-461.
[126] Gervaz, P., Scholl, B., Mainguene, C., Poitry, S., *et al.*, Angiogenesis of liver metastases: role of sinusoidal endothelial cells. *Dis Colon Rectum* 2000, *43*, 980-986.
[127] Zhang, J., Niu, D., Sui, J., Ching, C. B., Chen, W. N., Protein profile in hepatitis B virus replicating rat primary hepatocytes and HepG2 cells by iTRAQ-coupled 2-D LC-MS/MS analysis: Insights on liver angiogenesis. *Proteomics* 2009, *9*, 2836-2845.
[128] Vollmar, B., Siegmund, S., Menger, M. D., An intravital fluorescence microscopic study of hepatic microvascular and cellular derangements in developing cirrhosis in rats. *Hepatology* 1998, *27*, 1544-1553.
[129] Cheng, A. S., Chan, H. L., To, K. F., Leung, W. K., *et al.*, Cyclooxygenase-2 pathway correlates with vascular endothelial growth factor expression and tumor angiogenesis in hepatitis B virus-associated hepatocellular carcinoma. *Int J Oncol* 2004, *24*, 853-860.
[130] Majano, P., Lara-Pezzi, E., Lopez-Cabrera, M., Apolinario, A., *et al.*, Hepatitis B virus X protein transactivates inducible nitric oxide synthase gene promoter through the proximal nuclear factor kappaB-binding site: evidence that cytoplasmic location of X protein is essential for gene transactivation. *Hepatology* 2001, *34*, 1218-1224.
[131] Medina, J., Arroyo, A. G., Sanchez-Madrid, F., Moreno-Otero, R., Angiogenesis in chronic inflammatory liver disease. *Hepatology* 2004, *39*, 1185-1195.

[132] Sanz-Cameno, P., Martin-Vilchez, S., Lara-Pezzi, E., Borque, M. J., *et al.*, Hepatitis B virus promotes angiopoietin-2 expression in liver tissue: role of HBV x protein. *Am J Pathol* 2006, *169*, 1215-1222.
[133] Moon, E. J., Jeong, C. H., Jeong, J. W., Kim, K. R., *et al.*, Hepatitis B virus X protein induces angiogenesis by stabilizing hypoxia-inducible factor-1alpha. *Faseb J* 2004, *18*, 382-384.
[134] Braet, F., De Zanger, R., Sasaoki, T., Baekeland, M., *et al.*, Assessment of a method of isolation, purification, and cultivation of rat liver sinusoidal endothelial cells. *Lab Invest* 1994, *70*, 944-952.
[135] Yoo, Y. G., Oh, S. H., Park, E. S., Cho, H., *et al.*, Hepatitis B virus X protein enhances transcriptional activity of hypoxia-inducible factor-1alpha through activation of mitogen-activated protein kinase pathway. *J Biol Chem* 2003, *278*, 39076-39084.
[136] Isaacs, J. S., Jung, Y. J., Mole, D. R., Lee, S., *et al.*, HIF overexpression correlates with biallelic loss of fumarate hydratase in renal cancer: novel role of fumarate in regulation of HIF stability. *Cancer Cell* 2005, *8*, 143-153.
[137] Yu, Y., Liu, Y., Shen, N., Xu, X., *et al.*, Crystal structure of human tryptophanyl-tRNA synthetase catalytic fragment: insights into substrate recognition, tRNA binding, and angiogenesis activity. *J Biol Chem* 2004, *279*, 8378-8388.
[138] Otani, A., Slike, B. M., Dorrell, M. I., Hood, J., *et al.*, A fragment of human TrpRS as a potent antagonist of ocular angiogenesis. *Proc Natl Acad Sci U S A* 2002, *99*, 178-183.
[139] Tzima, E., Schimmel, P., Inhibition of tumor angiogenesis by a natural fragment of a tRNA synthetase. *Trends Biochem Sci* 2006, *31*, 7-10.
[140] Tanaka, S., Wands, J. R., Arii, S., Induction of angiopoietin-2 gene expression by COX-2: a novel role for COX-2 inhibitors during hepatocarcinogenesis. *J Hepatol* 2006, *44*, 233-235.
[141] Fazal, F., Bijli, K. M., Minhajuddin, M., Rein, T., *et al.*, Essential role of cofilin-1 in regulating thrombin-induced RelA/p65 nuclear translocation and intercellular adhesion molecule 1 (ICAM-1) expression in endothelial cells. *J Biol Chem* 2009, *284*, 21047-21056.
[142] Jiang, X., Takahashi, N., Ando, K., Otsuka, T., *et al.*, NF-kappa B p65 transactivation domain is involved in the NF-kappa B-inducing kinase pathway. *Biochem Biophys Res Commun* 2003, *301*, 583-590.
[143] Kim, J. Y., Kim, H., Suk, K., Lee, W. H., Activation of CD147 with cyclophilin a induces the expression of IFITM1 through ERK and PI3K in THP-1 cells. *Mediators Inflamm* 2010, *2010*, 821940.
[144] Dhar, S. K., Lynn, B. C., Daosukho, C., St Clair, D. K., Identification of nucleophosmin as an NF-kappaB co-activator for the induction of the human SOD2 gene. *J Biol Chem* 2004, *279*, 28209-28219.
[145] Ryo, A., Suizu, F., Yoshida, Y., Perrem, K., *et al.*, Regulation of NF-kappaB signaling by Pin1-dependent prolyl isomerization and ubiquitin-mediated proteolysis of p65/RelA. *Mol Cell* 2003, *12*, 1413-1426.
[146] Atkinson, G. P., Nozell, S. E., Harrison, D. K., Stonecypher, M. S., *et al.*, The prolyl isomerase Pin1 regulates the NF-kappaB signaling pathway and interleukin-8 expression in glioblastoma. *Oncogene* 2009, *28*, 3735-3745.
[147] Swiatkowska, M., Szemraj, J., Cierniewski, C. S., Induction of PAI-1 expression by tumor necrosis factor alpha in endothelial cells is mediated by its responsive element located in the 4G/5G site. *FEBS J* 2005, *272*, 5821-5831.
[148] Guzhova, I. V., Darieva, Z. A., Melo, A. R., Margulis, B. A., Major stress protein Hsp70 interacts with NF-kB regulatory complex in human T-lymphoma cells. *Cell Stress Chaperones* 1997, *2*, 132-139.

[149] Schulze-Osthoff, K., Schenk, H., Droge, W., Effects of thioredoxin on activation of transcription factor NF-kappa B. *Methods Enzymol* 1995, *252*, 253-264.
[150] Su, F., Theodosis, C. N., Schneider, R. J., Role of NF-kappaB and myc proteins in apoptosis induced by hepatitis B virus HBx protein. *J Virol* 2001, *75*, 215-225.
[151] Foo, S. Y., Nolan, G. P., NF-kappaB to the rescue: RELs, apoptosis and cellular transformation. *Trends Genet* 1999, *15*, 229-235.
[152] Moonen, R. M., Reyes, I., Cavallaro, G., Gonzalez-Luis, G., *et al.*, The T1405N carbamoyl phosphate synthetase polymorphism does not affect plasma arginine concentrations in preterm infants. *PLoS One* 2010, *5*, e10792.
[153] Schulz, L. C., Bahr, J. M., Glucose-6-phosphate isomerase is necessary for embryo implantation in the domestic ferret. *Proc Natl Acad Sci U S A* 2003, *100*, 8561-8566.
[154] Schepens, B., Tinton, S. A., Bruynooghe, Y., Beyaert, R., Cornelis, S., The polypyrimidine tract-binding protein stimulates HIF-1alpha IRES-mediated translation during hypoxia. *Nucleic Acids Res* 2005, *33*, 6884-6894.
[155] Okamura, K., Sato, Y., Matsuda, T., Hamanaka, R., *et al.*, Endogenous basic fibroblast growth factor-dependent induction of collagenase and interleukin-6 in tumor necrosis factor-treated human microvascular endothelial cells. *J Biol Chem* 1991, *266*, 19162-19165.

Supplement

Gene name	primer sequences
fatty acid synthase	Sense 5' CACCCACAACAGCCTCTTCC 3'
	Antisense 5' ACTTTCCCGTCGCATACCTG 3'
annexin A2	Sense 5' AATCATGGTCTCCCGCAGTG 3'
	Antisense 5' CGGGCTTCAGTCATCTCCAC 3'
galectin-1	Sense 5' CAATCATGGCTTGTGGTCTGG 3'
	Antisense 5' TGAAGCGAGGGTTGAAGTGC 3'
triosephosphate isomerase 1	Sense 5' GAGGGAATAAACCTGGCACTA 3'
	Antisense 5' GGCTATGACAGTCTGCTACGC 3'
enolase 1	Sense 5' CCTGCCCTGGTTAGCAAGAA 3'
	Antisense 5' AAGTCAGCGATGTGGCGGTA 3'
Peptidyl-prolyl cis-trans isomerase A	Sense 5' ACGAGCGGTTAAGTCAGAGG 3'
	Antisense 5' CAAGTTTCATTAGCCGAGGA 3'
peroxiredoxin 6	Sense 5' TTGAGAAGCGTAACGTGAAA 3'
	Antisense 5' TGTCCTTATCGTCCAGCATT 3'
lactate dehydrogenase β	Sense 5' TTGTCTTCTCCGCACGACTG 3'
	Antisense 5' CCAACTTGTCCAACACCCAC 3'
phosphoglycerate mutase 1	Sense 5' CGGTATCCCAATCGTGTATG 3'
	Antisense 5' TACTTGCTAGTCTGCGTGCC 3'
plectin 1	Sense 5' TTCTCCTGTGGACCTGTTATTG 3'
	Antisense 5' GCCCTGTAGCCAGTGTTTCT 3'
peroxiredoxin 2	Sense 5' CGTCAGTCAGGCTGGTCTCG 3'
	Antisense 5' AGTGTCCCACAGGCCAATCA 3'
GTP-binding nuclear protein Ran	Sense 5' GATGAATGGGCTTCGGAGTG 3'
	Antisense 5' ATGGGAATGACAGTGACAAACG 3'
β-actin	Sense 5' CTTAGTTGCGTTACACCCTTTC 3'
	Antisense 5' ACCTTCACCGTTCCAGTTTT 3'

fumarate hydratase (HepG2 cells)	Sense: 5'-GCATCCCAACGATCATGTTAA-3'
	Antisense: 5'-TGCCCAAGAGTAAGTGGAACA-3'
tryptophanyl-tRNA synthetase (HepG2 cells)	Sense: 5'-CAGAGGCATCTTCTTCTCACA-3'
	Anti sense: 5'-AATACATCCTGGAGCCACTTT-3'
fumarate hydratase (RPHs)	Sense: 5'-ATGGCAGACTGGATCAGGAAC-3'
	Anti sense: 5'-ATCGTTGGGATGCACAGGTAT-3'
tryptophanyl-tRNA synthetase (RPHs)	Sense: 5'-CCTGGTCTTGACTCGTCTGCT-3'
	Anti sense: 5'-TTCATCCTTTGACGCATTTCC-3'.
HBV core gene	Sense: 5’-ATGGACATTGACCCTTATAAAG-3’
	Anti sense: 5’-AGACTCTAAGGCTTCTCGAT-3’
Rat □ -actin (RPHs)	Sense: 5’ -TCTATCCTGGCCTCACTGT-3’
	Anti sense: 5’-TGTAAAACGCAGCTCAGTAA-3’
HBsAg gene	Sense: 5’-TCACCATATTCTTGGGAACAA-3’
	Anti sense: 5’-GTTTTGTTAGGGTTTAAATG-3’

Supplement table 1: Primer lists

mRNA ID	Gene
NM_006988	ADAMTS1
NM_001123041	chemokine (C-C motif) receptor 2 (CCR2
NM_001001548	CD36 molecule (thrombospondin receptor)
BC095432	ephrin-A1
NM_002467	v-myc myelocytomatosis viral oncogene homolog (avian) (MYC)
NM_002995	chemokine (C motif) ligand 1 (XCL1)
NM_002176	interferon, beta 1, fibroblast (IFNB1)
EU332844	integrin, alpha V (vitronectin receptor
NM_000212	integrin, beta 3 (platelet glycoprotein IIIa, antigen CD61) (ITGB3)
NM_002253	kinase insert domain receptor (a type III receptor tyrosine kinase) (KDR)
AK293055	highly similar to Homo sapiens SMAD, mothers against DPP homolog 1 (Drosophila) (SMAD1)
NM_004995	matrix metallopeptidase 14 (membrane-inserted)
NM_002422	matrix metallopeptidase 3
NM_002423	matrix metallopeptidase 7
NM_001024628	Neuropilin1
NM_006691.3	CD31
NM_000963	Cox2
NM_000582	Secreted phosphoprotein 1
NM_000459	Tie 2
NM_001135599	TGF beta2
NM_003255	Tim2
NM_000362	Tim3
NM_001078	vcam
NM_000029	angiotensinogen
NM_001872	Carboxypeptidase B 2
NM_001168319	endothelin 1
NM_000576	interleukin 1 beta
NM_000600	interleukin 6
NM_006528	tissue factor pathway inhibitor 2
NM_006404	protein C receptor
NM_000700	annexin A1
NM_016242	endomucin
NM_000591	CD14
NM_002526	5 nucleotidase
NM_000873	intercellular adhesion molecule 2
NM_001018111	podocalyxin-like
NM_001002857	annexin A2
NM_001432	epiregulin

Supplement table 2: lists of screened angiogenic genes

Abbreviations:

1D - one dimensional

2D - two dimensional

2D DIGE- Two-Dimensional Difference Gel Electrophoresis

2-DE- two-dimensional gel electrophoresis

AD- Alzheimer disease

APCI -atmospheric pressure chemical ionization

APPI-atmospheric pressure photoionization

ATCC- American Type Cell Culture Collection

bFGF- fibroblast growth factor

CI- Chemical ionization

CNS- Central Nervous System

Cox2- cyclooxygenase-2

CPS1-Carbamoyl-phosphate synthase

CyP-A -peptidyl-prolyl cis trans isomerase A

DCI- desorption chemical ionization

DDA- data-dependent acquisition

DEPC- Diethylpyrocarbonate

DMEM- Dulbecco's Minimum Essential Medium

DMEM-F12-Dulbecco's modified Eagle medium-Ham's nutrient medium

DMSO- dimethylsulphoxide

EBS-MD- epidermolysis bullosa simplex with muscular dystrophy

EC - endothelial cell

ECNI- electron-capture negative ionization

ECs- endothelial cells

EI- Electron ionization

ES-electrospray

ESI- electrospray ionization

FAB-fast-atom bombardment

FAIMS-High-Field Asymmetric Waveform Ion Mobility

FBS- Fetal Bovine Serum

FD- field desorption

FH - Fumarate hydratase

GFP- green fluorescent protein

GPI- Glucose-6-phosphate isomerase

HBSS- hanks' balanced salt solution

HBV - hepatitis B virus

HBx- hepatitis B virus x protein

HCC - hepatocellular carcinoma

HCV-Hepatitis C virus

HILIC- hydrophilic interaction chromatography

HUVECs- Human umbilical vein endothelial cells

ICAT- isotope-coded affinity tag

IFITM-1Interferon-induced transmembrane protein 1

IL6- interleukin 6

IMAC- immobilized metal ion affinity chromatography

IPTG-Isopropyl-β-D-thio-galactoside

IS- ion spray

iTRAQ - isobaric tags for relative and absolute quantification

IVC-inferior vena cava

LB -Luria-Bertani

LC - liquid chromatography

MALDI- matrix-assisted laser desorption ionization

MS - mass spectrometry

MTT- Dimethylthiazol

NFκB - nuclear factor kappa-light-chain-enhancer of activated B cells

NMR-Nuclear magnetic resonance

NO- nitric oxide

NSAIDs- Nonsteroidal anti-inflammatory drugs

PAI-1-Plasminogen activator inhibitor type 1

PBS- phosphate-buffered saline

PCR-Polymerase Chain Reaction

PD-liquid-SIMS, plasma desorption

PEs- proinflammatory eicosanoids

PGM1-Phosphoglycerate mutase 1

PGs- prostaglandins

Pin1- Peptidyl-prolyl cis-trans isomerase A

PPARa- peroxisome proliferator-activated receptor

Prx- peroxidases

PTB- polypyrimidine tract binding protein

ROS- Reactive Oxygen Species

RP - reversed-phase

RPH - rat primary hepatocyte

RT-PCR- Reverse Transcript Polymerase Chain Reaction

SCX - strong cation exchange

SDS-PAGE- sodium dodecyl sulfate polyacrylamide gel electrophoresis

SIMS-secondary-ion mass spectrometry

SPR- surface plasmon resonance

TBS- Tris-buffered saline

TGF ß- transforming growth factor ß

TOF- time-of-flight

TrkA- tyrosine kinase receptor

Trp RS - Tryptophanyl-tRNA synthetase

UHPLC- ultra-high pressure liquid chromatography

VEGF- vascular endothelial growth factor

List of representative publications

[1] Feng, X., **Zhang, J.**, Chen, W. N., Ching, C. B., Proteome profiling of Epstein-Barr virus infected nasopharyngeal carcinoma cell line: identification of potential biomarkers by comparative iTRAQ-coupled 2D LC/MS-MS analysis. J Proteomics 2011, 74, 567-576.

[2] Sui, J., Wang, M., **Zhang, J.**, Ching, C. B., Chen, W. N., Identification of differentially secreted proteins using two-dimensional liquid chromatography/tandem mass spectrometry in vascular smooth muscle cells incubated with S- and R-atenolol. Rap]d Communications in Mass Spectrometry 2010, 24, 1717-1719.

[3] Jia, J., Wang, J., Teh, M., Sun, W., et al., Identification of proteins differentially expressed between capillary endothelial cells of hepatocellular carcinoma and normal liver in an orthotopic rat tumor model using 2-D DIGE. Proteomics 2010, 10, 224-234.

[4] Bun Ching, C., **Zhang, J.**, Sui, J., Ning Chen, W., Proteomics profile of cellular response to chiral drugs: prospects for pharmaceutical applications. Proteomics 2010, 10, 888-893.

[5] **Zhang, J.,** Niu, D., Sui, J., Ching, C. B., Chen, W. N., Protein profile in hepatitis B virus replicating rat primary hepatocytes and HepG2 cells by iTRAQ-coupled 2-D LC-MS/MS analysis: Insights on liver angiogenesis. Proteomics 2009, 9, 2836-2845.

[6] Xu, J., Khor, K., Sui, J., **Zhang, J**., Chen, W. N., Protein expression profiles in osteoblasts in response to differentially shaped hydroxyapatite nanoparticles. Biomaterials 2009, 30, 5385-5391.

[7] Sui, J., **Zhang, J.**, Ching, C. B., Chen, W. N., Expanding proteomics into the analysis of chiral drugs. Mol Biosyst 2009, 5, 603-608.

[8] Niu, D., **Zhang, J.**, Ren, Y., Feng, H., Chen, W. N., HBx genotype D represses GSTP1 expression and increases the oxidative level and apoptosis in HepG2 cells. Mol Oncol 2009, 3, 67-76.

[9] Niu, D., Sui, J., **Zhang, J.**, Feng, H., Chen, W. N., iTRAQ-coupled 2-D LC-MS/MS analysis of protein profile associated with HBV-modulated DNA methylation. Proteomics 2009, 9, 3856-3868.

[10] Feng, H., **Zhang, J.,** Li, X., Chen, W. N., HBX-mediated migration of HBV-replicating HepG2 cells: insights on development of hepatocellular carcinoma. J Biomed Biotechnol 2009, 2009, 930268.

[11] **Zhang, J.**, Sui, J., Ching, C. B., Chen, W. N., Protein profile in neuroblastoma cells incubated with S- and R-enantiomers of Ibuprofen by iTRAQ-coupled 2-D LC-MS/MS analysis: possible action of induced proteins on Alzheimer's disease. Proteomics 2008, 8, 1595-1607.

[12] Xu, J., Khor, K. A., Sui, J., **Zhang, J.**, et al., Comparative proteomics profile of osteoblasts

cultured on dissimilar hydroxyapatite biomaterials: an iTRAQ-coupled 2-D LC-MS/MS analysis. Proteomics 2008, 8, 4249-4258.

[13] Tan, T. L., Fang, N., Neo, T. L., Singh, P., et al., Rac1 GTPase is activated by hepatitis B virus replication--involvement of HBX. Biochim Biophys Acta 2008, 1783, 360-374.

[14] Sui, J., **Zhang, J.**, Tan, T. L., Ching, C. B., Chen, W. N., Comparative proteomics analysis of vascular smooth muscle cells incubated with S- and R-enantiomers of atenolol using iTRAQ-coupled two-dimensional LC-MS/MS. Mol Cell Proteomics 2008, 7, 1007-1018.

[15] Sui, J., **Zhang, J.**, Ching, C. B., Chen, W. N., Comparative proteomic analysis of extracellular proteins reveals secretion of T-kininogen from vascular smooth muscle cells in response to incubation with s-enantiomer of propranolol. Mol Pharm 2008, 5, 885-890.

[16] Sui, J., Tan, T. L., **Zhang, J.**, Ching, C. B., Chen, W. N., iTRAQ-coupled 2D LC-MS/MS analysis on protein profile in vascular smooth muscle cells incubated with S- and R-enantiomers of propranolol: possible role of metabolic enzymes involved in cellular anabolism and antioxidant activity. J Proteome Res 2007, 6, 1643-1651.

[17] Lu, Y. W., Tan, T. L., **Zhang, J.**, Chen, W. N., Cellular apoptosis induced by replication of hepatitis B virus: possible link between viral genotype and clinical outcome. Virol J 2007, 4, 117.

[18] **Zhang, J.**, , I. S., , R. N., , P. C., , R. G., Molecular Characterisation of Sinusoidal Endothelial Cell Capillarisation Critical for Hepatocellular Carcinoma Progression. Annals of academy of medicine 2005, 34(Suppl), 262.

[19] **Zhang, J.,**and Chen, W. N., Inhibitory Effects of NASIAD Drug Ibuprofen on HBx-induced Angiogenesis. *Submitted*